Acute simulated hypoxia and ischemia in cultured C2C12 myotubes: decreased phosphatidylinositol 3-kinase (PI3K)/Akt activity and its consequences for cell survival

Mark Peter Thomas

Thesis presented in partial fulfilment of the requirements for the degree of

Master of Physiological Sciences at Stellenbosch University

Supervisor: Dr. Anna-Mart Engelbrecht

December 2008

DECLARATION

By submitting this thesis electronically, I declare that the entirety of the work contained therein is my own, original work, that I am the owner of the copyright thereof (unless to the extent explicitly otherwise stated) and that I have not previously in its entirety or in part submitted it for obtaining any qualification.

Date: 24 November 2008

Abstract

Cells are equipped with an array of adaptive mechanisms to contest the undesirable effects of ischemia and the associated hypoxia. Indeed, many studies have suggested that there is an increase in the PI3K/Akt pathway activation during hypoxia and ischemia. Damaged muscle can be regenerated by recruiting myogenic satellite cells which undergo differentiation and ultimately lead to the regeneration of myofibres. The C2C12 murine myogenic cell line is popular for studying myogenesis *in vitro*, and has been used in many studies of ischemic microenvironments. PI3K/Akt pathway activity is increased during C2C12 myogenesis and this is known to produce an apoptosis resistant phenotype. In this study, we provide evidence that high basal levels of PI3K activity exist in C2C12 myotubes on day ten post-differentiation. Ischemia is characterized by depleted oxygen and other vital nutrients, and ischemic cell death is believed to be associated with an increasingly harsh environment where pH levels decrease and potassium levels increase. By employing a model that mimics these changes in skeletal muscle culture, we show that both acute simulated ischemia and acute hypoxia cause decreases in endogenous levels of the p85 and p110 subunits of PI3K and a consequent reduction in PI3K activity. Supplementing skeletal muscle cultures with inhibitors of the PI3K pathway provides evidence that the protective effect of PI3K/Akt is subsequently lost in these conditions. Using Western blot analysis, a PI3K ELISA assay as well as known inhibitors of the PI3K pathway in conjunction with the MTT assay we are able to demonstrate that the activation of downstream

effectors of PI3K, including Akt, are concurrently decreased during acute simulated ischemia and acute hypoxia in a manner that is independent of PDK-1 and PTEN and that the decreases in the PI3K/Akt pathway activity produce a knock-on effect to the downstream signalling of transcription factors, such as Fox01 and Fox04, in our model. We proceed to provide compelling evidence that the apoptotic resistance of C2C12s is at least partially lost due to these decreases in PI3K/Akt pathway activity, by showing increased caspase-3 and PARP cleavage. Then, using vital staining techniques and a DNA fragmentation assay, we demonstrate increased cell membrane impairment, cell death and apoptosis after three hours of simulated ischemia and hypoxia in cultured C2C12 myotubes. In addition to the main findings, we produce evidence of decreased flux through the mTOR pathway, by showing decreased Akt-dependant phosphorylation at the level of TSC2 and mTOR during simulated ischemia and hypoxia. Finally, we present preliminary findings indicating increased levels of HIF1α and REDD-1, representing a possible oxygen sensing mechanism in our model. Therefore, we show that there is in fact a rapid decrease in PI3K/Akt activity during severe, acute simulated ischemia and hypoxia in C2C12 myotubes on day ten post-differentiation, and this causes a concomitant down regulation in cell survival pathways and increased activity of cell death machinery. Thereafter, we propose a possible mechanism of action and provide a platform for future studies.

Opsomming

Selle word met ‘n verskeidenheid beskermende meganismes toegerus om ontwrigting van normale sel funksionering – wat met iskemie en gevolgde hipoksie te paard gaan- te voorkom. Baie studies het, inderdaad, voorgestel dat daar ‘n verhoging in aktivering van die PI3K/Akt pad gedurende hipoksie en iskemie is. Beseerde spier kan regenereer word deur miogeniese satelliet selle te aktiveer, differensieër en tot die regenerasie van spier vesels lei. Miogenese *in vitro* word gereeld met die gewilde C2C12 sel lyn bestudeer. Hierdie sel lyn is ook in verskeie iskemiese mikro-omgewings bestudeer. PI3K/Akt aktiwiteit word gedurende miogenese verhoog, en dit word herken dat ‘n apoptose-weerstandige fenotipe sodoende bewerkstellig word. Ons voorsien bewyse dat hoë basale vlak aktiwiteit van PI3K op dag 10 post-differensiasie spier vesels bestaan. Iskemie word deur verpletterde suurstof vlakke en ander kern nutriente gekarakteriseer. Daar word geglo dat ‘n toenemende ru omgewing waar pH vlakke verlaag en kalium vlakke verhoog – met iskemiese sel dood assosieer word. Deur ‘n model wat die voorafgenoemde kondisies in skelet spier sel kultuur naboots te gebruik, demonstreer ons hier dat beide akute gesimuleerde iskemie en akute hipoksie ‘n verlaging in vlakke van die p85 en -110 subeenhede van PI3K (en gevolglike vermindering van PI3K aktiwiteit) te weeg bring. Deur skelet spier sel kulture met inhibeerders van die PI3K pad aan te vul, het bewys gelewer dat die beskermende rol wat PI3K/Akt het, gedurende hierdie kondisies verlore gaan. Deur van Western Blot analise, ‘n PI3K ELISA, asook herkende inhibeerders van die PI3K pad plus die MTT assay – was ons in

staat gestel om te wys dat die aktivering van stroom-af effektore van PI3K (insluitend Akt) gelyktydig verminder gedurende akute SI – en hipoksie, in ‘n wyse wat onafhanklik van PDK-1 en PTEN is. Daar is ook gewys dat verlagings in PI3K/Akt pad aktiwiteit in ons model ‘n ‘kern-reaksie’ effek tot die strroom-af sein transduksie van transkripsie faktore Fox01 en Fox04 het. Ons het voortgegaan om aangrypende bewyse te lewer dat die apoptotiese weerstand van C2C12s ten minste gedeeltelik gedurende akute SI- en hipoksie as gevolg van hierdie verlagings in PI3K/Akt pad aktiwiteit verloor word. Laasgenoemde word substansieer deurdat ons verhoogde kaspase-3 en PARP splitsing toon. Vervolgens, deur van kern vlekking tegnieke en ‘n DNA fragmentasie eksperiment gebruik te maak, demonstreer ons verhoogde sel membraan verswakking, sel dood en apoptose na drie ure van iskemie en hipoksie in gekweekte C2C12 spiervesels. Ter aanvulling tot die hoof bevindinge, voorsien ons bewyse van verlaagde fluks deur die mTOR pad – deur ‘n verlaagde Akt-afhanklike fosforilasie op die vlak van TSC2 en mTOR gedurende simuleerde iskemie en hipoksie te wys. Eindelik, voorsien ons preliminêre bevindinge wat verhoogde vlakke van HIFα en REDD-1 wys. Hierdie stel ‘n moontlike suurstof sensor meganisme in ons model voor. Dus wys ons dat daar inderdaad ‘n spoedige vermindering in PI3K/Akt aktiwiteit gedurende ernstige, akute gesimuleerde iskemie- en hipoksie in C2C12 spiervesels op dag 10 post-differensiasie is, en dat dit ‘n gevolglike af-regulasie in sel oorlewings paaie en verhoogde aktiwiteit van sel dood masjienerie veroorsaak.

Acknowledgements

I am sincerely indebted to all those mentioned here and some others that are not.

Most importantly, my dearest Celeste whom I adore. I am grateful for things to innumerable to mention.

My family and friends, both present and past, for their support and understanding.

The P and Team A for their unwavering support and kindnesses.

I thank my supervisor. Anna-Mart thank you for the opportunities and your subtle guidance, you help more than you know.

My friends and colleagues in the department, both current and former, for creating the labs and halls a pleasurable place to be every day.

Benji Loos for keen insights and frequent technical support.

Beverly Ellis for being there whenever you need her most, and for helping me to get started.

Finally, the inimitable Goose and unwavering Jimbo for always managing to keep tedium at bay, and for reminding me that life is meaningless if you don't enjoy it

Table of contents

List of Tables

List of Figures

Figure 1.5 Regulation of the mTOR pathway. *This schematic illustrates the regulation of mTOR as discussed in the text. Briefly, activated Akt is able to regulate mTOR through phosphorylation of TSC2 or mTOR directly. mTOR activity is also sensitive to changes in amino acids, nutrients, energy levels or hypoxia, which are all regulated through the TSC2/TSC1 complex upstream of Rheb.*

Figure 2.1 The Growth medium of proliferating C2C12 myoblasts is replaced with differentiating medium (DM) on day zero and cells are allowed to differentiate into multinucleated myofibres that are ready to treat on day ten.

Figure 2.2 Schematic representation of the experimental protocol. *C2C12 myotubes on day ten post-differentiation are randomly treated in four groups (independent experiments≥3) and incubated for three hours in the conditions illustrated above. Groups are described in detail in the text.*

Figure 3.1 Decrease in metabolic cell viability of C2C12 myotubes and myoblasts with increasing time spent in simulated ischemia. *Myoblasts and differentiated myotubes (day 10) were incubated in simulated ischemia, and their activities were assessed at 0,1,2,3,4 and 5 hours. Metabolic cell viability was measured using the MTT assay. Results are presented as means ± S.E.M (n ≥ 3).*

Figure 3.2 Linear relationship of time versus metabolic cell viability in C2C12 myotubes. *Differentiated C2C12 myotubes (day 10) were incubated in simulated ischemia, and their activities were assessed at 0,1,2,3,4,5,6 and 7 hours. Metabolic cell viabilities were measured by means of the MTT assay. The R^2 value was calculated for the time points ranging over 1 to 7 hours. Results are presented as means ± S.E.M (n ≥ 3).*

Figure 3.3 Difference in metabolic cell viability for C2C12 myotubes and myoblasts after 3 hours spent in simulated ischemia. *Myoblasts and differentiated myotubes (day 10) were incubated simulated ischemia, and their activities were assessed after three hours vs. their normoxic controls. Metabolic cell viability was measured by the MTT assay. Results are presented as their mean ± S.E.M (n=15 for myotubes and n ≥ 5 for myoblasts). *p<0.05 vs. control (myotubes), **p<0.05 vs. control (myoblasts).*

Figure 3.4 Differences in metabolic cell viability after 3 hours in normoxia or hypoxia, both with and without a modified Esumi buffer. *Myoblasts and differentiated myotubes (day 10) were incubated both with and without a modified Esumi buffer and differences in metabolic cell viability was measured vs. their normoxic or hypoxic controls after three hours. Cell activities were measured by the MTT assay. Results are presented as their mean ± S.E.M (n ≥ 3). *p<0.05 vs. untreated control, #p<0.05 vs. normoxia with ischemic buffer*

Figure 3.5A The effect of 3 hrs of hypoxia or simulated ischemia on protein expression of PI3K's regulatory p85 subunit. *Samples were examined by Western blot analysis with antibodies recognizing the p85 regulatory subunit of PI3K. Results are presented as their mean ± S.E.M, *p<0.05 vs. untreated control (n ≥ 3).*

Figure 3.5B The effect of a modified Esumi buffer on protein expression of PI3K's regulatory p85 subunit. *Samples were examined by Western blot analysis with antibodies recognizing the p85 regulatory subunit of PI3K. Results are presented as their mean ± S.E.M, (n ≥ 3).*

Figure 3.6A The effect of 3 hrs of hypoxia or simulated ischemia on protein expression of PI3K's catalytic p110 subunit. *Samples were examined by Western blot analysis with antibodies recognizing the p110 catalytic subunit of PI3K. Results are presented as their mean ± S.E.M, *p<0.05 vs. untreated control (n ≥ 3).*

Figure 3.6B The effect of a modified Esumi buffer on protein expression of PI3K's catalytic p110 subunit. *Samples were examined by Western blot analysis with antibodies recognizing the p110 catalytic subunit of PI3K. Results are presented as their mean ± S.E.M, (n ≥ 3).*

Figure 3.7 The effect of 3 hrs of hypoxia and simulated ischemia on the PI3Kα catalysed production of $PI(3,4,5)P_3$ in C2C12 myotubes. *The p85 subunit of PI3K was immunoprecipitated from cell lysates using an anti-PI3K antibody before a competitive ELISA assay was used to detect the amount of $PI(2,4,5)P_3$ produced from a substrate. Results are presented as their mean ± S.E.M, *p<0.05 vs. untreated control (n ≥ 3).*

Figure 3.8 Wortmannin decreases metabolic cell viability in C2C12 myotubes incubated in normoxia but not in those incubated in 3 hrs of simulated ischemia. *Wortmannin (200nM) was added to myotube cultures 20min prior to the incubation step. Simulated ischemia consisted of 3 hours in a modified Esumi buffer in 1.0% oxygen tension (B). Metabolic cell viability was measured using the MTT assay. Results are presented as their mean ± S.E.M, *p<0.05 vs. control (n ≥ 3).*

Figure 3.9 LY294002 decreases metabolic cell viability in C2C12 myotubes incubated in normoxia but not in those incubated in 3 hrs of simulated ischemia. *Only a high concentration, 100μM, of LY294002 shows decreased metabolic cell viability (B). LY294002 was added to myotube cultures 20min prior to the incubation step. Cell activities were measured using the MTT assay. Results are presented as their mean ± S.E.M, *p<0.05 vs. control (n ≥ 3); #p<0.05 vs. 10μM inhibitor (n ≥ 3)*

Figure 3.10 PTEN phosphorylation at serine 380 is not effected by incubation in 3 hrs of simulated ischemia. *Samples were examined by Western blot analysis with antibodies recognizing PTEN only when phosphorylated at the serine 380 position. Results are presented as their mean ± S.E.M, (n ≥ 3).*

Figure 3.11 PDK-1 phosphorylation at serine 241 is not effected by incubation in 3 hrs of hypoxia or simulated ischemia. *Samples were examined by Western blot analysis with antibodies recognizing PDK-1 only when phosphorylated at the serine 241 position. Results are presented as their mean ± S.E.M, (n ≥ 3).*

Figure 3.12 The effect of 3 hrs of hypoxia or simulated ischemia on phosphorylation of Akt (Ser473). *Samples were examined by Western blot analysis with antibodies recognizing phospho-Akt (Ser473). Results are presented as their mean ± S.E.M, *p<0.05 vs. control (n ≥ 3).*

Figure 3.13 LY294002 decreases phosphorylation of Akt (Ser473) in C2C12 myotubes during 3 hrs of simulated ischemia. *Samples were examined by Western blot analysis with antibodies recognizing phospho-Akt (Ser473). Results are presented as their mean ± S.E.M, *p<0.05 vs. control (n ≥ 3).*

Figure 3.14 Wortmannin decreases phosphorylation of Akt (Ser473) in C2C12 myotubes during 3 hrs of simulated ischemia. *Samples were examined by Western blot analysis with antibodies recognizing phospho-Akt (Ser473).*

Figure 3.15 The effect of a modified Esumi buffer on phosphorylation of Akt (Ser473) in C2C12 myotubes. *Samples were examined by Western blot analysis with antibodies recognizing phospho-Akt (Ser473). Results are presented as their mean ± S.E.M, (n ≥ 3).*

Figure 3.6 The effect of 3 hrs of hypoxia or simulated ischemia on phosphorylation of Akt (Thr308). *Samples were examined by Western blot analysis with antibodies recognizing phospho-Akt (Thr308). Results are presented as their mean ± S.E.M, *p<0.05 vs. control (n ≥ 3).*

Figure 3.17 LY294002 decreases the level of phosphorylation of Akt (Thr308) in C2C12 myotubes during 3 hrs of simulated ischemia. *Samples were examined by Western blot analysis with antibodies recognizing phospho-Akt (Thr308).*

Figure 3.18 Wortmannin decreases phosphorylation of Akt (Thr308) in C2C12 myotubes during 3 hrs of simulated ischemia. *Samples were examined by Western blot analysis with antibodies recognizing phospho-Akt (Thr308).*

Figure 3.19 The effect of 3 hrs of simulated ischemia and LY294002 on phosphorylation of Fox01 and Fox04. *Samples were examined by Western blot analysis with antibodies recognizing phospho-Fox01 (Ser193) and phospho-Fox04 (Ser256). Results are presented as their mean ± S.E.M, *p<0.05 vs. control (n ≥ 3).*

Figure 3.20 The effect of 3 hrs of hypoxia or simulated ischemia on phosphorylation of CREB. *Samples were examined by Western blot analysis with antibodies recognizing phospho-CREB (Ser133). Results are presented as their mean ± S.E.M, *p<0.05 vs. control (n ≥ 3).*

Figure 3.21 Caspase-3 cleavage in C2C12 myotubes incubated in 3 hrs of simulated ischemia. *Cultures were supplemented with LY294002 20min prior to incubation. Samples were examined by Western blot analysis with antibodies recognizing caspase-3 and cleaved caspase-3. Results are presented as their mean ± S.E.M, *p<0.05 vs. control (n ≥ 3).*

Figure 3.22 PARP-1 cleavage in C2C12 myotubes, triggered during 3 hrs of simulated ischemia. *Cultures were supplemented with LY294002 20min prior to incubation. Samples were examined by Western blot analysis with antibodies recognizing PARP-1 and the cleaved 85kD subunit of PARP-1. Results are presented as their mean ± S.E.M, *p<0.05 vs. control (n ≥ 3).*

Figure 3.23 The effect of acute of simulated ischemia and hypoxia on membrane permeability of C2C12 myotubes. *Cells were stained with Hoechst 33342 (blue) and PI (red) and analysed for membrane impairment using fluorescence microscopy. Healthy cells stain only for Hoechst, late apoptotic cells stain for PI and Hoechst while necrotic cells stain homogenously for PI and Hoechst (pink). NM (Normoxia), HM (Hypoxia), NE (Ischemic buffer), HE (Simulated ischemia), (n ≥ 3).*

Figure 3.24 Quantification of PI intensity in myotubes incubated in acute hypoxia and with a modified Esumi buffer. *Cells were stained with Hoechst 33342 (blue) and PI (red) and analysed using fluorescence microscopy. At least 250 cells were selected and assessed for the fluorescence intensity of PI. Results are presented as their mean ± S.E.M, *p<0.05 vs. control (n ≥ 3); #p<0.05 vs. SI (n ≥ 3)*

Figure 3.25 The effect of acute simulated ischemia and LY294002 on membrane permeability of C2C12 myotubes. *Cells were stained with Hoechst 33342 (blue) and PI (red) and analysed for membrane impairment using fluorescence microscopy. Healthy cells stain only for Hoechst, late apoptotic cells stain for PI and Hoechst while necrotic cells stain homogenously for PI and Hoechst (pink). NM (Normoxia), HE (Simulated ischemia), HELY (Simulated ischemia + 50 μM LY294002), (n ≥ 3).*

Figure 3.26 Quantification of PI intensity in myotubes incubated in acute simulated ischemia and LY294002. *Cells were stained with Hoechst 33342 (blue) and PI (red) and analysed using fluorescence microscopy. At least 145 cells were selected and assessed for the fluorescence intensity of PI. Results are presented as their mean ± S.E.M, *p<0.05 vs. control (n ≥ 3)*

Figure 3.27 The effect of acute hypoxia and simulated ischemia on apoptosis - Annexin V binding. *Cells were stained with Hoechst 33342 (blue) and Annexin V (green) and analysed for apoptosis using fluorescence microscopy. Healthy cells stain only for Hoechst whereas apoptotic cells stain for Hoechst and Annexin V. NM (Normoxia), HM (Hypoxia), HE (Simulated ischemia), (n ≥ 3).*

Figure 3.28 Quantification of Annexin V intensity in myotubes incubated in acute hypoxia and simulated ischemia. *Cells were stained with Hoechst 33342 and Annexin V and analysed using fluorescence microscopy. At least 75 whole myotubes were selected and assessed for the fluorescence intensity of Annexin V. Results are presented as their mean ± S.E.M, *p<0.05 vs. control (n ≥ 3)*

Figure 3.29 The effect of acute simulated ischemia and LY294002 on apoptosis in C2C12 myotubes - Annexin V binding. *Cells were stained with Hoechst 33342 (blue) and Annexin V (green) and for analysed apoptosis using fluorescence microscopy. Healthy cells stain only for Hoechst whereas apoptotic cells stain for Hoechst and Annexin V. NM (Normoxia), HELY (Simulated ischemia + 50 μM LY294002), HE (Simulated ischemia), (n ≥ 3).*

Figure 3.30 Quantification of Annexin V intensity in myotubes incubated in acute simulated ischemia supplemented with LY294002. *Cells were stained with Hoechst 33342 (blue) and Annexin V (green) and analysed using fluorescence microscopy. At least 75 whole myotubes were selected and assessed for the fluorescence intensity of Annexin V. Results are presented as their mean ± S.E.M, *p<0.05 vs. control (n ≥ 3)*

Figure 3.31 DNA fragmentation in C2C12 myotubes incubated in 3 hrs of hypoxia and simulated ischemia. *Genomic DNA was extracted from cells and then run on a 1% TAE-agarose gel. DNA was detected using ethidium bromide staining. Representative image of repeats>3.*

Figure 3.32 The effect of 3 hrs of simulated ischemia on the expression of TSC1 (Hamartin). *Samples were examined by Western blot analysis with antibodies recognizing endogenous TSC1. Results are presented as their mean ± S.E.M, *p<0.05 vs. control (n ≥ 3).*

Figure 3.33 The effect of 3 hrs of simulated ischemia on Akt-dependent phosphorylation of TSC2 (Tuberin). *Samples were examined by Western blot analysis with antibodies recognizing endogenous levels of TSC2 only when phosphorylated at the threonine 1462 position. Results are presented as their mean ± S.E.M, *p<0.05 vs. control (n ≥ 3).*

Figure 3.34 The effect of 3 hrs of simulated ischemia on the Akt-dependent phosphorylation of mTOR. *Samples were examined by Western blot analysis with antibodies recognizing endogenous levels of mTOR only when phosphorylated at the serine 2448 position. Results are presented as their mean ± S.E.M, *p<0.05 vs. control (n ≥ 3).*

Figure 3.35 The effect of 3 hrs of hypoxia or simulated ischemia on REDD1 levels in C2C12 myotubes. *Samples were examined by Western blot analysis with antibodies recognizing endogenous levels of HIF1α and REDD1. Results are presented as their mean ± S.E.M, *p<0.05 vs. control (n ≥ 3).*

Figure 4.1 Proposed mechanism of decreased PI3K/Akt activity during acute SI and hypoxia in C2C12 myotubes on day ten post-differentiation. *Explained in detail in the text*

Abbreviations

4E-BP1	4E binding protein
AIF	Apoptosis Inducing Factor
AMP	Adenosine Monophosphate
AMPK	AMP-activated protein kinase
AP-1	Activated Protein-1
ARNT	Aryl Hydrocarbon Receptor Nuclear Translocator
ASK-1	Apoptosis Signal Regulating Kinase 1
ATP	Adenosine Triphosphate
bHLH	basic Helix Loop Helix
Bid	BH3 interacting domain death agonist
bp	base pair
CREB	c-AMP response element binding protein
Con	Control
DD	Death Domain
DED	Death Effector Domain
DISC	Death-Inducing Signalling Complex
DMEM	Dulbecco's Modified Eagle's Medium
DNA	Deoxyribonucleic acid
ECACC	European Collection of Cell Cultures
EDTA	Ethylenediaminetetraacetic Acid

ELISA	Enzyme-Linked Immunosorbent Assay
ER	Endoplasmic Reticulum
ERK	Extracellular Regulated Kinase
FADD	Fas-Associated Death Domain
FGF	Fibroblast Growth Factor
FIH	Factor Inhibiting HIF
FITC	Fluorescein isothiocyanate
FoxO	Forkhead box binding transcription factors (O-subgroup)
Gab1	Grb2-associated binder-1
GPCR	G-protein-coupled receptor
Gβγ	Guanine nucleotide binding protein βγ
H_2O_2	Hydrogen peroxide
HE	simulated ischemia
HEPES	4-(2-hydroxyethyl)-1-piperazineethanesulfonic acid
HGF	Hepatocyte Growth Factor
HIF	Hypoxic Inducible Factor
HM	Hypoxia only
IAP	Inhibitor of Apoptosis Protein
IGF	Insulin-like Growth Factor
JAK/STAT	Janus kinase/Signal Transducers and Activators of Transcription
JIP-1	JNK-interacting protein 1
JNK	c-jun NH_3-terminal Kinases
LY294002	2-(4-morpholino)-8-phenyl-4H-1-benzopyran-4-one

MAPK	Mitogen Activated Protein Kinase
MRF	Myogenic Regulatory Factor
MTT	3-(4,5-dimethylthiazol-2-yl)-2,5-diphenyltetrazoliumbromide
mTOR	mammalian Target Of Rapamycin
NADPH	Nicotidamine Adenine DiPhosphate Hydroxylase
NE	modified Esumi buffer only
NFκB	Nuclear Factor Kappa B
NM	untreated control
ODDD	Oxygen Dependent Degradation Domain
PARP	Poly (ADP-ribose) polymerase enzyme
PBS	Phosphate Buffered Saline
PDK1	3-phosphoinositide-dependent kinase
PH	Pleckstrin-Homology
PHLPP	PH domain leucine-rich repeat protein phosphatase
PHs	Prolyl Hydroxylases
PI	Phosphatidylinositol
PI3K	Phosphatidylinositol 3-Kinase
PIP	Phosphatidylinositol-4-phosphate
PIP_2	Phosphatidylinositol-4,5-biphosphate
PIP_3	Phosphatidylinositol-3,4,5-triphosphate
PMSF	PhenylMethylSulfonyl Fluoride
pO_2	partial oxygen tension

PTEN	Phosphatase and tensin homologue deleted on chromosome ten
PTPs	Protein Tyrosine Phosphatases
PVDF	Polyvinylidine Fluoride
REDD	DNA-damage-inducible transcript
ROS	Reactive Oxygen Species
RTK	Receptor Tyrosine Kinase
S6K	S6 kinase
SDS-PAGE	Sodium Dodecyl Sulphate Polyacrylamide Gel Electrophoresis
SEM	Standard Error of the Mean
Ser	Serine
SH2	src homology 2
SHIP	src homology 2-containing inositol 5'-phosphatase
SI	Simulated Ischemia
SIN1	Stress activated MAP kinase Interacting protein Sin1
siRNA	small interfering Ribonucleic Acid
SMAC/DIABLO	Diablo homolog (Drosophila)
SODD	Silencer of Death Domains
TAE	Tris-acetate-EDTA
TBS	Tris Buffered Saline
TBS-T	Tris Buffered Saline- Tween20
TGFβ	Transforming Growth Factor beta
Thr	Threonine
TNFR	Tumour Necrosis Factor Receptor

TOR	Targets Of Rapamycin
TRADD	TNF Receptor-Associated Death Domain
TSC	Tubular Sclerosis Complex
UV	UltraViolet
VEGF	Vascular Endothelial Growth Factor
VHL	von Hippel-Lindau

Chapter 1

Introduction

The cells of all living organisms are being continually exposed to a toxic gas, oxygen. The same facility as a powerful oxidizer that makes oxygen so reactive towards organic material also lends to its suitability as the final electron acceptor in the mitochondrial respiratory chain. Accordingly, oxygen is essential for the generation of ATP, the invaluable energy currency of the cell, underlining its role as one of the most pressingly vital molecules for all anaerobes.

Oxygen homeostasis is crucial for optimal physiological functioning and is necessary for normal growth and differentiation of cells. There are several pathological conditions, most notably cancerous tumours (Pouyssegur *et al.*, 2006) as well as myocardial, cerebral and retinal ischemia (Semenza, 2000), where acute or chronic low oxygen conditions disrupt favourable cellular operations and lead to cell and tissue damage. Also, various acute and chronic conditions (most commonly atherosclerosis) can lead to peripheral vascular diseases that manifest as limb ischemia with low survival rates in critical cases (Santilli and Santilli, 1999). Consequently, cells are equipped with a range of adaptive mechanisms that combat

unwelcome reductions in oxygen availability. For example, adult skeletal muscle displays the incredible potential to regenerate following chronic ischemic stresses (Aranguren *et al.*, 2008; Heemskerk *et al.*, 2007; Scholz *et al.*, 2003). Ischemic muscle damage is thought to trigger the recruitment of myogenic satellite cells which rapidly proliferate before undergoing differentiation in response to certain cues. This process ultimately leads to the regeneration of damaged myofibres (Aranguren *et al.*, 2008; Hawke and Garry, 2001). Although continued exposure to severe hypoxia is thought to have harmful effects, the extreme plasticity of skeletal muscle has been demonstrated by athletes who conduct exercise training sessions in hypoxic conditions for its proposed beneficial effects. Locally induced hypoxia during high altitude exercise training (Vogt *et al.*, 2001) or in hypobaric conditions (Terrados *et al.*, 1990) has shown positive effects on performance not seen during normoxic training. These effects have been attributed to a variety of muscle adaptations. Moreover, chronic exposure to low oxygen tension at high altitudes leads to dramatic decreases in muscle fibre size and mass leading to phenotypic variation in high-altitude populations and in lowlanders exposed to acute bouts of severe hypoxia (Hoppeler and Vogt, 2001).

During myogenesis, many of the signalling cascades that participate in the regulation of cell proliferation and growth are up-regulated. Akt, the principle downstream target of phosphoinositide 3-kinase (PI3K), is one such family of protein kinases (Jiang *et al.*, 1998). The PI3K/Akt pathway is important for muscle differentiation and lies upstream of both key death and energy consuming pathways. Under conditions of chronic, decreased cellular oxygen availability, PI3K signalling pathways are thought to mediate in cellular survival. Indeed, many reports suggest an increase in PI3K/Akt activation during chronic hypoxia (Barry *et al.*, 2007).

The protein kinase mammalian target of rapamycin (mTOR) is a key component that acts as a gateway to ensure that protein synthesis and its associated energy consumption remain in equilibrium with nutrient supply. mTOR is believed to manage valuable energy stores in response to a depletion of nutrients like amino acids, oxygen and mitogens, a situation that might occur during decreased blood flow observed in pathophysiological conditions such as ischemic diseases (Zhou *et al.*, 2008; Sarbassov *et al.*, 2005a; Vaupel *et al.*, 1989). Decreased flux through the mTOR pathway, situated downstream of PI3K/Akt, aims to conserve valuable energy resources during these states. These actions may contribute to cell survival during a chronic hypoxic or ischemic insult in some cell lines. Hitherto, few studies have examined the role of the PI3K/Akt/mTOR pathway in acute ischemia or hypoxia in skeletal muscle.

1.1 Chapter outline

Section 1.2 begins by describing and defining hypoxia and ischemia and the proposed mechanisms by which they lead to cell damage. It then goes on to illustrate some of the well known pathophysiologic and physiological circumstances in which hypoxia and ischemia occur. *Section 1.3* begins by delving into the more abstruse topic of oxygen sensing before discussing cellular adaptation to low oxygen levels through the foremost regulators of the homeostatic response to oxygen shortage, the hypoxic inducible factors. *Section 1.4* concerns the development and function of skeletal muscle as well as the pertinent subject of myogenic satellite cells and their response during muscle injury. While the *subsection 1.4.4* briefly examines *in vitro* differentiation of the C2C12 skeletal muscle cell line. *Section 1.5* gives a broad overview of PI3K signalling and discusses its downstream target Akt. Their roles in hypoxia and ischemia are discussed in *sections 1.5.6.1* and *1.5.6.2* respectively. A brief overview of the literature concerning cell death, particularly apoptosis, is given in *section 1.6*.

Thereafter, explicit attention is given to the specific role of the PI3K/Akt pathway in apoptosis in *section 1.6.4*. Lastly, the mTOR pathway is overviewed in *section 1.7*. Special consideration is given to its regulation through PI3K/Akt and to its involvement in C2C12 myotube development.

1.2 Normoxia, hypoxia and ischemia

Oxygen acts as the final electron acceptor in the mitochondrial respiratory chain, where the catalysed generation of ATP provides the essential energy currency of the cell. For that reason, correct maintenance of cellular oxygenation levels is pressingly vital for normal energy production in all aerobic organisms. Devoid of oxygen homeostasis, mammalian cells are incapable of normal growth and differentiation. Normoxia has been defined as a state where ambient oxygen partial pressure is 150 mm Hg whereas hypoxia can be described as a state where the concentration of oxygen reaching the blood, lungs or tissue is abnormally low (1973). While a practical definition for hypoxia is when the demand for oxygen exceeds the vascular supply reaching the tissues of the body (Lee *et al.*, 2007), ischemic hypoxia is best described as reduced generalized or local tissue perfusion (Hockel and Vaupel, 2001). Hypoxia is therefore a predominant feature of ischemia. The reduction of blood flow in ischemia causes decreased oxygen as well as nutrient supply to, and a concurrently diminished removal of waste products from, vital organs (Semenza, 2000; Dirnagl *et al.*, 1999).

Within mammalian tissue, there is no defined threshold discriminating normoxia from hypoxia. Inspired air moves though the air passages and alveoli of the respiratory system and diffuses into the blood down slight oxygen gradients. The outcome is a normal circulating arterial blood oxygen concentration of around 14% O_2 (Roy *et al.*, 2003). The oxygen

concentrations of mammalian organs span over a wide range and can be anywhere from 12% O_2 to less than 0.5% O_2 in normoxic, healthy tissue (Roy *et al.*, 2003). In fact, many tissues ordinarily reside in a range of 2-8% stable oxygenation (Barbazetto *et al.*, 2004). These differences in average tissue oxygen levels necessitate working definitions of hypoxia specific to the tissues, cells or organs being investigated. The physiological oxygen concentration in skeletal muscle is approximately 5% O_2 (Brevetti *et al.*, 2003) while experimentally, pathological hypoxia has been described as <0.5% O_2 for cultured C2C12 skeletal muscle cells (Yun *et al.*, 2005).

1.2.1 Mechanism of cell damage in hypoxia and ischemia

Divergent results have been reported in studies investigating hypoxia induced cell death (Long *et al.*, 1997; Webster *et al.*, 1999; Santore *et al.*, 2002). The mechanisms by which decreases in oxygen might initiate cell death remains controversial, but recent results indicate that cell death is triggered indirectly by secondary mechanisms and not directly by a decrease in oxygen as such (Webster *et al.*, 1999). It is accepted that hypoxia and ischemia cause severe acidosis and lead to the alteration of ion concentrations in cells and tissue (Yao and Haddad, 2004). During hypoxia and ischemia, the lack of available oxygen causes a rapid deceleration or even cessation of oxidative phosphorylation and an increase in anaerobic glycolysis. When a switch away from oxygen-dependent energy production to anaerobic glycolysis takes place, there is a reduced consumption of H^+ due to a decreased ATP turnover (King and Opie, 1998). The production of lactate generates more H^+ still, augmenting that produced by decreased ATP return. The net result is a decrease in pH and an increase in intracellular acidosis. The resultant microenvironment is believed to be responsible for most of the harmful effects seen during ischemia (Neely and Grotyohann, 1984).

Acidosis that develops in hypoxia and hypoxia/ischemia is thought to initiate a series of mechanisms involved in necrotic and apoptotic signalling (Banasiak *et al.*, 2000). The interaction between pH, proton pumps and coupled exchangers during hypoxia and ischemia leads to an accumulation of deleterious Ca^{2+} (Kristian and Siesjo, 1998), Na^{+} (Allen and Xiao, 2003) and K^{+} (Mo and Ballard, 2005). Hypoxia induced acidosis triggers the activation of the Na^{+}/H^{+} exchanger among other membrane transporters. The subsequent increase in intracellular Na^{+} activates the Na^{+}/Ca^{2+} coupled exchanger which increases intracellular Ca^{2+} concentrations in turn (Allen and Xiao, 2003; Yao and Haddad, 2004). It has also been shown that hypoxia and acidosis can cause a coordinated, programmed cell death response in some cells (Gottlieb *et al.*, 1995; Webster *et al.*, 2005) (discussed in section 1.6.6).

The controlled extracellular environment in tissue culture allows research to be conducted in simulated hypoxic and ischemic conditions. An acute ischemic insult in which nutrients and growth factors as well as oxygen are deprived from cultured cells can be simulated in order to mimic decreased oxygen and blood flow (Long *et al.*, 1997). Additionally, the decreases in pH, the altered ion concentrations and compromised metabolic activity seen during physiological ischemia can be replicated with suitable buffers *in vitro* (Esumi *et al.*, 1991).

1.2.2 Occurrence of hypoxia and ischemia

The decline in supply versus demand of molecular oxygen, characteristic of hypoxia and ischemia, can be attributed to pathophysiological circumstances (as in tumours and peripheral vascular diseases) or physiologic circumstances (as in exercising skeletal muscle or travels to high-altitudes).

1.2.2.1 Hypoxia and ischemia in pathophysiological circumstances

Oxygen homeostasis is crucial for normal functioning, and a disruption of this balance occurs in many pathophysiological states. Hypoxia is a characteristic property of tumours and tumour progression (Harris, 2002). Rapidly growing tumours quickly exceed the capacity to form new blood vessels, resulting in a hypoxic microenvironment during tumour development (Vaupel and Mayer, 2007). The tissue responds by activating angiogenic machinery (Coleman *et al.*, 2002), but the resultant neovascularization is chaotic and irregular with intermittent blood flow (Denko *et al.*, 2000) which is usually a sign of poor prognosis (Vaupel and Mayer, 2007). Other pathophysiological conditions such as myocardial and retinal ischemia, stroke and pulmonary hypertension are also associated with hypoxic insults and can lead to reduced cell viability (Semenza, 2000). Whereas acute and chronic hypoxia, a common consequence of atherosclerosis, can lead to peripheral vascular diseases that manifest as limb ischemia with low survival rates in critical cases (Santilli and Santilli, 1999).

1.2.2.2 Hypoxia and ischemia in physiologic circumstances

Persistent exposure to harsh hypoxic conditions has been established to have destructive effects on muscle tissue. Accordingly, chronic exposure to low oxygen tension at high altitudes leads to dramatic decreases in muscle fibre size and mass in high-altitude climbers (Howald and Hoppeler, 2003). However, high-altitude hypoxia has also been associated with significant adaptations in blood flow (Erzurum *et al.*, 2007) as well as muscle structure and performance capacity (Kayser *et al.*, 1991) in high-altitude populations. This extreme plasticity and adaptability of skeletal muscle in low oxygen environments has been demonstrated by athletes who conduct exercise training sessions in hypoxic conditions for its proposed beneficial effects. Locally induced hypoxia during high altitude exercise training

(Vogt *et al.*, 2001) or in hypobaric conditions (Terrados *et al.*, 1990) have shown positive effects on performance not found when training in normoxic conditions. These effects have been attributed to muscle adaptations such as an increase in myoglobin content and capillarity in response to low oxygen tensions (Vogt *et al.*, 2001; Reynafarje, 1962). It has also been postulated that modest chronic hypoxia may even be cardioprotective, by activating cardiac remodelling machinery in response to hypoxia, by means of oxygen-sensitive adaptations at the transcriptional level (Essop, 2007).

1.3 Molecular response to hypoxia: Oxygen sensing and cellular adaptation

A decrease in oxygen availability lends toward a tendency away from the preferred mechanism of oxidative phosphorylation to an increased dependence on anaerobic glycolysis. This shift towards a decrease in oxidative capacity negatively influences normal metabolic operations, so cells are equipped with a range of adaptive mechanisms that are able to detect and hastily attempt to redress any unwelcome reductions in oxygen availability (Papandreou *et al.*, 2005).

1.3.1 Detecting changes in oxygen

In order to bring about an adaptive response to alterations in tissue oxygen levels, a system capable of sensing changes in oxygen concentration must be present. Although the complexities of the true sensing system remain to be unravelled, it seems as if reactive oxygen species (ROS) play a central role amongst what may include several detection mechanisms (Acker *et al.*, 2006; Semenza, 1999). If this is indeed the case, then ROS would have to be generated in proportion to cellular oxygen concentrations. The most likely contenders of ROS generation in these circumstances are NAD(P)H oxidase and the mitochondrial electron transport chain (Semenza, 1999). Even though controversies over

whether or not ROS are actually generated or even dissipated during hypoxia still exist (Clanton, 2005), it has been inferred from many experiments that mitochondrial ROS generated at complex III in the electron transport chain is important for oxygen sensing in hypoxia (Brunelle *et al.*, 2005; Chandel *et al.*, 2000). It is generally believed that production of ROS is a normal physiological response to hypoxia in skeletal muscle, but that redox homeostasis is not preserved during extreme or chronic hypoxia (Clanton, 2007). It has also been demonstrated that a burst of intracellular ROS is formed in skeletal muscle during acute hypoxia, before re-oxygenation (Zuo and Clanton, 2005).

1.3.1.1 Mitochondrial ROS as oxygen sensor

A controlled response, to low doses of endogenously generated ROS, can occur through specific signalling cascades (Thannickal and Fanburg, 2000). In fact, many signalling responses are dependent on small transient increases in ROS production for their optimal functioning (Thannickal and Fanburg, 2000; Hancock *et al.*, 2001). The mitochondrial electron transport chain has been well documented as a possible source of ROS (Mattiasson, 2004), and it seems as though mitochondrial electron transport function might be important for conventional cellular signalling (Bogoyevitch *et al.*, 2000; Nemoto *et al.*, 2000; Kulisz *et al.*, 2002). Under normal conditions, a balance between intracellular oxidizing and reducing species exists. Molecular oxygen can be reduced to form superoxide ($O_2^{-}\cdot$), although any superoxide produced in the cell is rapidly converted to hydrogen peroxide (H_2O_2) by dismutases present in the mitochondria and cytosol. The resulting H_2O_2 is a weak oxidant, with a half life of seconds. However, H_2O_2 represents an ideal candidate as molecular messenger in oxygen dependent signalling (Kietzmann *et al.*, 2000). An important factor contributing to the reactivity of H_2O_2 is that it is not a free radical and is therefore soluble in both lipid and aqueous environments. Catalase and glutathione peroxidase will rapidly

disassociate H_2O_2 to water while Fenton reactions produce highly reactive hydroxyl radicals from H_2O_2 (Kietzmann *et al.*, 2000). At cellular pH, protein cysteine residues are de protonated to thiolate ions, the protein motifs that are most susceptible to oxidation by H_2O_2 (Forman *et al.*, 2004). They can react with H_2O_2 and become oxidized to yield sulfenate ions. The resulting sulfenate is able to react with a thiol, such as cytosolic GSH in a process known as S-glutathiolation, to form a disulfide which is capable of being reduced back to its original sulphate (Forman *et al.*, 2004). Additional, less well described oxidative protein modification, such as creation of disulphide linkages and cross linking to form dityrosine, have been suggested as alternative methods by which ROS may act as signalling messengers (Thannickal and Fanburg, 2000).

Redox sensitive proteins are those that are able to undergo a posttranslational modification in response to changes in the redox state of a cell. These posttranslational modifications can be achieved by an increase in ROS production and the subsequent oxidation of vulnerable protein motifs. H_2O_2 is thought to act on several branches along the tree of cellular signalling cascades. Upstream, the oxidation of protein tyrosine phosphatases (PTPs) by H_2O_2 has been demonstrated as a probable concerted mechanism by which the activity of growth factors and mitogenic G-coupled receptor activation is enhanced (Bae *et al.*, 1997; Chiarugi *et al.*, 2002). This reversible inactivation of PTPs leads to enhanced receptor tyrosine kinase (RTK) phosphorylation which in turn induces phosphorylation of cytoplasmic protein kinases. The outcome is a signalling cascade that leads to the downstream activation of the extracellular regulated kinase (ERK), p38 and c-jun NH_3-terminal kinase (JNK) mitogen activated protein (MAP) kinases (Lee and Esselman, 2002). Moreover, it is possible that the JAK/STAT pathway, which is known to be stimulated by ROS, is activated by a similar mechanism (Simon *et al.*, 1998). Furthermore, some protein kinase C isoforms contain cysteines in their

regulatory sites that are also capable of being oxidized by H_2O_2 (Wu, 2006). Notably, redox sensitive transcription factors such as nuclear factor kappa B (NF-kB), activated protein-1 (AP-1) and hypoxia inducible factor-1 (HIF-1) could also be targets for H_2O_2, thereby allowing changes in oxygen concentrations to regulate transcriptional activity (Kietzmann *et al.*, 2000).

In a response proportional to diminished cellular oxygen concentrations, skeletal muscle mitochondrial complex III, or possibly some other sensing mechanism, responds by causing a transient increase in intracellular ROS (Guzy *et al.*, 2005). ROS generated in hypoxia, are able to act on multiple signalling pathways in order to modulate muscle modifications in a response to reduced oxygen availability (Hoppeler *et al.*, 2003). Most notably, ROS generated in hypoxia by the mitochondrial transport chain have been implicated in the activation of the hypoxic inducible transcription factors (Chandel *et al.*, 2000).

1.3.2 Cellular adaptations to hypoxia: Hypoxic inducible factors

The foremost regulators of the homeostatic response to oxygen shortage must be the hypoxic inducible factor (HIF) family of transcription factors. Hypoxia has been reported to elicit a direct or indirect response from more than 2% of human genes in arterial endothelial cells (Manalo *et al.*, 2005). Furthermore, most of the genes expressed during hypoxia are believed to be controlled by HIF-1 (Greijer *et al.*, 2005). By becoming active during periods of low oxygen, HIF induces the transcription of a series of genes that bring about cellular changes that attempt to compensate for any alterations caused by the hypoxic state. HIF accomplishes this by controlling, among others, genes regulating angiogenesis (Pugh and Ratcliffe, 2003), glucose metabolism (Chen *et al.*, 2001) and erythropoiesis (Semenza *et al.*, 1991). In this way, it attempts to restore oxygen homeostasis and normal metabolic functioning.

HIFs are hetrodimers made up of an inducible, regulated alpha subunit and a constitutively expressed beta subunit. Both constituents of the HIF complex are members of the basic-Helix-Loop-Helix (bHLH)–containing PER-ARNT-SIM (PAS) domain superfamily (Wang *et al.*, 1995). Multiple HIF-alpha chain isoforms have been described (Gleadle *et al.*, 2006). However HIF1, composed of the HIF1α isoform and the aryl hydrocarbon receptor nuclear translocator (ARNT) beta subunit, is thought to be the foremost regulator of the hypoxic cellular response (Semenza, 1998).

1.3.2.1 Hypoxic inducible factors in normoxia

Under normoxic conditions, and therefore in the presence of sufficient oxygen, the von Hippel-Lindau (VHL) E3 ubiquitin ligase complex tags the alpha subunit of HIF for proteosomal degradation (Huang *et al.*, 1998). Degradation of the alpha subunit occurs rapidly within approximately five minutes in normoxic conditions (Salceda and Caro, 1997). This, in effect, deactivates the action of HIF, as its constituent alpha and beta subunits need to combine to produce an active HIF hetrodimer complex (Huang *et al.*, 1998). The proteosomal mediated decomposition of HIFα occurs promptly subsequent to a requisite, post-translational hydroxylation at two HIFα proline residues by so-called prolyl hydroxylases (PHs) (Bruick and McKnight, 2001). The oxygen required enzymatic hydroxylation at Pro 402 (Yu *et al.*, 2001) and Pro 564 (Masson *et al.*, 2001), in the oxygen dependent degradation domain (ODDD) of HIFα, provide an interface for VHL, resulting in the eventual destruction of the alpha subunit. Another inhibitory hydroxylase enzyme, factor inhibiting HIF (FIH), regulates the recruitment of certain transcriptional co-activators by way of asparaginyl hydroxylation. In the presence of adequate amounts of available oxygen, hydroxylation of asparagine 803 on the HIFα subunit takes place. In this way FIH effectively blocks co-activator support and thereby inhibits selected translational activity of the HIF complex (Mahon *et al.*, 2001). This partial impairment of the transcriptional capability of the HIF dimer is thought to be caused

by preventing the co-activator p300 from binding to HIFα (Lando *et al.*, 2002). For that reason, p300 dependent HIFα transcription is impaired in normoxia.

So, HIF itself does not directly detect changes in pO_2. It is unclear though, whether FIH or the PHs themselves possess a true oxygen sensing ability either (Semenza, 2001). One theory suggests that the PHs and FIH are indeed genuine oxygen sensors and can act alone in detecting decreases in oxygen tension. However, it seems clear that ROS play an essential role in oxygen sensing, and it has been demonstrated that ROS are an essential component in the stabilization of HIF-1 in hypoxia (Brunelle *et al.*, 2005; Chandel *et al.*, 2000). It should also be noted that HIF can be controlled by factors other than the hydroxylases. Phosphorylation of HIF1α by MAPK is thought to enhance its transactivation but not its stabilization or DNA binding ability (Hur *et al.*, 2001). Instead MAPK is said to regulate HIF by effecting the p300 co-activator (Sang *et al.*, 2003). Although the oxygen sensing mechanisms of HIF are not fully understood, it is obvious that the alpha subunit of HIF becomes destabilized and promptly destroyed during normoxia thereby abolishing any of its potential effects.

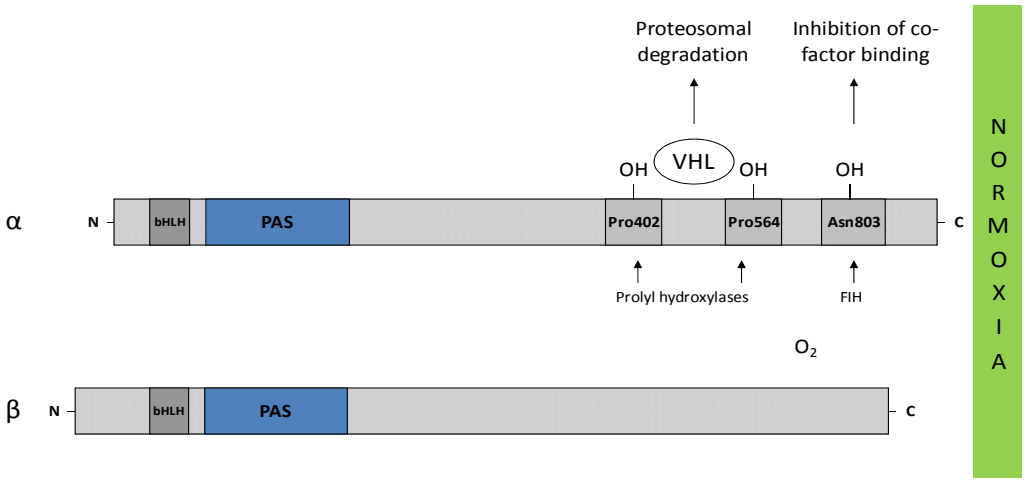

Figure 1.1 Amino acid sequence of the α and β subunits of HIF1 during normoxia. This demonstrates proteosomal degradation and inhibition of co-factor binding in the presence of oxygen.

In hypoxia, the decreased availability of molecular oxygen greatly diminishes HIFα hydroxylation and thus the ubiquinated proportion of the HIFα subunit decreases markedly (Sutter *et al.*, 2000). This leads to the rapid stabilization and accumulation of the alpha subunit (Kallio *et al.*, 1997). HIF1α can then subsequently translocate into the nucleus, where it is able to dimerize with the beta subunit and attain a new conformational state (Kallio *et al.*, 1997). The HIF hetrodimer is now able to interact with hypoxia response elements (HREs) in the regulatory regions of target genes and affect suitable adaptive modifications to the cell (Semenza *et al.*, 1991).

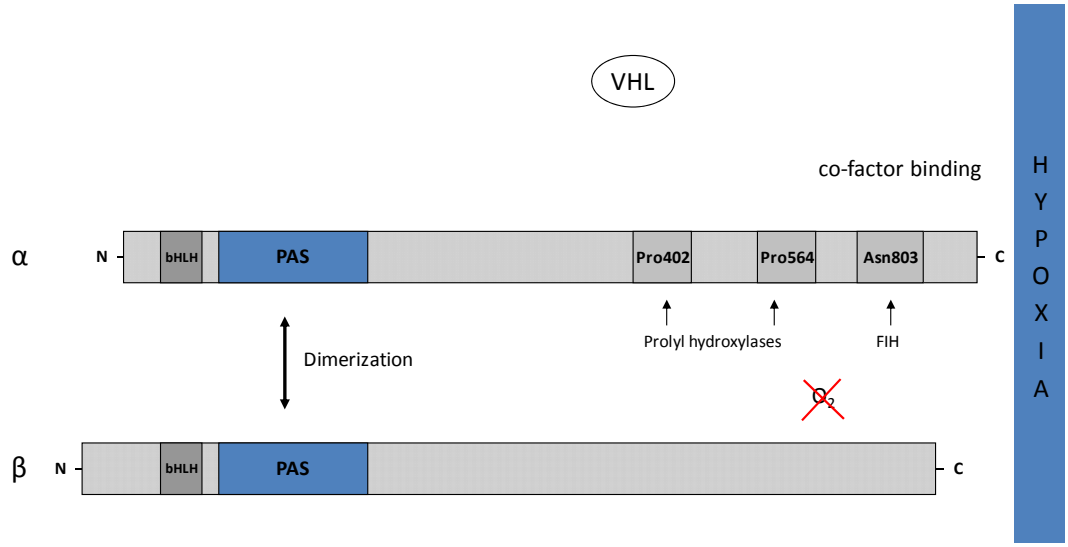

Figure 1.2 Amino acid sequence of the α and β subunits of HIF1 during hypoxia. This demonstrates dimerization and co-factor binding in the absence of oxygen. FIH (factor inhibiting HIF).

1.3.2.3 Oxygen independent regulation of HIF

HIFs interact with a multitude of angiogenic and metabolic genes in a potent and rapid fashion. This powerful resource has been cunningly employed by many cells with the intention of using HIFs remodelling capabilities, albeit in an oxygen independent manner (Richard *et al.*, 2000). Of particular interest here is the fact that growth factors and cytokines

influence HIF activity in non-hypoxic conditions. Insulin like growth factors have been shown to control HIF activity (Feldser *et al.*, 1999), and HIF1α has been shown to require the activity of PI3K/Akt pathway (Gort *et al.*, 2006) and NFkB for its expression (Belaiba *et al.*, 2007). This does seem to be cell line specific however (Arsham *et al.*, 2002). In a recent experiment, during skeletal muscle differentiation of C2C12 myoblasts grown in normoxic conditions, HIF1α was knocked down using siRNA technology. Researchers showed that HIF1α expression increased upon myogenic induction and that HIF1α is required for C2C12 myogenesis *in vitro* (Ono *et al.*, 2006). Importantly, it has also been shown that, unlike in most other cell lines, the effects of hypoxia on myogenesis of C2C12 cells operates independently of HIF1 (Yun *et al.*, 2005).

1.3.2.4 HIF in cancer and ischemia

It is not unexpected that HIFs have been implicated in a range of pathophysiological conditions in which hypoxia and ischemia play a part. HIFs play an integral role in tumour progression, and there is a strong positive association between HIF1α expression in cancerous tumours and patient mortality (Vaupel and Mayer, 2007; Harris, 2002). The over-expression of HIFs in cancer is probably a consequence of the increased hypoxia/ischemia in the central portions of poorly vascularized tumours. Consequently, hypoxic signalling in cancer leads to increased angiogenesis and tumour progression (Pouyssegur *et al.*, 2006). Knockdown of the HIF1α isoform of the alpha subunit of HIF has shown reduced tumour sizes and increased sensitivity of tumour cells to chemotherapeutic reagents (Gort *et al.*, 2006). These relationships are complex however, as the reduced nutrients and growth factors (as might be expected in ischemic tumours) might have divergent effects on the induction of HIF in hypoxic tumours (Gort *et al.*, 2006). Besides tumours, HIF is involved in myocardial and cerebral ischemic insults (Semenza, 2000) and has also been connected with vascular

endothelial growth factor (VEGF) expression in retinal ischemia (Ozaki *et al.*, 1999). By decreasing HIF expression in cancer or increasing it in other ischemic conditions, HIF therapy is a potentially valuable clinical target (Lee *et al.*, 2007).

1.4 Skeletal muscle: Development and the activation of satellite cells in response to damage

Mammalian skeletal muscle exhibits an incredible potential to adapt to external stresses. This adaptive ability includes the capacity to endure unwelcome reductions in oxygen availability via several types of muscle tissue alterations (Hoppeler and Vogt, 2001). Indeed, adult skeletal muscle displays an extraordinary capability to regenerate following chronic ischemic stresses (Aranguren *et al.*, 2008; Heemskerk *et al.*, 2007; Scholz *et al.*, 2003). However, this ability of skeletal muscle to regenerate seems to be reduced with aging (Grounds, 1998). Ischemic muscle damage is thought to trigger the recruitment of myogenic satellite cells which rapidly proliferate before undergoing differentiation in response to certain cues. This ultimately leads to regeneration of damaged myofibres (Aranguren *et al.*, 2008; Hawke and Garry, 2001).

1.4.1 Skeletal muscle structure and characteristics

Skeletal muscle is made up of several elongated, multinucleated fibres, each of which extends over the entire length of the muscle. Each muscle fibre is surrounded entirely by a sarcolemmal membrane which fuses with tendon fibres and connects the muscle to bone (Guyton, 2006). Myofibres are individually innervated, and the nature of this innervation during myogenesis defines its contractile properties. Also, adult skeletal muscle comprises a combination of different myofibre types with distinct physiological properties. Hence, the type of neuronal support and the ratio of different fibre types in a muscle determine its

functional and physiological characteristics (Charge and Rudnicki, 2004). Organized skeletal muscle is comprised of numerous bundles of muscle fibres, packaged together into what are known as muscle fasciculi. Contained within each muscle fibre are hundreds or even thousands of myofibrils composed of polymerized protein units known myosin and actin filaments. Together, these filaments make up the contractile apparatus of the muscle (Guyton, 2006).

1.4.1.1 The mechanics of skeletal muscle contraction

Large numbers of mitochondria are present within the intracellular matrix of a muscle fibre, wherein the myofibrils are suspended. These mitochondria provide the energy for muscle contraction, in the form of high energy ATP (Guyton, 2006). Muscle shortening, or contraction, comes about subsequent to a neuronal stimulus, by a mechanism known as the 'sliding filament theory'. The heads of myosin molecules in a myosin filament attach to a flanking actin filament to form 'cross-bridges'. A cyclical detaching and successive reforming of cross-bridges ever further up the actin filament causes the myosin chain to 'walk' up the actin chain which results in shortening (Huxley, 2000; Rassier *et al.*, 1999). A maximum contraction is believed to occur when there is greatest overlap between actin filaments and myosin cross-bridges (Rassier *et al.*, 1999).

1.4.2 Myogenic satellite cells

Residing in distinct pockets situated between the basal lamina and sarcolemma of muscle fibres exist a population of quiescent, undifferentiated myogenic cells (Hawke and Garry, 2001; Seale *et al.*, 2001). These cells are defined by stringent morphological criteria and are known as satellite cells, named so owing to their relative position in the muscle fibre (Mauro, 1961). Stem cells are unspecialized cells capable of self-renewal through division as well as

growth, prior to differentiation into specialized cell types. Stem cells present during the first few divisions of the fertilized oocyte are able to form placental trophobalsts and embryonic cell types. These cells are said to be totipotent. Pluripotent cells, descendants of these totipotent cells, are able to differentiate into almost any cells that arise from the three germ layers. Most mature tissue has what are known as adult stem cells which are said to be multipotent, cells capable of differentiating down only a few limited cell lineages, or unipotent/committed progenitor cells that are capable of differentiating into one cell type only (Alison *et al.*, 2002).

C2C12 primary myoblasts have shown the potential to differentiate into adipose-like cells (Teboul *et al.*, 1995) and osteoblasts (Katagiri *et al.*, 1994) when prompted with certain cues *in vitro*. In fact, these recent experiments indicate that myogenic progenitor cells possess many of the characteristics of multipotent stem cells. Actually, it seems as though adult muscle satellite cells may have multipotential properties, something that may be of great clinical significance in the future (Hawke and Garry, 2001; Seale *et al.*, 2001).

1.4.3 Satellite cell driven muscle regeneration in response to injury

Following chronic ischemic stress, skeletal muscle is able to regenerate (Aranguren *et al.*, 2008; Heemskerk *et al.*, 2007; Scholz *et al.*, 2003). However, chronic exposure to low oxygen tension leads to dramatic decreases in muscle fibre mass and size (Hoppeler and Vogt, 2001). It is believed that satellite cells abandon their quiescent state and begin proliferating in response to myotrauma. Furthermore, it has been shown that satellite cells grown in culture can form new muscle fibres and re-establish the satellite cell population upon transplantation into damaged tissue (Seale *et al.*, 2001). When a muscle becomes injured, myoblasts (proliferating satellite cells) migrate to the injured area to begin the

process of repair (Charge and Rudnicki, 2004). This system of restoration is regulated by a family of bHLH transcription factors know as myogenic regulatory factors (MRFs) (Hawke and Garry, 2001). These factors up-regulate the expression of genes required for myogenesis and include myoD, myf5, MRF4 and myogenin (Olson, 1990). First, the expression of the MRFs myf5 and myoD increase and eventually cause myoblasts to commit to myogenic differentiation. Thereafter, the MRFs myogenin and MRF4 become up-regulated and facilitate the process of terminal muscle differentiation and muscle fibre development (Charge and Rudnicki, 2004; Sabourin *et al.*, 1999).

Following myotrauma, the inflammatory response and its associated cytokines, in addition to a shifting profile of growth factors, play an essential part in muscle development (Charge and Rudnicki, 2004). Hepatocyte growth factor (HGF) is an essential mitogen that increases proliferation and attracts satellite cells to the injured area in a chemotatic manner (Miller *et al.*, 2000). Expression of the HGF receptor (Anastasi *et al.*, 1997) and a secondary chemotactic effect (Suzuki *et al.*, 2000), in response to HGF stimulation, has been demonstrated for C2C12 cells. Fibroblast growth factors (FGFs), in particular FGF-6 in skeletal muscle (Floss *et al.*, 1997), play an important role in muscle regeneration by increasing satellite cell proliferation in response to injury (Charge and Rudnicki, 2004). Although a comprehensive description of their roles in muscle regeneration remain unclear, it has also been shown that, in addition to their proliferative function, expression of both FGFs and HGFs during injury suppress satellite cell differentiation (Charge and Rudnicki, 2004). Proliferation precedes differentiation and the fusion of myoblasts into myotubes. The latter is accomplished by the paracrine/autocrine regulation of the insulin like growth factors (IGFs) (Charge and Rudnicki, 2004). It has been shown that a decreased expression of growth factors (such as basic fibroblast growth factor [bFGF] and transforming growth factor [TGF-

β]), but an increased expression of IGF-I and IGF-II by myoblasts results in the eventual differentiation and ensuing fusion of myotubes (Yoshiko *et al.*, 2002; Charge and Rudnicki, 2004). In summary, it is clear that myogenic precursors, regulated by various mitogenic factors, can respond to injury in an ordered fashion to cause migration, proliferation and eventual differentiation so as to replace damaged muscle fibres.

1.4.4 Muscle differentiation *in vitro*: C2C12 murine myogenic cell line

C2C12 murine myogenic cell line models are popular for studying myogenesis *in vitro*, and have been used in the study of ischemic microenvironments in various unrelated investigations (Loos *et al.*, 2008; Lacerda *et al.*, 2006; Yun *et al.*, 2005). Although generally considered a committed progenitor cell line, *in vitro* studies have demonstrated the multipotent potential of C2C12 myoblasts (Katagiri *et al.*, 1994; Teboul *et al.*, 1995). Using muscle satellite cells, muscle differentiation can be replicated *in vitro* (Hawke and Garry, 2001). Myoblasts grown in normal cell culture conditions proliferate without differentiating, and myoblast differentiation will only take place when the profile of growth factors in culture medium changes where the decreased expression of growth factors results in myoblasts exiting the cell cycle. Although this procedure occurs with a dearth of growth factor expression, a concomitant increase in IGF expression is needed for differentiation to proceed (Yoshiko *et al.*, 2002). This microenvironment is commonly achieved by decreasing the concentration of serum in culture media, although left to themselves the cells would eventually regulate their own growth factor expression profile and begin to differentiate (Yoshiko *et al.*, 2002).

1.5 Phosphoinositide 3-kinase (PI3K) signalling

The PI3Ks are a family of intracellular lipid kinase enzymes that play a pivotal role in, amongst other things, metabolism, growth and survival. Hitherto, the PI3K signalling pathway has proven to be one of the most diverse yet significant signalling systems in the cell (Cantley, 2002). PI3K enzymes generate lipid second messengers by catalysing the phosphorylation of phosphoinositides and phosphatidylinositol, basic building blocks of lipid membranes in mammalian cells, at their 3'-hydroxy groups (Cantrell, 2001). By binding to these newly formed lipid products, intracellular proteins accumulate in localized regions at the plasma membrane. Here, their activation is made more thermodynamically favourable, and various downstream signalling cascades can therefore become primed. Due to its intimate association with cellular metabolism and survival, it is not surprising that abnormally altered expression or mutations in this pathway have been implicated in a wide range of human cancers (Luo *et al.*, 2003; Shaw and Cantley, 2006).

1.5.1 Classification of PI3K members

The PI3K family is divided into three classes (I, II and III) based on their protein domain structure, substrate preference and associated regulatory subunits (Foster *et al.*, 2003). Of the three classes, class I members are the best studied and most well understood (Foster *et al.*, 2003). This is most likely due to the fact that they represent an important link between external stimuli and downstream effectors. Class I members are hetrodimers made up of a p110 catalytic subunit accompanied by a non-catalytic, regulatory subunit. Four isoforms of the p110 subunit have so far been described, and it is through their catalytic activity that the generation of phosphatidylinositol-3,4,5-trisphosphate (PIP_3) from phosphatidylinositol-4,5-bisphosphate (PIP_2), phosphatidylinositol-4-phosphate (PIP) and phosphatidylinositol (PI) is instituted (Cantrell, 2001). Class I members can be divided into two classes (class IA and

class IB) which are further subdivided based on the sequence similarity of their catalytic subunits. Class IA consists of three isoforms (p110α, p110β and p110δ) encoded by three separate genes, whereas class IB consists of only the p110γ isoform (Foster *et al.*, 2003). Class I PI3Ks have been implicated in a broad array of cellular processes and have been shown to participate in the regulation of cell migration, cell metabolism, survival, growth and proliferation (Foster *et al.*, 2003). Although class I PI3Ks were originally thought to act exclusively at the cell membrane, some reports have indicated that they may act at locations other than cell membranes as well (Rameh and Cantley, 1999). To date, class II and III PI3Ks have not been as extensively studied. Class II are the least well understood of the three PI3K classes and many extracellular signal events have been shown to activate class II PI3K activity, a clear mechanism of action is not yet known (Foster *et al.*, 2003; Engelman *et al.*, 2006). On the other hand, more is known about class III than class II PI3Ks. Unlike the other classes, they are thought capable of phosphorylating phosphatidylinositol. Recent studies indicate that class III PI3Ks may be important regulators of mTOR (Nobukuni *et al.*, 2005), and are important in controlling certain aspects of cell growth as well as cellular responses to nutrient starvation (Engelman *et al.*, 2006).

1.5.2 Activation of class I PI3Ks

Class IA is a heterodimer made up of a regulatory p85 subunit and a catalytic p110 subunit. In un-stimulated cells, the p85 regulatory subunit stabilizes and suppresses the catalytic ability of the p110 subunit (Wu *et al.*, 2007). Following stimulation by extracellular signals, phosphotyrosine residues on the cytoplasmic tails of activated RTKs expose binding sites for the p85 subunit. This is mediated through Src homology 2 (SH2) domains on adapter proteins or by direct binding to the two SH2 domains of the p85 subunit itself (Cantrell, 2001). Once bound to SH2 domains of adapters (such as those from the IRS family) or to RTKs, the

suppression of p110's catalytic ability is released and PIP_3 lipid second messengers can be generated by the catalysed phosphorylation of the D3 inositol ring of plasma membrane lipids in the inner leaflet of the plasma membrane bilayer. In this way, pools of second messenger lipids are created at the cell membrane. PI3Ks can also become activated through other signalling cascades by recruitment and transphosphorylation of adapter proteins and stimulation of integrin dependent cell adhesion (Cantley, 2002). Scaffolding proteins such as Grb2-associated binder-1 (Gab1) are recruited to the plasma membrane in response to specific signalling events. Here, their phosphorylation regulates binding to p85 (Rocchi *et al.*, 1998). In contrast to class IA, class IB PI3Ks do not have p85 regulatory subunits and are exclusively activated by heterotrimeric G-protein-coupled receptor (GPCR) stimulation. This occurs by binding to Gβγ (guanine nucleotide binding protein βγ) (Engelman *et al.*, 2006). In addition, all class I PI3Ks become reactive towards the small GTPase Ras by direct interface with p110. This interaction is believed to simulate PI3K activity even further (Cantrell, 2001).

1.5.3 Activation of PI3K effectors

The PIP_3 lipids generated upon activation of class I PI3Ks are able to interact with specialized phosphoinositide-binding domains present on certain protein effectors. Many of these proteins, including Akt and 3-phosphoinositide-dependent kinase (PDK1), adapter proteins (e.g. Gab-1) and small GTPases (e.g. Ras), contain a consensus, pleckstrin-homology (PH) domain (Vanhaesebroeck *et al.*, 2001). These proteins are able to associate directly with PIP_2 or PIP_3 at the cell membrane. As a result of high affinity binding to these newly formed PIP lipid products, intracellular proteins containing a PH domain can therefore accumulate in localized regions at the plasma membrane. Here, their activation is made more

thermodynamically favourable, and various downstream signalling cascades can therefore become primed (Vanhaesebroeck *et al.*, 2001).

1.5.4 Endogenous and artificial inactivation of the PI3K pathway

PI3K activation is contradicted naturally by phosphatases within the cell or artificially by means of experimental supplementation with specific inhibitors. These deactivators and negative regulators of PI3K are important clinical targets or potential therapeutic agents in many cancers, and are also utilized in the research into PI3K signalling networks.

1.5.4.1 PI3K phosphatases

Multiple, endogenous inositol lipid phosphatases exist and are involved in countering PI3K signalling through dephosphorylation of their lipid second messengers (Vanhaesebroeck *et al.*, 2001). Phosphatase and tensin homologue deleted on chromosome ten (PTEN) is an important phosphoinositide 3-phosphatase and tumor suppressor that has been incriminated in many mammalian cancers (Cantley and Neel, 1999). PTEN de-phosphorylates the lipid second messenger PIP_3, and in so doing it negatively regulates PI3K signalling (Vanhaesebroeck *et al.*, 2001). The phosphatase activity of PTEN rapidly diminishes the membrane recruitment and localization of Akt and its co-activators resulting in decreased flow through the PI3K/Akt pathway (Wu *et al.*, 1998). Having said this, PTEN regulation and function is still incompletely understood at present (Vanhaesebroeck *et al.*, 2001). Another important negative regulator of PI3K, src homology 2-containing inositol 5′-phosphatase (SHIP), belongs to a different family of PI-phosphatases, specifically, the type II 5-Phosphatases. Akin to PTEN, type II 5-phosphatases are able to de-phosphorylate PIP_3, alternatively they can also hydrolyse PIP_2 (Vanhaesebroeck *et al.*, 2001). More than one SHIP has thus far been cloned, and together these SHIPs are believed to be primary PI3K

phosphatases *in vivo* (Krystal *et al.*, 1999). Again therefore, similar to PTEN, SHIPs have the ability to oppose PI3K/Akt signalling.

1.5.4.2 PI3K inhibitors

Two of the most widely used PI3K inhibitors are wortmannin and LY294002. Both are low molecular weight, cell-permeable complexes that are relatively specific PI3K inhibitors in low concentrations (Vanhaesebroeck *et al.*, 2001). Wortmannin is a fungal metabolite that acts as a powerful inhibitor of PI3K by binding irreversibly to its p110 catalytic subunit. It is thought to have an IC_{50} of approximately 3 nM (Ui *et al.*, 1995). Judicious use of wortmannin is often advised as it is fairly unstable in tissue culture media, with a half-life of around only 10 min in most cases (Holleran *et al.*, 2003). Even though the biological effect of wortmannin persists for up to a few hours, there is little, if any, wortmannin present after about one hour of incubation in culture medium (Holleran *et al.*, 2003). Although it is a less potent inhibitor than wortmannin, LY294002 is an attractive option as a PI3K inhibitor due to its extended half-life in culture conditions. LY294002 can inhibit purified PI3K with an IC_{50} of ~1.4 μM (Vlahos *et al.*, 1994). LY294002 functions as a competitive binder of ATP, and it has been demonstrated to inhibit PI3K dependent signalling processes, such as the activation of Akt via phosphorylation (Vanhaesebroeck *et al.*, 2001).

1.5.5 PI3K and the serine/threonine kinase Akt

Akt (also known as PKB or Rac) is a family of serine/threonine protein kinases that participate in many key signalling pathways concerning cell survival (Song *et al.*, 2005) as well as several pathways relating to growth and metabolism (Yang *et al.*, 2004). Three mammalian Akt isoforms are known, all of which are downstream effectors of the class I PI3Ks, intracellular lipid kinases that are activated following interaction with ligand-bound

growth factor RTKs or GPCRs. PI3K lipid second messengers located on the inner leaflet of the cell membrane are able to interact with the N-terminal PH domains of Akt with high affinity, thereby providing any Akt molecules in the vicinity with docking sites at the plasma membrane. This results in the recruitment and ensuing conformational change of passing Akt molecules. This, as well as the consequent localization with other PH domain containing protein molecules required for their activation, results in a greatly enhanced probability of their becoming activated (Vanhaesebroeck *et al.*, 2001).

Membrane bound Akt becomes activated only after dual phosphorylation by PDK1 and what is now known to be the mTOR in complex with rictor and SIN1, also known as rictor-mTORC2 (mammalian target of rapamycin) (Sarbassov *et al.*, 2005b). Phosphorylation by both of these protein kinases is thought to be mandatory for the complete activation of Akt and its downstream targets. Following activation of PI3K, both rictor-mTORC and Akt are recruited to the plasma membrane though binding of their PH domains. Here they are spatially localized, and rictor-mTORC phosphorylates Akt at the Ser473 position in the hydrophobic motif of its C-terminal regulatory domain (Sarbassov *et al.*, 2005b). After this, PDK1 leads to the full activation of Akt by means of a second phosphorylation event that takes place at the Thr308 motif within the activation loop in the kinase domain (Stephens *et al.*, 1998). Alternatively, a decrease in the recruitment of Akt to the plasma membrane can be attained by the intracellular de-phosphorylation of PIP_3 by PTEN, the major phosphatase inhibiting PI3K generation of lipid second messengers. On the other hand, Akt phosphorylation is also controlled directly by a family of protein phosphatases. PH domain leucine-rich repeat protein phosphatase (PHLPP) causes de-phosphorylation of Ser473 on the hydrophobic motif of Akt (Gao *et al.*, 2005). This markedly reduces downstream, Akt-dependent functioning.

Akt is a major regulator of cell survival (discussed in section 1.6) as well as the physiological processes concerned with growth and development (Yang *et al.*, 2004). Subsequent to its dual phosphorylation and activation, Akt disassociates from the cellular cytoskeleton and moves into the cytosol and nucleus. Here, by virtue of its kinase activity, phospho-Akt manages the activity of many cytosolic and nuclear proteins and is known to have a hand in the control of cell metabolism (Cross *et al.*, 1995), growth (Potter *et al.*, 2002) and angiogenesis (Shiojima and Walsh, 2002) among other things.

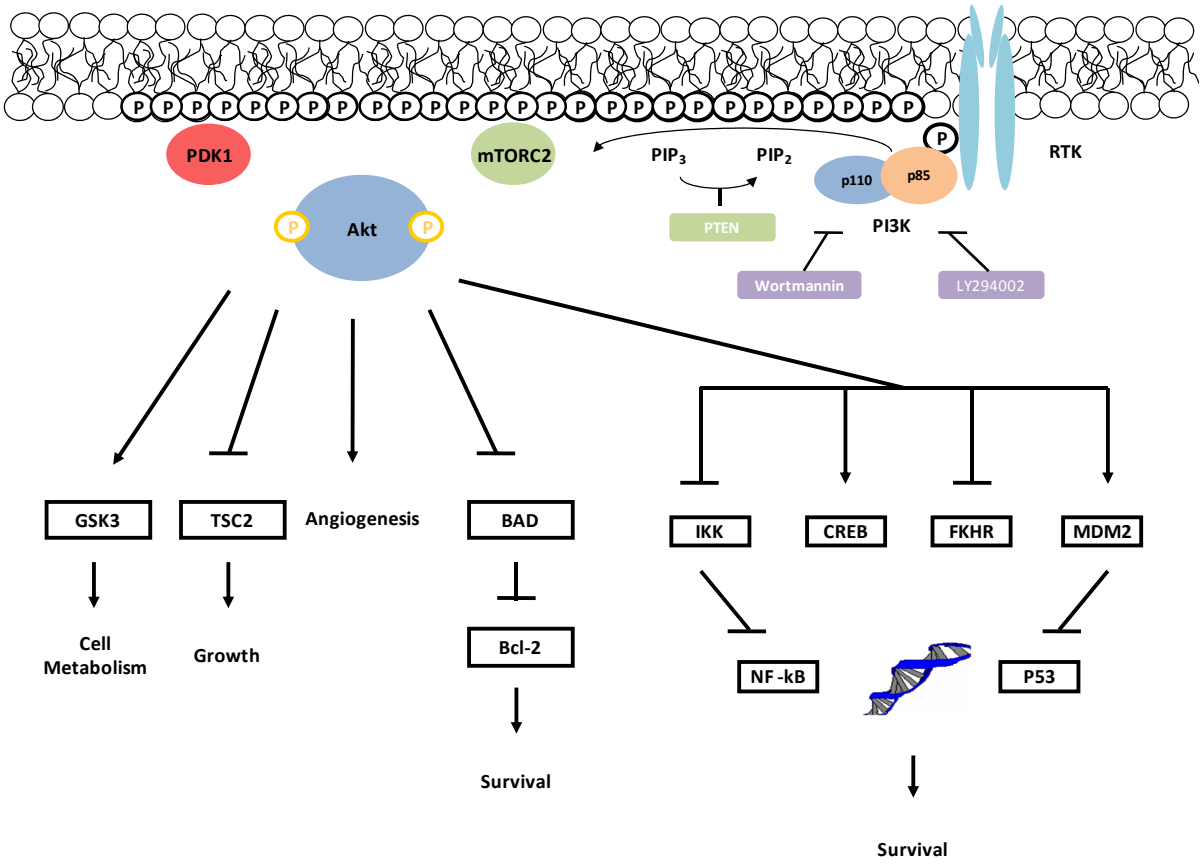

Figure 1.3 Schematic of the PI3K/Akt pathway. Activation and inhibition of PI3K, Akt and downstream effectors as described in detail in the text. Briefly, RTK activation recruits PI3K to the cell membrane where it catalyses the generation of lipid second messengers on the inner leaflet of the plasma membrane, and thereby creating docking sites for Akt and it's co-activators. Akt disassociates from the membrane and activates downstream effectors. Adapted from (Song *et al.*, 2005).

1.5.6 PI3K/Akt signalling in hypoxia and ischemia

Akt is a major controller of cell survival in many cells. Akt functions downstream of PI3K, and its induction and activation have been reported to be important to the survival of many cell types during hypoxia and ischemia (Barry *et al.*, 2007; Fukunaga and Kawano, 2003).

1.5.6.1 PI3K/Akt in hypoxia

Hypoxia increases Akt phosphorylation in many cell lines including adventitial fibroblasts (Gerasimovskaya *et al.*, 2005), PC12 cells (Beitner-Johnson *et al.*, 2001), human proximal tubular epithelial cells (HK-2), human embryonic kidney fibroblasts (HEK293) and rat L6 myotubes (Barry *et al.*, 2007). These increases in phospho-Akt levels have been shown to promote the viability of cells during hypoxic conditions (Barry *et al.*, 2007). Although understood to be a common response in hypoxia, activation of the PI3K/Akt pathway is not observed in all cell lines. For example, increased levels of phospho-Akt were not induced during hypoxia, in a study examining a series of breast cancer cell lines representing the different genetic stages seen during breast cancer development. No changes in Akt activation was seen for either short or longer hypoxic exposures in any of these breast cancer cell lines, when incubated in hypoxia in media containing serum (Blancher *et al.*, 2001). Hypoxia had no effect on Akt phosphorylation in PC-3, human prostate cancer cells after 8 hrs in serum free media either (Zhong *et al.*, 2000). Some authors have shown PI3K/Akt pathway activation or phospho-Akt levels to actually be decreased by hypoxia in some cells. Significantly reduced levels of phospho-Akt were found for a vascular smooth muscle cell line (A7r5) and COS-7 cells when incubated in glucose and serum free medium in acute hypoxia, for instance. This was accompanied by a correlated, increased apoptosis for these cell lines, when incubated in similar settings (Loberg *et al.*, 2002). Elsewhere, hypoxia was also shown to cause phospho-Akt levels to diminish in opossum kidney cells in a time

dependent manner (Kwon *et al.*, 2006). Interestingly, this occurred only when cells were exposed to hypoxia alone, in the absence of a re-oxygenation step. Hypoxia caused a similar decrease in Akt phosphorylation at both the Ser473 and the Thr308 positions in neonatal rat cardiomyocytes. Here too, reactivation of Akt was only detected after re-oxygenation (Shao *et al.*, 2006). Notably, in a cell line presenting with a constitutively active PI3K/Akt pathway in normoxia, hypoxia leads to decreased PI3K/Akt activation as well (Mottet *et al.*, 2003). The PI3K/Akt pathway activation in the HepG2 human hepatoma cell line declined after five hours of hypoxia, and it was almost completely inactivated after sixteen hours of exposure. This trend was observed both in the presence or absence of serum. In another report, 3T3 fibroblasts seemed to also show decreased phospho-Akt levels in response to hypoxia (Laughner *et al.*, 2001).

PI3K activity and Akt phosphorylation are also important for HIF1α expression in the hypoxic regions of tumours (Gort *et al.*, 2006). This is correlated with the transcription of genes aiding in cell survival. Indeed, Akt and associated HIF-1 have been shown to be predictors of clinical outcome in some cancers (Gort *et al.*, 2006).

1.5.6.2 PI3K/Akt in ischemia

Both amplified and reduced Akt phosphorylation levels have been described by experiments investigating ischemia. Different cell lines and diverse experimental procedures and conditions are probably accountable, in part, for these differential analyses. Many possible mechanisms have been suggested to regulate flux through the PI3K/Akt pathway during ischemia. Some of these are expounded upon here.

It has been postulated that increased activity of the PI3K/Akt pathway, found in ischemic skeletal muscle *in vivo,* is associated with enhanced levels of VEGF (Germani *et al.*, 2003); (Takahashi *et al.*, 2002). Accordingly, this enhanced expression of VEGF is known to increase cell survival during ischemia. It has also been demonstrated that JNK was shown to reactivate Akt after hypoxia *in vitro* and ischemia-reperfusion *in vivo* (Shao *et al.*, 2006). It is believed that this reactivation is thought to aid in cell survival and decrease the harmful effects of injury. This sentiment is echoed by a study showing the necessity of PDK1, one of the co-activators of Akt, in ischemic preconditioning (Budas *et al.*, 2006).

An interesting report showed an increase in phospho-Akt levels after global cerebral ischemia in a rat model (Jin *et al.*, 2000). While elsewhere, a transient focal cerebral ischemia in mice showed that constitutively expressed phospho-Akt levels decreased after an ischemic event (Noshita *et al.*, 2003). This state persisted till well after reperfusion had occurred. Another investigation, using cultured cerebral cortical astrocytes, showed variable levels of Akt phosphorylation, above and below control levels, throughout ischemic incubation (Jiang *et al.*, 2002). However, a relative increase in phospho-Akt was observed over time. Studies have shown that ischemic preconditioning (Tsang *et al.*, 2005) and transient ischemia (Matsui *et al.*, 2001) in the heart lead to increase Akt activation. Others have shown that apoptosis promoted in ischemia reperfusion of the rat heart can be attributed, in part, to decreased levels of Akt operating downstream of PI3K (Takada *et al.*, 2004). In another recent study it was discovered, by measuring the phosphorylation of one of its substrates, that Akt-1 activation was significantly decreased in hypertrophied ischemic hearts (Barillas *et al.*, 2007).

In a novel pathway, investigators proposed an ER stress-induced apoptosis after ischemia-reperfusion, in human choriocarcinoma cells. Here, levels of activated Akt and, to a lesser

degree, levels of total Akt protein expression were decreased after simulated ischemia (Yung *et al.*, 2007).

1.5.7 PI3K/Akt and the C2C12 murine myogenic cell line

PI3K is important for the proliferation, differentiation and survival in differentiating myoblasts (Jiang *et al.*, 1998). It is already known that activation of PI3K as well as its main downstream effector Akt is necessary for differentiation to occur (Jiang *et al.*, 1999; Wilson *et al.*, 2004), and that PI3K inhibitors such as Wortmannin and LY294002 are able to block myogenesis (Kaliman *et al.*, 1996). In addition, it was recently shown that during differentiation of skeletal muscle myoblasts, and in conditions favourable to muscle differentiation, PI3K lipids become greatly accumulated at the plasma membrane in an unconventional manner (Mandl *et al.*, 2007). These lipids are thought to act as second messengers relaying communication to the major signalling molecule downstream of PI3K, namely Akt. In fact, it has been demonstrated that the induction of Akt is greatly enhanced as myoblasts exit the cell cycle and begin to differentiate (Fujio *et al.*, 1999). Akt activation is increased, and this has been shown to be sustained in terminal differentiated cells, even after serum re-stimulation (Fujio *et al.*, 1999; Rommel *et al.*, 1999). Akt activity is complex and differentially regulated however, with different isoforms and phosphorylation sites having different levels of activation during different stages of myogenesis. It is believed that this increase in PI3K/Akt activation is mainly responsible for the relatively apoptotic resistant phenotype of differentiated C2C12 myotubes (Fujio *et al.*, 1999).

Increased expression of PI3K occurs during the serum starved conditions usually used to induce differentiation, and serum withdrawal from myoblasts causes PI3K activation and accumulation of lipids in an unconventional manner (Mandl *et al.*, 2007). This may seem

counter intuitive, as growth factors are known to promote proliferation and inhibit differentiation in myoblasts (Coolican *et al.*, 1997). Still, unlike in most cell lines, serum starvation promotes the induction and activation of Akt during myogenesis, in a process facilitated by PI3K. This fact is supported by an investigation showing that the constitutive expression of an Akt isoform enhances myotube formation, even when PI3K activity had been inhibited (Jiang *et al.*, 1999). The activation of PI3K during differentiation is now widely understood to be due to an increased autocrine expression of insulin like growth factor-II (IGF-II) operating through the IGF-I receptor (Bach *et al.*, 1995). Transfer of C2C12s to a low-serum environment causes a marked increase in the expression of the IGF-II gene which is sustained during and after terminal differentiation of myoblasts (Yoshiko *et al.*, 2002). In the presence of insulin, IGF-I or IGF-II in serum free medium in cell culture, myoblasts have been shown to differentiate and maintain their apoptosis resistant phenotype (Bach *et al.*, 1995; Conejo and Lorenzo, 2001). This lends credence to the observation that decreased expression of growth factors and an increased autocrine/paracrine expression of IGF-II, acting through the PI3K/Akt pathway, is what causes myoblast to differentiate and gives them an apoptotic resistant phenotype (Florini *et al.*, 1991; Stewart and Rotwein, 1996). The precise mechanisms by which this occurs are not yet known.

1.6 Cell death

As our understanding of the processes coordinating regulated cell death develops, it is becoming increasingly obvious that most cellular death is governed by a strict system of controls and that the different forms of regulated cell death are dynamically linked to one another. Cell death takes place is an extremely complicated milieu, and current evidence suggests that it varies along a spectrum of death styles (Assuncao Guimaraes and Linden, 2004). While ischemic cell death is believed to be caused mainly by changes in the cellular

environment (discussed in section 1.2.1), the precise role of hypoxia in the development of cellular death remains controversial. The PI3K/Akt signalling pathway is concerned with protection against the apoptotic mode of cellular death (Vanhaesebroeck *et al.*, 2001). It has also been reported to play a role in cell survival during hypoxia and ischemia (discussed in section 1.5.6.1). Alternatively, it has been demonstrated that, together, hypoxia and acidosis can lead to a coordinated, programmed cell death response in some cells (Gottlieb *et al.*, 1995; Webster *et al.*, 2005).

1.6.1 Précis of apoptosis regulation

Apoptosis is an essential, genetically controlled system of catabolic processes involved in the confined dismantlement and removal of cells under various circumstances. As opposed to the cellular swelling and eventual lyses seen during necrosis, the apoptotic cell keeps its membrane intact while the cellular contents and nuclear chromatin condenses (pyknosis) before becoming marginalized (Afford and Randhawa, 2000). The apoptotic cell then ruptures into membrane bound fragments called apoptotic bodies which exhibit phagocytotic ligands, such as phosphatidylserine, that are recognized by phagocyte receptors. Thereafter, a sophisticated clearance process, that culminates in phagocytosis of these bodies, takes place (Krysko *et al.*, 2006).

1.6.2 Caspases

The enzymes central to apoptosis are the caspases (***c***ysteine ***asp***art***ases***), a family of cysteine proteases that are able to catalyse the cleavage of certain vital cytoplasmic proteins. This process results in the systematic degradation of a cell in reaction to a death stimulus. Caspase precursors are expressed constitutively in cells, allowing for rapid induction of apoptosis. An intricate system of controls ensures that initiator caspase activation occurs only when

triggered to do so by appropriate pro-apoptotic stimuli (Nicholson and Thornberry, 1997) ; (Thornberry and Lazebnik, 1998). Activation of the upstream initiator caspases (2,8 & 9) sets in motion a process which causes activation of the effector caspases (3,6 & 7), by the selective cleavage of their inactive pro-caspase forms (Figure 1.4) (Nunez *et al.*, 1998). Different caspase initiators respond to distinct, separate pro-apoptotic stimuli. Initiator caspase-8, for example, reacts to apoptotic stimuli, triggered mainly in response to death receptor activation (Cohen, 1997). Caspase-9, on the other hand, promulgates the message of cell death in response to a wider variety of signals from both inside and outside the cell (Cohen, 1997). Caspase-3 is one of the key transmitters of the verdict of cell death, and is responsible wholly or in part for the proteolytic cleavage of many important proteins (Nunez *et al.*, 1998). The cleavage of pro-caspase-3, and subsequent generation of caspase-3, leads to the activation of the other effector caspases (6 & 7). The effector caspases are able to cleave specific proteins thereby activating or inactivating them. In addition to caspases, other proteins such as Bid can also be proteolytically cleaved and activated as part of the caspase pathway.

1.6.3 Apoptotic pathways

Apoptosis can become initiated by means of either an intrinsic or by an extrinsic pathway (Lawen, 2003). The extrinsic or receptor-mediated pathway is characterized by the binding of an extracellular ligand to a death receptor such as Fas (Wajant, 2002) or TNF-R1 (Chen and Goeddel, 2002), initiating the apoptotic cascade (Figure 1.4). In the Fas signalling pathway, receptor trimerization is prompted by the binding of a Fas agonist. This arrangement permits the binding of Fas associated death domain protein (FADD) to Fas, and the binding of pro-caspase-8 death effector domains (DED) to the DED of FADD. Together, these molecular associations are termed the death-inducing signalling complex (DISC). Once the DISC is in

place, transactivation of the pro-caspases occurs, initiating effector caspase cleavage and hence apoptosis. Additionally, a caspase-8 mediated activation loop can also stimulate release of mitochondrial apoptotic factors and initiate the intrinsic apoptotic pathway (Wajant, 2002); (Lawen, 2003). Agonist binding to TNF-R1 results in the release of the intracellular inhibitory protein designated silencer of death domains (SODD) which enables TNF receptor-associated death domain (TRADD) to identify and bind to the intracellular domain of TNF-R1. Bound TRADD then recruits FADD which is responsible for apoptotic signalling. Notably, under certain conditions, TNF-R1 will take part in anti-apoptotic signalling since it is the molecules that are directly accessible to TRADD, in its bound state, that will determine its action (Chen and Goeddel, 2002; Lawen, 2003).

The intrinsic apoptotic pathways are exemplified by stress conditions that lead to the release of the small heme protein cytochrome c, a constituent of the mitochondrial electron transport chain, into the cytosol (Lawen, 2003). This process is mediated by the Bcl-2 family of proteins. The pro-apoptotic members Bax, Bak and Bid are thought to facilitate cytochrome c release from the mitochondria whereas Bcl-2, an anti-apoptotic member, opposes it (Figure 1.4) (Jiang and Wang, 2004). The loss of cytochrome c results in the cessation of ATP synthesis by the mitochondria and a consequent increase in superoxide generation. Once released, cytosolic cytochrome c combines with dATP, pro-caspase-9 and the adapter protein Apoptotic Protease Activating Factor-1 (Apaf-1). Pro-caspase-9 molecules then become auto-activated, and their combination with cytochrome c and Apaf-1 is now termed an apoptosome. In turn, Caspase-9 enables the activation of effector caspases resulting in the proteolytic cleavage of proteins (Lawen, 2003; Jiang and Wang, 2004). Exposure to some apoptotic stimuli can result in the release of other caspase dependent apoptotic factors from the mitochondria as well. For instance SMAC/DIABLO disables members of the inhibitor of

apoptosis protein (IAP) family and thereby indirectly activates pro-caspase-3 and promotes enzymatic activity of caspase-3 (Chai *et al.*, 2000). More recently, it has been found that apoptotic stimuli may also cause the release of apoptosis inducing factor (AIF) and Endonuclease G, mitochondrial proteins that instigate a caspase independent cell death (Cregan *et al.*, 2004; Joza *et al.*, 2001). The Poly (ADP-ribose) polymerase-1 (PARP-1) enzyme, which undergoes distinct cleavage during caspase dependent apoptosis (Soldani and Scovassi, 2002), is thought to be a key regulator in caspase independent, AIF mediated cell death (Yu *et al.*, 2006).

1.6.4 The PI3K/Akt signalling pathway and apoptosis

PI3K-dependent protection against apoptosis is understood to come about via activation of its downstream target Akt. Akt (also known as PKB) is a family of serine/threonine protein kinases that participate in many key signalling pathways concerning cell survival (Song *et al.*, 2005) as well as several pathways relating to growth and metabolism (Yang *et al.*, 2004). Phosphorylated Akt regulates and manages the activity of downstream apoptotic effectors, directly or indirectly, through their phosphorylation. One of the major functions of Akt is to impede cytochrome c mediated apoptosis probably by inducing the phosphorylation, and thus obstructing the function of, the pro-apoptotic protein BAD. It is possible that Akt may function in an anti-apoptotic manner by influencing certain factors at a postmitochondrial level as well (Zhou *et al.*, 2000). Moreover, the regulation of various transcription factors by substrates that have been phosphorylated by Akt has also been shown (Song *et al.*, 2005). Thus, Akt can be described as a crucial regulator of cellular survival both directly and at the level of transcription factors.

Table 1.1 Some of the Akt effectors known to control cell survival. Provided herein is an incomplete list of well known Akt effectors along with their biological action.

Effector	Biological action & effect on apoptosis	Reference
Androgen receptor	Supression of AR target genes that mediate apoptosis	(Lin *et al* ., 2001)
ASK-1	Decreases ASK-1 activity via phosphorylation at Ser83	(Kim *et al* ., 2001)
BAD	14-3-3 association blocks apoptotic function	(Datta et al., 1997)
Caspase-9	Akt phosphorylation inhibits protease activity	(Cardone et al., 1998)
CREB	Results in transcription of survival genes	(Pugazhenthi et al., 2000)
FOXO family	Results in nuclear exclusion and FOXO degradation	(Reagan-Shaw and Ahmad, 2007)
GSK-3β	Reduces apoptosis through GSK-3β inhibition	(Lin *et al* ., 2007)
Hsp90	Operates as a kinase chaperone to decrease apoptosis	(Zhang *et al* ., 2005)
IKK	Activates NF-Kβ causing transcription of survival genes	(Barkett and Gilmore, 1999)
JIP-1	Akt binding blocks JNK binding which delays apoptosis	(Song and Lee, 2005)
MDM2	Causes MDM2 nuclear translocation & p53 degradation	(Mayo and Donner, 2001)
p21	Promotes survival by enhancing p21 stability	(Li *et al* ., 2002)
XIAP	Prevents XIAP degradation	(Dan *et al* ., 2004)
YAP	14-3-3 association attenuates p73-mediated apoptosis	(Basu *et al* ., 2003)

1.6.4.1 Transcriptional regulation of apoptosis by the Akt signalling pathway

Akt is strongly associated with cell survival through transcriptional control of survival genes and pro-apoptotic genes. FoxO1 (FKHR), FoxO3 (FKHRL1) and FoxO4 (AFX) have all been shown to induce apoptosis (Burgering and Medema, 2003). These transcription factors belong to the large Forkhead family of proteins known as the 'O' subgroup (FoxO), and they are characterized by a conserved DNA-binding motif (Reagan-Shaw and Ahmad, 2007). Target genes for these FoxO isoforms are thought to include the apoptosis inducing Fas and TRADD ligands as well as members of the pro-apoptotic Bcl-2 family (Burgering and Medema, 2003). By phosphorylating its members, PI3K/Akt inhibits the transcriptional activity of the FoxO family. It accomplishes this feat by enabling FoxO to bind to 14-3-3 chaperone proteins which results in their eventual exclusion from the nucleus, a position from which they are unable to convey their transcriptional instructions. In addition, PI3K/Akt

dependent 14-3-3 binding also impedes DNA binding. Once excluded from the nucleus, the FoxO proteins are also available for proteosomal degradation. Therefore PI3K/Akt activity not only prevents FoxO-dependent transcription, but it also encourages FoxO degradation (Reagan-Shaw and Ahmad, 2007). Inhibition of the FoxO family, through Akt phosphorylation, has also been shown to be essential for C2C12 myotube formation (Hribal *et al.*, 2003). Akt governs apoptosis through several other transcription factors including NF-κB (Barkett and Gilmore, 1999) and the c-AMP response element binding protein (CREB). Phosphorylation of CREB by Akt causes an increase in its transcriptional activity, and has been shown to increase the expression of the anti-apoptotic Bcl-2 (Pugazhenthi *et al.*, 2000).

1.6.4.2 Direct regulation of apoptosis by the Akt signalling pathway

Akt is also thought to increase cell survival by directly targeting activators of apoptosis (Song *et al.*, 2005). The Bcl-2 member BAD binds to certain anti-apoptotic proteins and thereby inhibits their ability to propagate cell survival. By phosphorylating BAD, Akt causes it to liberate coupled anti-apoptotic proteins and then associate with the 14-3-3 protein (Datta *et al.*, 1997). This leads to the obstruction of its apoptotic function, as the integrity of the mitochondria is upheld and the release of pro-apoptotic factors can not occur. Akt has also been shown to directly phosphorylate the initiator and effector caspase-9 in humans, and in doing so, it is able to lessen its apoptotic action (Cardone *et al.*, 1998). Refer to table 1.1 for a summary of these as well as other downstream effectors of Akt and a short description of their role in apoptosis.

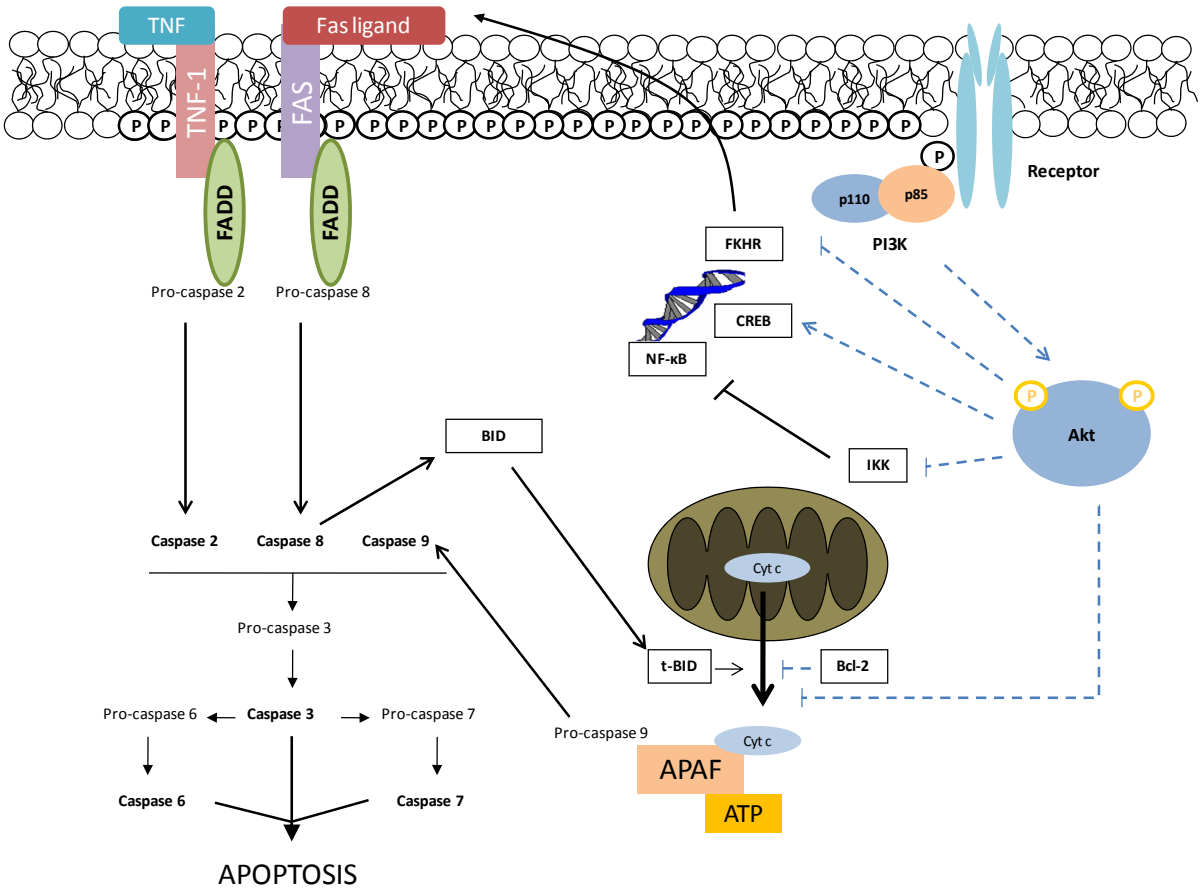

Figure 1.4 Regulation of apoptosis. Akt is able to control cell survival at the level of transcription factors as well as by blocking cytochrome c exit from the mitochondria. Intrinsic, extrinsic and caspase mediated cell death are discussed in detail in the text.

- - - indicates pro-survival pathways ——— indicate pro-apoptotic pathways.

1.6.4.3 Apoptosis regulation through protein binding of Akt

One of the major aspects of signal transduction is the communication of cellular signals by the movement of high energy phosphate groups. These phosphate groups are able to act as switches inside cells and by their presence or absence, depending on the signal involved, signal cascades can be switched off or on. In this way, the protein kinase Akt can switch protein function on or off by the transfer of phosphate groups to specific amino acid motifs. However, Akt is also able to regulate programmed cell death by binding directly to certain proteins, important for apoptosis regulation, without phosphorylating them. For example, Akt

associates with JIP-1 to block JNK binding and delay apoptosis (Song and Lee, 2005). Also, it is known that the Hsp90-Akt complex can phosphorylate apoptosis signal regulating kinase (ASK-1) and prevent apoptosis (Zhang *et al.*, 2005).

1.6.5 The Map kinases and apoptosis

The mitogen activated protein kinases (MAPKs) belong to a prominent group of serine/threonine protein kinases that are components in numerous signalling pathways, including some that control apoptosis. The MAPKs JNK and P38-MAPK are known to respond to cellular stresses and are ordinarily associated with apoptosis rather than cell survival. However, the roles of these two protein kinases with regard to apoptosis regulation have proved to be complex, and, under certain conditions, apoptotic behaviour has been reported for both JNK and P38-MAPK (Wada and Penninger, 2004). In contrast to JNK and P38-MAPK, many accounts portray ERK related signalling pathways to be involved in anti-apoptosis (Wada and Penninger, 2004). Yet, as with JNK and P38-MAPK, apoptosis regulation with ERK is complicated and situational, and under certain conditions ERK may act to encourage apoptosis (Zhuang and Schnellmann, 2006). In addition, ASK1, which is an upstream MAP3K in both the JNK and P38-MAPK pathways, has been demonstrated to be phosphorylated by Akt, and in that way reducing ASK1 activity (Kim *et al.*, 2001).

1.6.6 Hypoxia and acidosis can cause a programmed cell death response

It has been concluded that severe hypoxia or ischemia alone is not enough to cause apoptosis in cardiac myocytes and that apoptosis only occurs when there is a decrease in extracellular pH accompanying these states (Webster 1999). Moreover, the decrease in ATP levels associated with hypoxia and ischemia exacerbate acidosis even further and result in additional initiation of the programmed death pathways (Webster *et al.*, 2005). Hence,

apoptotic cell death during the hypoxic and ischemic states is believed to be caused by the secondary effects to hypoxia and not directly by hypoxia itself. Having said this, the activation of Akt has been shown to protect against hypoxia induced apoptosis during ischemia and hypoxia (Matsui *et al.*, 1999; Matsui *et al.*, 2001). Also, levels of the Bcl-2 protein have been shown to decline in some animal models of ischemia (Webster *et al.*, 2005). BNip3 is a member of the BH3-only subfamily of Bcl-2 proteins that is associated with both hypoxia and acidosis, and it has been shown to play a critical role in apoptosis of cardiac myocytes in hypoxia and ischemia (Webster *et al.*, 2005). The transcription of Bnip3 becomes increased during hypoxia. Bnip3 then translocates into mitochondria, but is only able to do so at decreased pH. Here it stimulates the release of pro-apoptotic factors which leads to apoptosis. This apoptotic pathway seems to be cell line specific and has not been shown in some models. Together, hypoxia and acidosis can cause a coordinated, programmed cell death response.

1.6.7 Autophagy

Cell death takes place is an extremely complicated environment, and current evidence suggests that it varies along a spectrum of death styles (Assuncao Guimaraes and Linden, 2004). Much evidence now exists to substantiate claims that several, overlapping cell death styles operate collectively or alone as so-called programmed cell death pathways (Lockshin and Zakeri, 2004). Cell death can be partitioned into three main categories (Lockshin and Zakeri, 2004), two of which, apoptosis (type I) and necrosis (type III), have been described above. Although widely accepted as a programmed cell death type, autophagy (type II cell death) is yet to be definitively defined as such (Tsujimoto and Shimizu, 2005). In fact autophagy might more accurately be described as a cell survival mechanism that acts alongside cell death but does not necessarily lead to it (Tsujimoto and Shimizu, 2005). Autophagy, first described in the 1960's (Stromhaug and Klionsky, 2001), is characterised by

the development of autophagosomes that engulf organelles and other cellular components before fusing with large autophagic vacuoles and thereby results in mass proteolysis (Lockshin and Zakeri, 2004). This is believed to occur mainly in response to nutrient starvation or signals prompting cellular remodelling and is thought to be controlled mainly by mTOR (Meijer and Codogno, 2004). It has recently been shown that C2C12 myoblast death begets both apoptosis and autophagy (Martinet *et al.*, 2005).

1.7 mTOR

It is essential that cell proliferation and growth be coordinated with nutrient availability to the cell. By assigning meagre resources to the less vital process of protein synthesis, the cell factory could unwittingly strip itself of critical energy supplies. The serine/threonine protein kinase mTOR is a key component in an important cellular network acting to ensure that protein synthesis and its associated energy consumption remain in equilibrium with nutrient supply (Wullschleger *et al.*, 2006). By receiving communications from growth factors through PI3K and Ras related pathways, mTOR participates in the management of growth and metabolism by governing the rate of protein synthesis in the cell. mTOR is also able to react to any fluctuations in nutrient availability, including lowered oxygen (Sarbassov *et al.*, 2005a). These nutrient sensing processes are mediated through signalling pathways that work independently of mitogenic signals and growth factors. Thus, mTOR is believed to manage valuable energy stores in response to a depletion of nutrients like amino acids, oxygen and mitogens, a situation that might occur during decreased blood flow observed in pathophysiological conditions such as ischemic diseases (Zhou *et al.*, 2008; Sarbassov *et al.*, 2005a; Vaupel *et al.*, 1989).

1.7.1 Two separate mTOR complexes

The antifungal compound rapamycin was found to be potentially immunosuppressive and to cause growth inhibition in yeast. This was established to be caused by indirect inhibition of the eponymous targets of rapamycin (TOR) genes (Wullschleger *et al.*, 2006). Under favourable conditions, where sufficient nutrients are at hand, cells will enlarge and increase in number. While all the time the process of cell growth must be in concordance with the cells environmental status, to ensure the preservation of homeostasis. Two separate TOR complexes are believed to exist, both having different effects on growth in response to environmental conditions and to receptor tyrosine kinase activation (Sarbassov *et al.*, 2005a).

Mammals have a single TOR gene, the functionally and structurally conserved mammalian homologue mTOR. mTOR forms two known protein complexes, mTORC1 and mTORC2, both of which are acknowledged serine/threonine protein kinases (Inoki *et al.*, 2005). mTORC1 is composed of mTOR as well as other proteins including raptor and is sensitive to rapamycin. Rapamycin is able to bind to the FKBP12-binding domain on mTORC1 *in vitro* which results in its inhibition by a mechanism that is not yet known (Sarbassov *et al.*, 2005a). mTORC1 controls among other things protein synthesis, temporal cell growth (Wullschleger *et al.*, 2006) and autophagy (Meijer and Codogno, 2004), while lowered nutrient levels are known to inhibit its functioning (Wullschleger *et al.*, 2006). On the other hand, mTORC2 is insensitive to rapamycin as FKBP-12 does not bind to it. It functions differently to mTORC1, and manages the spatial growth of cells by controlling the actin cytoskeleton (Wullschleger *et al.*, 2006). mTORC2 in combination with the rictor protein is able to phosphorylate Akt at the serine 473 position. Interestingly, this action may enhance the phosphorylation of PKB/Akt at its threonine 308 position by PDK1 (Sarbassov *et al.*, 2005b).

1.7.2 Upstream of mTOR

mTOR is controlled upstream by a complex interplay of nutrient and growth factor controls as well as by other signals independent of mitogenic influence. These are able to act at various levels of the mTOR pathway (reviewed in Hay and Sonenberg, 2004). Only those aspects pertinent to the PI3K/Akt and hypoxia/ischemia are discussed in any detail here.

1.7.2.1 Regulation of mTOR by the TSC1/TSC2 complex

mTOR functioning is negatively regulated by a heterodimer made up of the tubular sclerosis proteins TSC1 (hamartin) and TSC2 (tuberin) (Tee *et al.*, 2002). In circumstances of diminished nutrients, the TSC1/TSC2 complex will decrease mTOR signalling through the Rheb complex (Figure 1.5). Rheb is a small GTP-binding protein that acts as an upstream activator of mTOR, and, although it is thought to act downstream of the TSC1/TSC2 heterodimer, its mechanistic action on mTOR remains unknown. At the moment, a basic model suggests that the TSC1/TSC2 complex inhibits the mTOR pathway by stimulating the GTP hydrolysis of Rheb through TSC2 GAP activity (Inoki *et al.*, 2005). Following this, Rheb is believed to positively stimulate mTOR activity.

1.7.2.2 Regulation of mTOR by nutrients

mTOR signalling is extremely sensitive to changes in nutrient levels, especially amino acids (Wullschleger *et al.*, 2006). A number of mechanisms as to how mTOR senses nutrient changes have been described. Among these is a direct sensing capability of mTOR itself (Hay and Sonenberg, 2004) or a proposed sensitivity of upstream regulators of mTOR such as TSC2 or Rheb to fluctuating nutrient concentrations (Wullschleger *et al.*, 2006).

Conditions of hypoxia, ischemia and exercise as well as other situations that decrease circulating amino acid or glucose levels lead to the activation of AMP-activated protein kinase (AMPK) through escalating cellular AMP and phosphorylation of the catalytic subunit (Tokunaga *et al.*, 2004). Rising AMPK activation could act directly to inhibit mTOR (Tokunaga *et al.*, 2004). On the other hand, an increasing AMP/ATP ratio is thought to lead to the phosphorylation of TSC2 and subsequent stimulation of its GAP activity (Figure 1.5) (Inoki *et al.*, 2003). This could inhibit Rheb and most probably mTOR. The decreasing energy levels seen during hypoxia interact with mTOR signalling through the AMPK/mTOR pathway. However, hypoxia can inhibit mTOR functioning more directly via the TSC1/TSC2 complex and the hypoxia-inducible gene REDD1 (Brugarolas *et al.*, 2004). It was found that, increased HIF-1α stability during hypoxia increases expression of REDD1 which is thought to lead to TSC1/TSC2-dependent inhibition of mTOR signalling (Brugarolas *et al.*, 2004).

1.7.2.3 Regulation of mTOR by PI3K/Akt

Although a well known regulator of cell survival, PI3K/Akt is also critical manager of the mTOR pathway, mainly through growth factor control. In this way it can convert increased growth factor signalling into pleiotropic effects of mitogenesis and growth (Plas and Thompson, 2005). Akt becomes phosphorylated through the PI3K pathway in response to growth factor receptor stimulation. In turn, phosphorylation of the TSC1/TSC2 complex by activated Akt causes its inhibition and leads to decreased inhibition of mTOR downstream (Manning *et al.*, 2002). TSC2 has been identified as the target for Akt phosphorylation *in vivo* and *in vitro* (Manning *et al.*, 2002), and Akt has been found to phosphorylate TSC2 at both the threonine 1462 and the serine 939 positions (Manning *et al.*, 2002). A potential mechanism of action is increased association of TSC2 with the 14-3-3 chaperone resulting in its decreased activity (Li *et al.*, 2002b). Akt has also recently been found to regulate mTOR

activity through phosphorylation of serine 2448 (Nave *et al.*, 1999). It has also been hypothesized that Akt could regulate mTOR activity by regulating the AMP/ATP ratio and thus inhibit AMPK activity (Hahn-Windgassen *et al.*, 2005). Interestingly, in a potentially significant clinical finding, it was recently shown that a negative feedback loop results from growth signals operating through mTOR and the downstream p70 S6 kinase (S6K) to inhibit PI3K signalling (Harrington *et al.*, 2005).

1.7.3 Downstream of mTOR

The most important and well studied downstream targets of mTOR are said to be constituents of the cells translational apparatus, particularly those responsible for ribosomal recruitment to mRNA (Hay and Sonenberg, 2004). The activators of translation, p70 ribosomal protein S6 kinase 1 are important for cell growth and are direct targets for mTOR (Hay and Sonenberg, 2004). mTOR also activates an inhibitor of translational initiation, the eukaryotic initiation factor 4E binding protein 1 (4E-BP1) (Wullschleger *et al.*, 2006). In addition, mTOR is known to control many other growth related processes.

1.7.4 mTOR and the C2C12 cell line

Unsurprisingly, the mTOR pathway has been found to be essential in development, growth and hypertrophy of C2C12 myotubes (Erbay and Chen, 2001). C2C12 myoblasts are known to cease differentiation in a rapamycin sensitive manner, and therefore mTOR signalling is thought to be crucial for normal C2C12 myotube development (Erbay and Chen, 2001). Is has been demonstrated that mTOR increases the expression of IGF-II, the most vital component in C2C12 myotube development, and that it lies upstream of PI3K/Akt mediated C2C12 myogenesis (Erbay *et al.*, 2003). However, it has also been shown that insulin and IGF-I lie upstream of mTOR protein synthesis in C2C12s as well (Shen *et al.*, 2005).

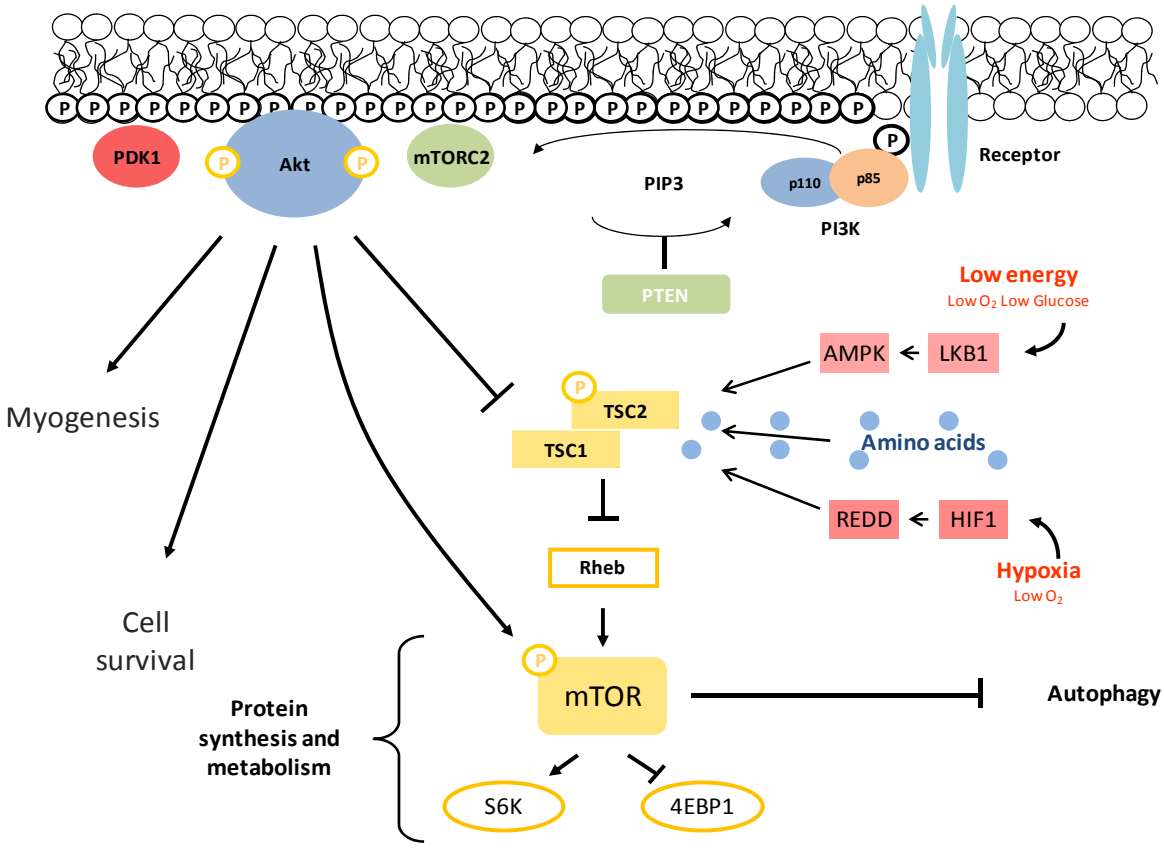

Figure 1.5 Regulation of the mTOR pathway. This schematic illustrates the regulation of mTOR as discussed in the text. Briefly, activated Akt is able to regulate mTOR through phosphorylation of TSC2 or mTOR directly. mTOR activity is also sensitive to changes in amino acids, nutrients, energy levels or hypoxia, which can all be regulated through the TSC2/TSC1 complex upstream of Rheb.

1.8 Study aims and objectives

The aims of this thesis are the following:

1. To elucidate whether acute simulated ischemia or acute hypoxia leads to changes in PI3K activity or expression in C2C12 myotubes on day ten post-differentiation
2. To assess if acute simulated ischemia and acute hypoxia lead to changes in metabolic cell viability, and to establish if PI3K plays a role in these changes
3. To establish whether changes in PI3K activity or expression during acute simulated ischemia and acute hypoxia, if there are indeed any, are reflected in the activity of the downstream effector Akt
4. To assess if changes in the PI3K/Akt pathway during acute simulated ischemia and acute hypoxia lead to changes in the levels of apoptosis and cell survival

Chapter 2

Materials and methods

2.1. Cell culture

C2C12 murine skeletal muscle myoblasts were obtained from the European Collection of Cell Cultures (ECACC). Dividing myoblasts were maintained at 37°C, 20% O_2 and 5% CO_2 in a humidified atmosphere. Myoblasts were cultured in Dulbecco's Modified Eagle's Medium (DMEM) (Sigma Aldrich) supplemented with 10% foetal bovine serum (Highveld Biological (PTY) Ltd, RSA), 4% L-glutamine (Sigma Aldrich) and 1% penicillin/streptomycin (Sigma Aldrich), which will be collectively referred to as growth medium from this point onwards. Cells were first allowed to proliferate in T75 flasks (75cm^2 flasks, Greiner Bio One) until they reached 80% confluence and were split and seeded in growth medium into six well plates (Greiner Bio One) at a seeding density of 100 000 cells. Splitting was accomplished by washing the cell monolayer with warm Phosphate Buffered Saline (PBS) followed by incubation with 2 ml trypsin/EDTA (Sigma Aldrich) at 37°C, with occasional agitation, until cells loosened completely or for a maximum of four minutes. When cells reached 90% confluence (typically after 24 hrs) growth medium was replaced with DMEM (Sigma Aldrich) supplemented with 1% horse serum (Sigma Aldrich), 4% L-glutamine (Sigma Aldrich) and 1% penicillin/streptomycin (Sigma Aldrich), which will collectively be referred to as differentiation medium from this point onwards. Differentiating

C2C12s were maintained at 37°C, 20% O_2 and 5% CO_2 in a humidified atmosphere. Mature multinucleated, myotubes were allowed to develop and were ready to use on day 10 post-differentiation. A complete step by step protocol of C2C12 cell culture procedures is reproduced in appendix A (protocol 1).

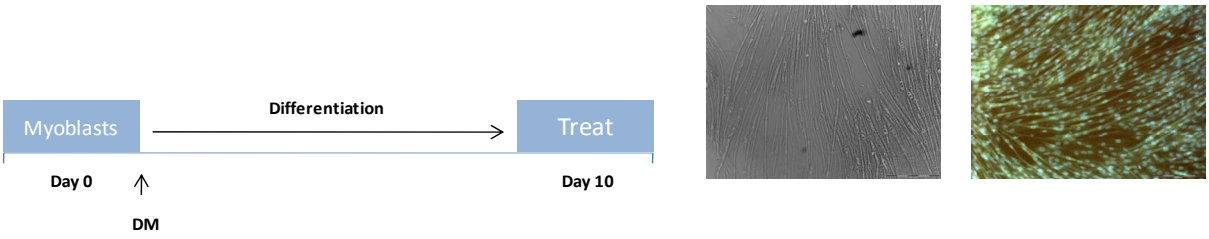

Figure 2.1 The growth medium of proliferating C2C12 myoblasts is replaced with differentiating medium (DM) on day zero and cells are allowed to differentiate into multinucleated myofibres that are ready to treat on day ten.

2.2. Experimental protocol

Differentiated C2C12 myotubes (always treated in sub-groups of three wells) were randomly divided into four groups as follows: group 1: untreated controls (Con or NM), group 2: simulated ischemia (SI or HE), group 3: three hours hypoxia (HM) and group 4: three hours in ischemic buffer (NE). Untreated controls (group 1) were maintained in differentiation medium in normoxic conditions in a humidified 5% CO_2 atmosphere. SI cells (group 2) were incubated under hypoxic conditions (1% O_2, 5% CO_2 and balance N_2) in a modified Esumi buffer (Esumi *et al.*, 1991) with a pH 6.4, containing in mM: 12 KCl, 0.5 $MgCl_2$, 0.9 $CaCl_2$, 137 NaCl and 20 HEPES. Cells from group three were incubated in differentiation medium under hypoxic conditions (1% O_2, 5% CO_2 and balance N_2). Finally, cells from group four were incubated in the modified Esumi buffer in a normoxic environment. Experimental protocol consisted of each of the aforementioned groups being incubated for a period of three hours (acute incubation). However, in the pilot study both myoblasts and myotubes were incubated in SI for several time points spanning five and seven hours respectively.

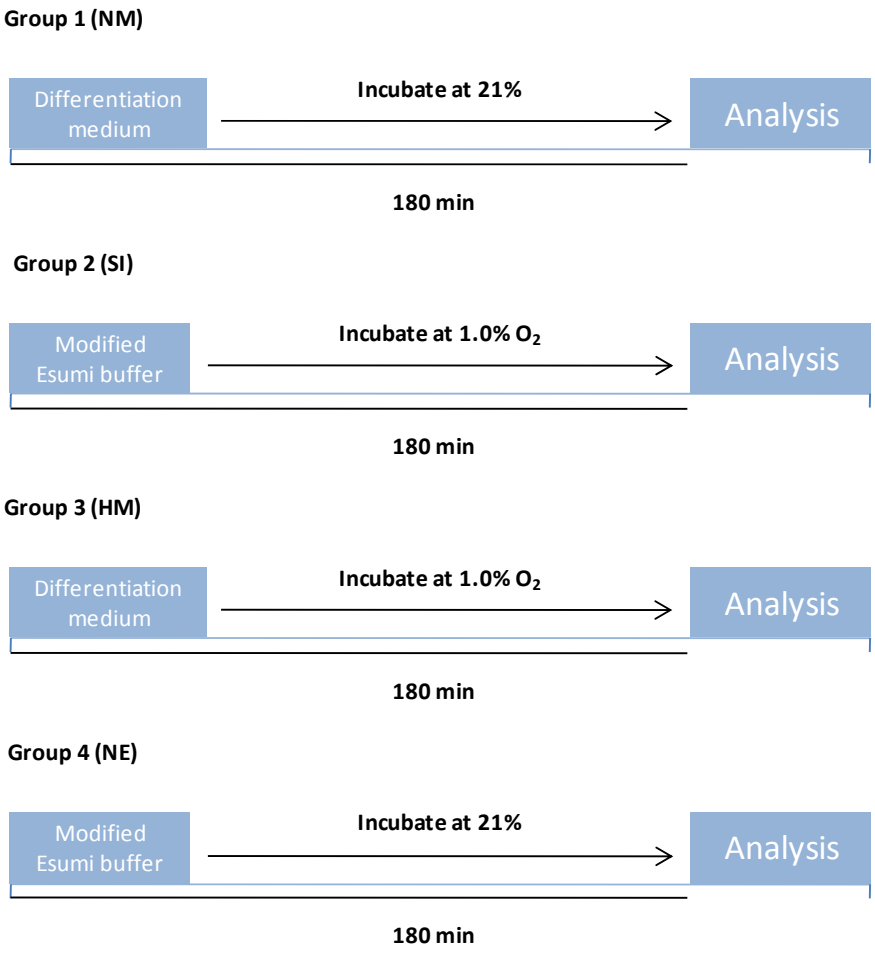

Figure 2.2 Schematic representation of the experimental protocol. C2C12 myotubes on day ten post-differentiation are randomly treated in four groups (independent experiments ≥ 3) and incubated for three hours in the conditions illustrated above. Groups are described in detail in the text. Percentages indicate oxygen tension.

2.3. PI3K inhibitors

Two pharmacological inhibitors specific for the PI3K pathway, namely wortmannin and 2-(4-morpholino)-8-phenyl-4H-1-benzopyran-4-one (LY294002), were used in the study. In experiments where inhibition of the PI3K pathway was desired, applicable cultures were supplemented with inhibitors at appropriate concentrations, 20 min prior to the treating of cells as described in the experimental protocol (section 2.2). Both pharmacological inhibitors were obtained from Sigma Aldrich and were prepared and stored as per manufactures instructions.

2.4. MTT cell activity assay

The 3-(4,5-dimethylthiazol-2-yl)-2,5-diphenyltetrazoliumbromide (MTT) cell activity assay indicates the percentage of metabolically viable cells post intervention, where absorption measurements correlate directly with the ability of vital reduction enzymes in the mitochondria of healthy cells to reduce MTT. Briefly, C2C12 myotubes were treated as described previously in the experimental protocol (section 2.2). However, for the MTT cell activities performed in the pilot study both C2C12 myoblasts and myotubes were incubated in SI for several time points spanning five and seven hours respectively. Subsequent to treatments, supernatants were discarded and 1.5 ml of warm PBS and 500 µl of MTT solution (0.01 g MTT/ml PBS) was added to each well containing the cell monolayer which was then incubated for 2 hrs at 37ºC in a humidified 5% CO_2 atmosphere. After incubation, 2 ml of isopropanol-HCl/Triton-X-100 (50:1) was added to each well and vigorously agitated for 5 min in order to dissolve formazan crystals that had been generated in healthy cells. The suspension was then centrifuged for 2 min at 1400 rpm and the supernatant spectrophotometrically analysed to determine absorbance at a wavelength of 540 nm versus a blank. Groups were analysed in triplicate in at least three separate experiments and absorbance values calculated as a percentage versus untreated controls. MTT was obtained from Sigma Aldrich. A complete step by step protocol for the MTT assay is reproduced in appendix A (protocol 2).

2.5. Western blot analysis

2.5.1 Protein extraction and quantification

Complete protocols for the extraction and quantification of proteins from our cells are provided in appendix A. Consequently, they are described only in brief here. After treatment,

as described in the experimental protocol (section 2.2), cells immediately had their supernatants discarded and were placed on ice. Cell monolayers were then rinsed three times in 5 ml of a pre-lysis buffer (20 mM Tris-HCl, pH 7.4, 137 mM NaCl, 1 mM $CaCl_2$, 1 mM $MgCl_2$ and 0.1 mM sodium orthovanadate). Total cell protein was extracted by incubating cells on ice for 10 min in 1 ml of a modified radioimmunoprecipitation (RIPA) buffer, pH 7.4, containing: Tris–HCl 2.5 mM, EDTA 1 mM, NaF 50 mM, NaPPi 50 mM, dithiothreitol 1 mM, phenylmethylsulfonyl fluoride (PMSF) 0.1 mM, benzamidine 1 mM, 4 mg/ml SBTI, 10 mg/ml leupeptin, 1% NP40, 0.1% SDS and 0.5% Na deoxycholate. Adherent cells were then harvested from culture dishes by scraping. Whole cell lysates were sonicated in order to disrupt the cell membranes to release their contents before being centrifuged at 4°C and 8000 rpm for 10 min. Lysates were then stored at -80°C or had their protein content determined immediately. A complete step by step protocol for protein extraction is reproduced in appendix A (protocol 3). Protein content was quantified using the Bradford protein determination method (Bradford, 1976), directly before the preparation of cell lysates. A complete step by step protocol for protein quantification by the Bradford method is reproduced in appendix A (protocol 4).

2.5.2 Sample preparation (cell lysates)

Following protein quantification, aliquots diluted in Laemmli sample buffer were prepared for all samples, each containing 50 μg protein. Aliquots were then stored at -80°C for future analysis by Western blotting. A complete step by step protocol for sample preparation and storage is reproduced in appendix A (protocol 5).

2.5.3 SDS-PAGE and Western blot analysis

Whole cell lysates were separated on 10% polyacrylamide gels by sodium dodecyl sulphate polyacrylamide gel electrophoresis (SDS-PAGE). A pre-stained protein marker ladder

(peqGOLD) was loaded in the left most well on each gel for orientation and electrophoretic determination of molecular weights of specific bands. Previously prepared protein samples were boiled for 5 min before 50 μg of protein (sample preparation described above) was loaded per lane. Gels were run for 60 minutes at 130 V (constant) and 400 mA (Mini Protean System, Bio-Rad, Hercules). Following SDS-PAGE, proteins were transferred to polyvinylidine fluoride (PVDF) membranes (Immobilon, Millipore, USA) using a semi-dry electrotransfer system (Bio-Rad, USA) for 60 min at 15 V and limit 0.5 A. In order to prevent non-specific binding, membranes were blocked in 5% (w/v) fat-free milk in 0.1% Tris Buffered Saline-Tween20 (TBS-T) for 2 hours at room temperature with gentle agitation. Membranes were then incubated with specific primary antibodies (table 2.1) diluted in TBS-T (1:1000), overnight at 4°C. The following day, membranes were washed in copious volumes of TBS-T (3X5 min) before being incubated in anti-rabbit (Amersham Biosciences, UK limited, and Dako Cytomation, Denmark) horseradish peroxidase-conjugated secondary antibody for 1 hr at room temperature with gentle agitation. Following the incubation period, membranes were washed a further three times in TBS-T (3x5 min), followed by a final 10 minute wash in TBS. Antibodies were detected with the LumiGLO Reserve™ chemiluminescent substrate kit (KPL, Inc., USA) as per the manufacturer's instructions, and bands were exposed to autoradiography film (Hyperfilm, Amersham Biosciences, UK limited). Exposed bands were visualised and then quantified by densitometry using the UN-SCAN-IT© densitometry software (Silk Scientific Corporation, Utah, USA). All bands were expressed as optical density readings relative to a control present on the same blot. A complete step by step protocol for SDS-PAGE and Western blot analysis is reproduced in appendix A (protocol 6).

Table 2.1 Antibodies used in Western blotting analysis. The thickness of the polyacrylamide gel used is given for each antibody along with its catalogue number.

Antibody	Size (kD)	Cat. No*	Gel thickness
p-Akt (Ser473)	60	9271	1 mm
p-Akt (Thr308)	60	9275	1 mm
Akt	60	9272	1 mm
p-TSC2	200	3617	1 mm
TSC2	200	3612	1 mm
p-CREB (Ser133)	41	9198	0.75 mm
CREB	41	9197	0.75 mm
p-PTEN (Ser380)	60	9551	0.75 mm
PTEN	60	9559	0.75 mm
p-PDK1 (Ser241)	63	3061	0.75 mm
PDK1	63	3062	0.75 mm
p-FKHR (Ser193)	72-82	9401	0.75 mm
FKHR	72-82	9462	0.75 mm
p-mTOR (Ser2448)	120	2971	0.75 mm
mTOR	120	2972	0.75 mm
cleaved PARP	85	9541	0.75 mm
PARP	116	9542	0.75 mm
REDD	41	2516	0.75 mm
HIF1α	120	3716	0.75 mm
TSC1	150	4906	0.75 mm
PI3K (p85)	85	4292	1 mm
PI3K (p110)	110	4254	1 mm

*All antibodies obtained from Cell Signaling

2.6 PI3K activity assay (competitive ELISA)

2.6.1 Immunoprecipitation of PI3K

After treatment of applicable groups, as described in the experimental protocol (section 2.2), C2C12 myotube monolayers were each rinsed three times with 5 ml of ice-cold lysis buffer (20 mM Tris-HCl, pH 7.4, 137 mM NaCl, 1 mM $CaCl_2$, 1 mM $MgCl_2$ and 0.1 mM sodium

orthovanadate). This was removed and cells were incubated on ice for 20 min in 1 ml of a second, modified lysis buffer (Tris–HCl 2.5 mM, pH 7.4, EDTA 1 mM, NaF 50 mM, NaPPi 50 mM, dithiothreitol 1 mM, phenylmethylsulfonyl fluoride (PMSF) 0.1 mM, benzamidine 1 mM, 4 mg/ml SBTI, 10 mg/ml leupeptin, 1% NP40, 0.1% SDS and 0.5% Na deoxycholate). Adherent cells were then harvested from culture dishes by scraping, and whole cell lysates were sonicated and centrifuged as described in protocol 3 (appendix A). Protein content was quantified using the Bradford protein determination method (Bradford, 1976), which is reproduced in detail in protocol 4 (appendix A). PI3K was immunoprecipitated by adding 10 µl of a rabbit polyclonal anti-PI3K p85/protein A-agarose slurry conjugate (Upstate Biotechnology, catalog #16-107) to cell lysates containing 1000 µg of protein. This was allowed to agitate gently overnight at 4ºC. The immunoprecipitated enzyme was collected by pulsing on a desktop centrifuge (5 sec at 14 000 rpm) and discarding the supernatant. The beads were then washed three times in the following buffers: buffer A (20 mM Tris-HCl, pH 7.4, 137 mM NaCl, 1 mM $CaCl_2$, 1 mM $MgCl_2$, 1% NP-40, 0.1 mM sodium orthovanadate), buffer B (0.1 M Tris-HCl, pH 7.4, 5 mM LiCl and 0.1 mM sodium orthovanadate) and buffer C (10 mM Tris-HCl, pH 7.4, 150 mM NaCl, 5 mM EDTA and 0.1 mM sodium orthovanadate). A complete step by step protocol for the immunoprecipitation of PI3K from our cells is reproduced in appendix A (protocol 7).

2.6.2 PI3K activity competitive ELISA

PI3K activity in the immunoprecipitates was analysed with a PI3K enzyme-linked immunosorbent assay (ELISA) (from Echelon Biosciences, Salt Lake City, UT; product # K-1000), according to the manufacturer's instructions. Briefly, immunoprecipitated enzyme (obtained as described previously in section 2.6.1 and protocol 7 in appendix A) and $PI(4,5)P_2$ substrate were incubated for 3 hrs at room temperature in a reaction buffer specific

for the α isoform of PI3K (50 mM HEPES, pH 7, 25 mM $MgCl_2$ and 250 μM ATP). Kinase reactions were stopped by adding of 1 N H_2SO_4 and transferring the reaction mixture to the incubation plate provided. This was incubated overnight at 4ºC with a PI(3,4,5)P_3 detector protein, then added to a PI(3,4,5)P-coated microplate for 1 h, in order to permit competitive binding to take place. Following several wash steps, a peroxidase-linked secondary detection reagent was added so as to calorimetrically detect the PI(3,4,5)P_3 detector protein binding to the plate (absorbance measured at 450 nm on a plate reader). The colorimetric signal is inversely proportional to the amount PI(3,4,5)P_3 produced by PI3K, and the enzyme activity was expressed as amounts of PIP_3 (picomoles/ml) produced by cell extracts containing equal amounts of protein.

2.7 Vital staining (immunohistochemistry)

C2C12 myotubes for vital staining were cultured in six well plates (Nunc, NY, USA), and induced to differentiate as described previously (section 2.1).

2.7.1 Propidium iodide and Hoechst staining

After treatment of applicable groups, as described in the experimental protocol (section 2.2), cells were washed three times with sterile 0.1 M PBS before being incubated for 20 min at room temperature with Propidium iodide (PI) (5 mg/ml in a 1:200 dilution). Thereafter, the cell monolayers were again rinsed three times with sterile PBS and fixed and permeabilised with an ice-cold 1:1 methanol/acetone mixture for 10 min at 4ºC. After being left to air dry for 20 min in the dark, cells were, once more, washed three times in sterile PBS and enough Hoechst 3342 (10 mg/ml in a 1:200 dilution) was then added to cover the entire cell monolayer. This was left to incubate for 10 min at 4ºC. Thereafter, cells were washed five times in sterile PBS and images were immediately acquired with an Olympus IX81

microscope fitted with CellR® software. Cells were evaluated on spectrum for apoptosis and necrosis as follows: propidium iodide is usually excluded from healthy cells whereas Hoechst 33342 is able to diffuse through cell membranes regardless of their condition. Therefore cells with slightly permeable membranes stain with PI to a small degree, while late apoptotic and necrotic cells exhibit enlarged nuclei, stain homogeneously for PI and Hoechst and appear pink when co-stained. A minimum of three randomly chosen fields, of at least 3 independent experiments per experimental condition, with a total number of at least 250 individual cells was analysed using Simple PCI (C-Imaging Systems) software. Data was expressed in arbitrary pixel values and was exported to Microsoft excel where it was statistically analysed for the degree of membrane permeabilisation, as a percentage relative to untreated controls. A complete step by step protocol for propidium iodide and Hoechst staining is reproduced in appendix A (protocol 8).

2.7.2 Annexin V and Hoechst staining

After treatment of applicable groups, as described in the experimental protocol (section 2.2), cell monolayers were washed three times with sterile 0.1 M PBS before being fixed and permeabilised with an ice-cold 1:1 methanol/acetone mixture for 10 min at 4ºC. After being left to air dry for 20 min in the dark, cells were, once more, washed three times in sterile PBS. The following steps were conducted in a dark, humidified environment at room temperature. Non-specific binding was blocked by incubating in 5% donkey serum for 20 min. Cells were then incubated with anti-Annexin V primary antibody for 90 min. Cells were then rinsed three times with sterile PBS and incubated with a FITC bound secondary antibody for 30 min. Immediately thereafter, cells were washed three times in sterile PBS and enough Hoechst 3342 (10 mg/ml in a 1:200 dilution) was then added to cover the entire cell monolayer. This was left to incubate for 10 min at 4ºC. Finally, cells were washed five times

in sterile PBS and images were immediately acquired with an Olympus IX81 microscope fitted with CellR® software. A minimum of three randomly chosen fields, of at least 3 independent experiments per experimental condition, with a total number of at least 75 individual myotubes was analysed with Simple PCI (C-Imaging Systems) software. Data was expressed in arbitrary pixel values and was exported to Microsoft excel where it was statistically analysed for the degree of Annexin V binding, as a percentage relative to untreated controls. A complete step by step protocol for Annexin V and Hoechst staining is reproduced in appendix A (protocol 9).

2.8 DNA fragmentation assay

C2C12 myotubes were treated as described previously in the experimental protocol (section 2.2). After treatment, the cell monolayer was washed with warm Phosphate Buffered Saline (PBS) and cells were collected by incubation and agitation with trypsin/EDTA (Sigma Aldrich) at 37°C, until cells loosened completely or for a maximum of four minutes. Double the amount of warm medium was then added to the trypsin/cell suspension which was then pelleted by centrifugation for 10 min at 1200 rpm and 10ºC. The resultant cell pellets were then washed twice by re-suspension in sterile PBS, with centrifuging between washes. Thereafter, the supernatant was discarded and the pellets re-suspended in 3 ml of DNA extraction buffer (2 mM EDTA, 100 mM Tris-HCl, pH 8.0, 0.8% SDS (w/v) and 10 mM NaCl) and RNase (Sigma Aldrich), to a final concentration of 20 µg/ml. The re-suspension was incubated on a heating block at 37ºC for 1 hr before being supplemented with proteinase K (Whitehead Scientific), to give a final concentration of 100 µg/ml. This was then incubated on a heating block at 45ºC overnight. The following day, the proteinase K was inactivated by heating to 70ºC for 5 min. After that, all the samples were quenched on ice for 5 min before DNA was extracted with two rounds of Tris-buffered phenol/chloroform (1:1) (Sigma

Aldrich) extraction and once with a chloroform/isoamyl alcohol (24:1) (Sigma Aldrich) extraction. The DNA was then precipitated by adding 40 µl NaCl and 1 ml of ice-cold 100% ethanol. The suspension was centrifuged for 20 min at 14 000 rpm, and the supernatant was removed, and the precipitated DNA washed once with 70% (v/v) ethanol and 2 volumes of ice cold 100% ethanol. The genomic DNA was then centrifuged for 5 min on a desktop centrifuge at 14 000 rpm, and the resulting DNA pellet was left to air-dry for 5 min before being re-suspended in 40 µl of Tris-EDTA, pH 7.5 and left at 4ºC overnight. The following day, 10 µl of each DNA sample and 1 µl of 100 bp DNA ladder (New England BioLabs) was mixed with 2 µl of 5X loading dye (0.25% bromophenol blue, 50% glycerol in 5X Tris-acetate-EDTA [TAE]) and resolved by electrophoresis through a 1% TAE-agarose gel in 1X TAE buffer at 4 V/cm. DNA was visualized by staining with ethidium bromide (1 µg/ml) (Sigma Aldrich), followed by examination on a UV transilluminator. A complete step by step protocol for DNA fragmentation is reproduced in appendix A (protocol 10).

2.9 Statistical analysis

All the data concerning untreated controls was set equal to 100 unless otherwise stated. All data were expressed as means ± SEM and as a percentage relative to untreated controls. Means were compared to untreated controls using the student's t-test. Data were considered significant if p-value<0.05. All statistical analyses were conducted with the aid of *Statistica* version 7 software.

Chapter 3

Results

Note on data representation in this chapter: Qualitative data will be represented in the form of images herein. DNA fragmentation images are used for their qualitative advantages and as such have not been appraised statistically. *Key* – Quantitative data is represented by means of bars graphs the colours of which correspond to the following: MTT data for myotubes, MTT data for myoblasts, ELISA data, densitometry data for western blots and vital staining fluorescence intensity.

3.1 Preliminary work (MTT cell activities)

Our initial aim was to determine the sensitivity of C2C12s to a modified Esumi buffer which mimics the decreased nutrient and pH levels as well as the altered ion concentrations seen during ischemia. C2C12 myotubes were exposed to simulated ischemia (SI) which entailed incubation in the modified Esumi buffer in hypoxia (1.0% O_2, 5% CO_2 and balance N_2). We wanted to establish if cellular functioning would be impaired when compared with those cells incubated at standard normoxic conditions under which the cells are usually cultured. Furthermore, we wished to compare the responses of C2C12 myoblasts (grown with 10% FBS) and differentiated myotubes (maintained in 1% HS) in equivalent conditions. The 3-(4,5-dimethylthiazol-2-yl)-2,5-diphenyltetrazoliumbromide (MTT) cell activity assay was chosen for the pilot work. This assay

indicates the percentage of metabolically viable cells post intervention, where ultimate absorption measurements correlate directly with the ability of vital reduction enzymes in the mitochondria to reduce MTT. C2C12 cells were seeded in high density, cultured in the standard manner and treated (as myoblasts) or differentiated upon reaching 90% confluence. Cell activity was shown to decrease dramatically to 40% and 20% in myotubes and myoblasts respectively after one hour in SI. Thereafter, the cell activities of the myotubes were shown to decrease with each successive hour until reaching 14.6% of the baseline (0 hrs hypoxia) at five hours (Figure 3.1). Notably, mean cell activity measurements dropped to approximately one quarter that of the baseline after only three hours. Myoblasts proved to be less robust and showed less MTT reducing capacity at each time point when compared to myotubes under complementary conditions. Ultimately, a trend towards a decrease in cell activity with an increase in time spent in SI was displayed for both myoblasts and myotubes.

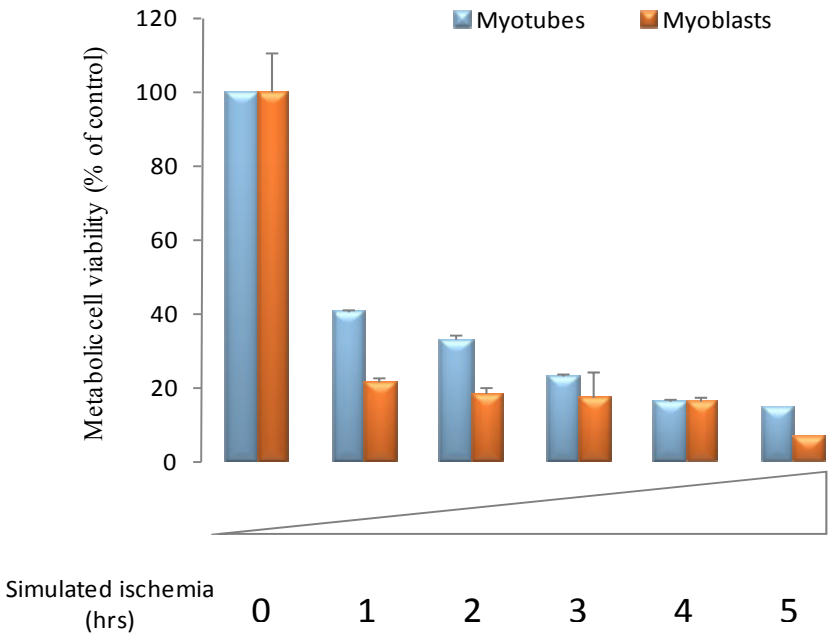

Figure 3.1 Decrease in metabolic cell viability of C2C12 myotubes and myoblasts with increasing time spent in simulated ischemia. Myoblasts and differentiated myotubes (day 10) were incubated in simulated ischemia, and their activities were assessed at 0,1,2,3,4 and 5 hours. Metabolic cell viability was measured using the MTT assay. Results are presented as means ± S.E.M ($n \geq 3$).

Next, we wished to determine if the cell enzyme activities in our myotube model decreased linearly over an appreciable time period. Moreover, we desired to discern if our 'acute' time points fell within a linear trend, if one did indeed exist, or if cell activities would behave appreciably differently if the cells were exposed for longer. A similar experiment was performed where cells on day 10 of differentiation were subjected to SI for several time points spanning seven hours. An R^2 (coefficient of determination) value of 0.949% was found for the one to seven hour time points (Figure 3.2), thereby indicating a linear relationship of time versus enzyme reducing capacity in our myotube model.

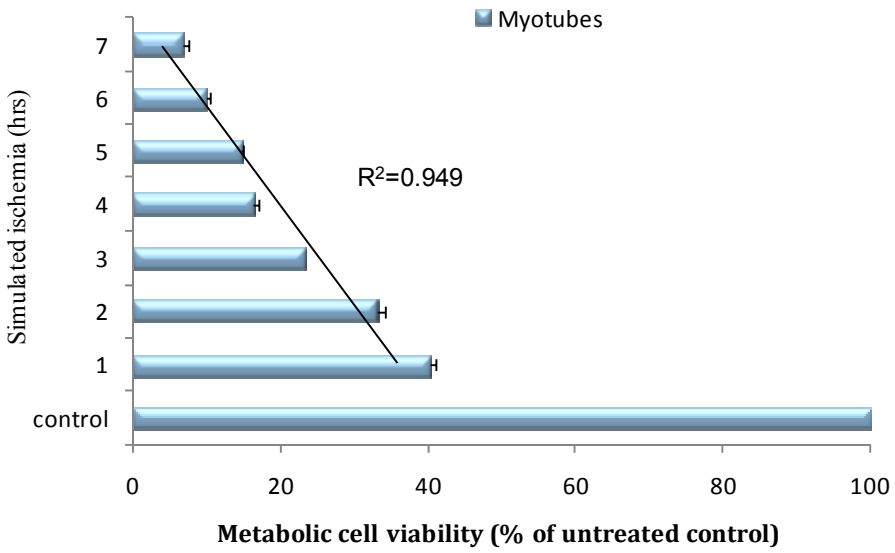

Figure 3.2 Linear relationship of time versus metabolic cell viability in C2C12 myotubes. Differentiated C2C12 myotubes (day 10) were incubated in simulated ischemia, and their activities were assessed at 0,1,2,3,4,5,6 and 7 hours. Metabolic cell viabilities were measured by means of the MTT assay. The R^2 value was calculated for the time points ranging over 1 to 7 hours. Results are presented as means ± S.E.M ($n \geq 3$).

3.2 Metabolic cell viability after 3 hrs 'acute' intervention

After preliminary work was completed our attention was turned to the three hour time point which we labelled 'acute'. C2C12 cells were exposed to SI (modified Esumi buffer and 1.0% O_2) as myoblasts or after being differentiated in the usual manner. Metabolic cell viability was then evaluated for C2C12 myotubes in numerous, separate experiments (total n=15). Compared to controls, metabolic cell viability was shown to decrease significantly to a mean 25.8% (Figure 3.3). Metabolic cell viability was evaluated for C2C12 myoblasts in a similar way ($n \geq 5$). Myoblasts proved less robust than the corresponding myotubes with cell enzyme activity decreasing significantly to 21.4% of the controls.

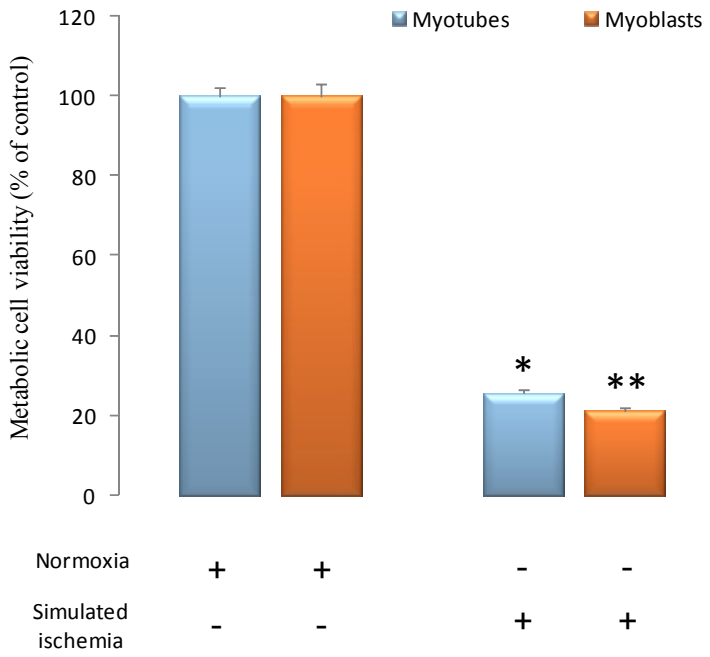

Figure 3.3 Difference in metabolic cell viability for C2C12 myotubes and myoblasts after 3 hours spent in simulated ischemia. Myoblasts and differentiated myotubes (day 10) were incubated simulated ischemia, and their activities were assessed after three hours vs. their normoxic controls. Metabolic cell viability was measured by the MTT assay. Results are presented as their mean ± S.E.M (n=15 for myotubes and $n \geq 5$ for myoblasts). *p<0.05 vs. control (myotubes), **p<0.05 vs. control (myoblasts).

Next, myotubes were incubated with and without the modified Esumi buffer in both normoxia and hypoxia (1.0% O_2). The difference in metabolic cell viability between baseline (cells incubated in culture medium at normoxia) and hypoxic conditions (cells incubated in culture medium at 1% O_2) were found to achieve only near significance (p=0.05, data not shown). Likewise, the corresponding myoblast groups too, showed no significant difference in metabolic cell viability. In myotubes, the difference in metabolic cell viability for the 'normoxia Esumi' group versus the 'normoxia medium' group was measured to be 67.37%. The difference between the 'hypoxia medium' group versus the SI group was calculated to be a slightly less 65.59% (Figure 3.4A). As predicted, myoblasts proved less robust (statistical data not shown), and they presented a similar trend to that of the myotubes. The difference in metabolic cell viability for the 'normoxia Esumi' group versus the 'normoxia medium' group was measured to be 75.94%. As with myotubes, the difference between the 'hypoxia medium' group versus the SI group was calculated to be slightly less, this time at 72.57% (Figure 3.4B).

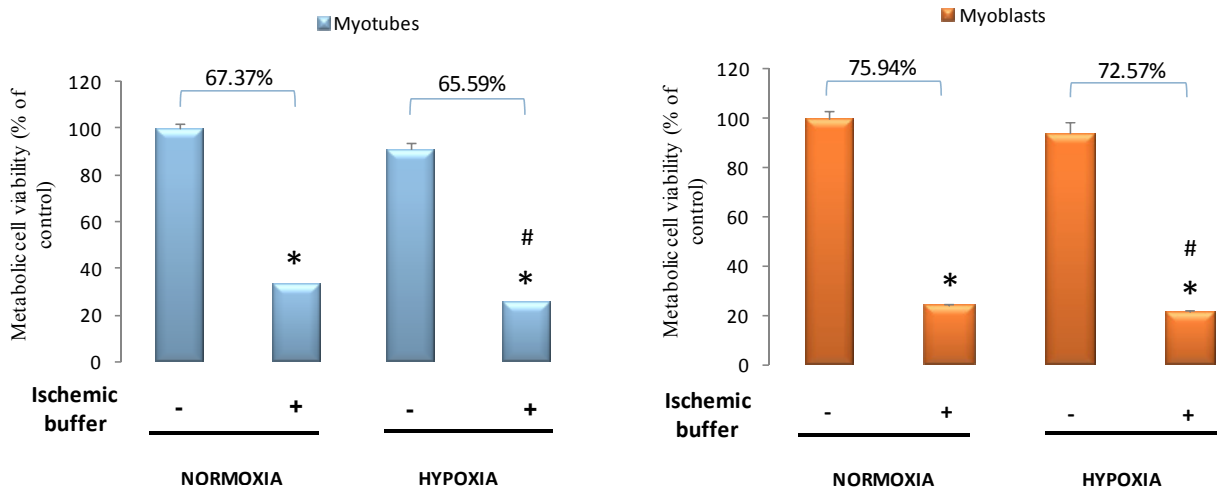

Figure 3.4 Differences in metabolic cell viability after 3 hours in normoxia or hypoxia, both with and without a modified Esumi buffer. Myoblasts and differentiated myotubes (day 10) were incubated both with and without a modified Esumi buffer and differences in metabolic cell viability was measured vs. their normoxic or hypoxic controls after three hours. Cell activities were measured by the MTT assay. Results are presented as their mean ± S.E.M ($n \geq 3$). *p<0.05 vs. untreated control, #p<0.05 vs. normoxia with ischemic buffer

3.3 Effects of 3 hrs 'acute' intervention on PI3K

Phosphatidylinositol 3 kinase (PI3K) is an integral signalling node that plays a role in many cellular processes including the regulation of cell death. PI3K is considered in this section.

Note on representation of Western blot analysis in this chapter: protein expression intensities are expressed relative to baseline levels (always the untreated, normoxic control, unless stated otherwise). Controls present on each Western blot data were normalized (to 1), and all protein levels were expressed as a percentage relative to their control. All of the Western blot analysis presented herein is that of protein expression in C2C12 myotubes only. Also, blots showing total protein levels or β-actin were obtained from stripped membranes.

3.3.1 p85 subunit of PI3K (Western blots)

The p85 subunit of PI3K was found to be constitutively expressed in C2C12 myotubes on day ten post-differentiation. Compared to the untreated controls, endogenous levels of the p85 subunit decreased significantly ($p<0.05$) during acute SI. Cell extracts from myotube cultures incubated in hypoxia in the absence of the modified Esumi buffer showed a statistically insignificant trend towards a decrease in p85 protein levels (Figure 3.5A). Although p85 levels for myotubes incubated in three hours of hypoxia were lower than untreated controls, they were higher in contrast to the myotubes in SI. These changes were found to be statistically insignificant however.

As an aside, C2C12 myotubes were incubated in the modified Esumi buffer for three hours, this time in the absence of hypoxia (i.e. normoxic conditions). Interestingly, no prominent difference in p85 was found between this and the baseline state (Figure 3.5B).

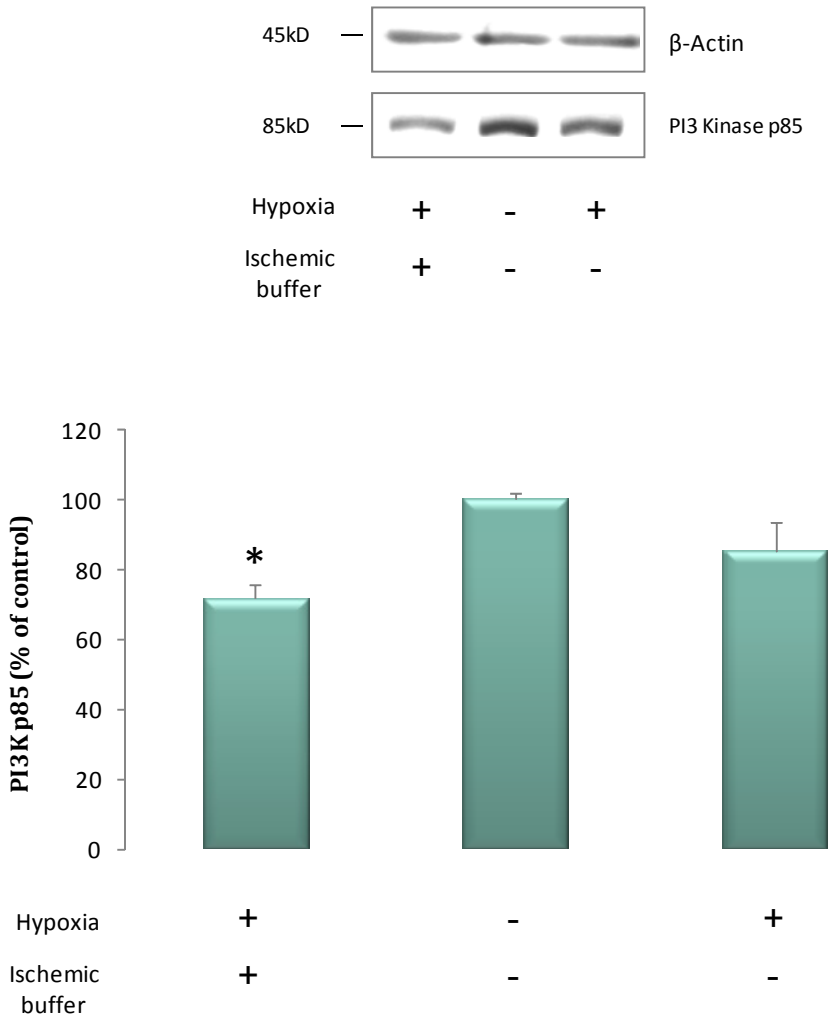

Figure 3.5A The effect of 3 hrs of hypoxia or simulated ischemia on protein expression of PI3K's regulatory p85 subunit. Samples were examined by Western blot analysis with antibodies recognizing the p85 regulatory subunit of PI3K. Results are presented as their mean ± S.E.M, *p<0.05 vs. untreated control (n ≥ 3).

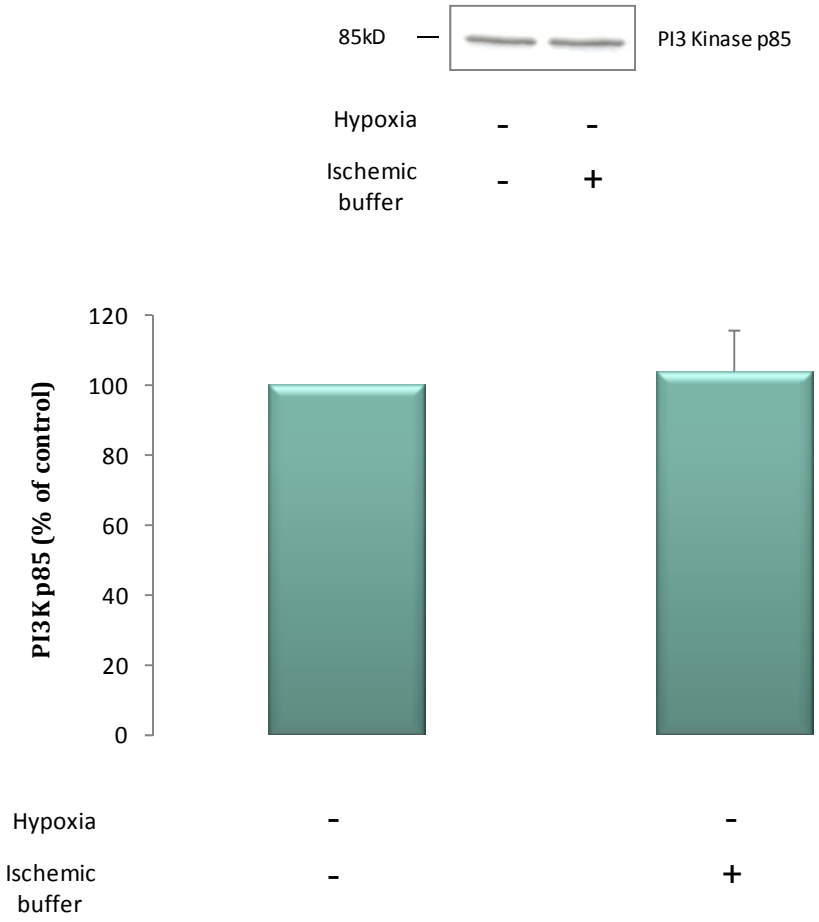

Figure 3.5B The effect of a modified Esumi buffer on protein expression of PI3K's regulatory p85 subunit. Samples were examined by Western blot analysis with antibodies recognizing the p85 regulatory subunit of PI3K. Results are presented as their mean ± S.E.M, ($n \geq 3$).

3.3.2 p110 subunit of PI3K (Western blots)

Protein levels of the catalytic p110 subunit echo those found for the p85 subunit (p85 subunit results given in section 3.1). The p110 subunit was found to be expressed constitutively in myotubes on day ten post-differentiation. Compared to the normoxic controls, protein levels of the p110 subunit decreased significantly during acute SI. In a reflection of previous results, myotube cultures incubated in three hours of hypoxia showed a statistically non-significant tendency towards decreased endogenous levels of the p110 subunit (Figure 3.6A). The cell extracts of myotubes incubated in hypoxia showed elevated p110 levels compared to myotubes in SI.

C2C12 myotubes were also incubated in the modified Esumi buffer for three hours in the absence of hypoxia, as before. Again, no marked difference was found for p110 levels between this and the baseline state (Figure 3.6B).

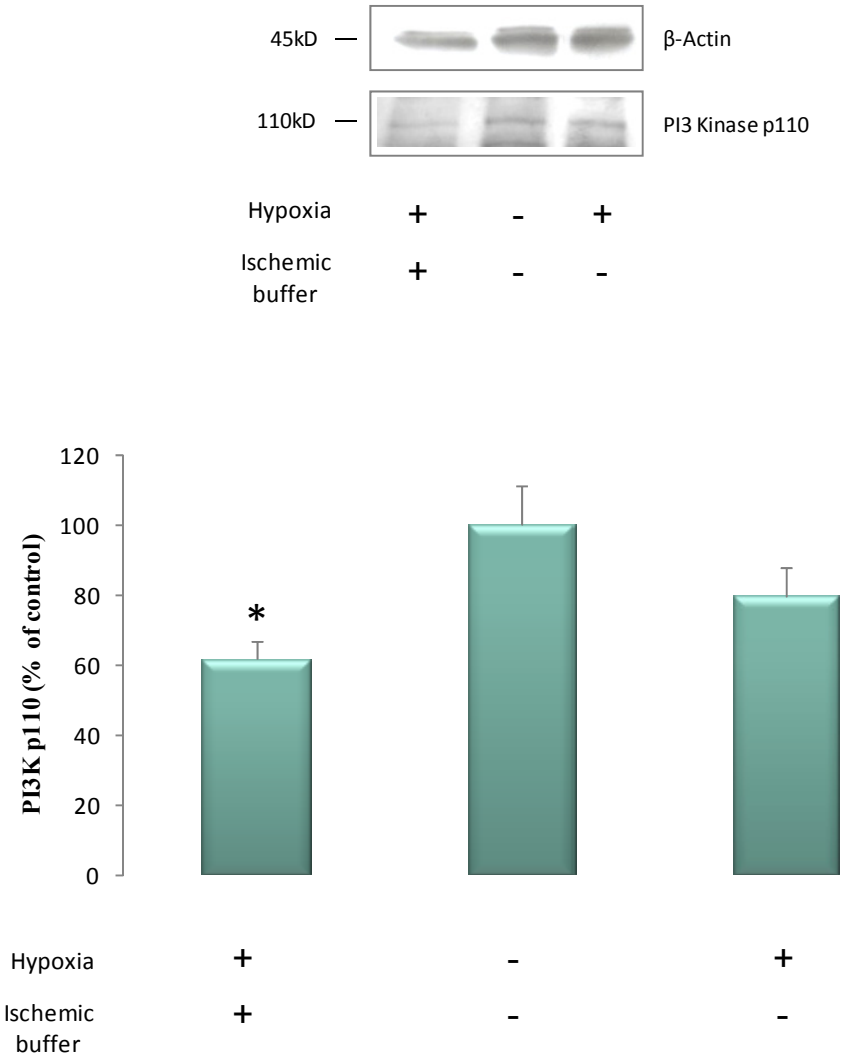

Figure 3.6A The effect of 3 hrs of hypoxia or simulated ischemia on protein expression of PI3K's catalytic p110 subunit. Samples were examined by Western blot analysis with antibodies recognizing the p110 catalytic subunit of PI3K. Results are presented as their mean ± S.E.M, *p<0.05 vs. untreated control (n ≥ 3).

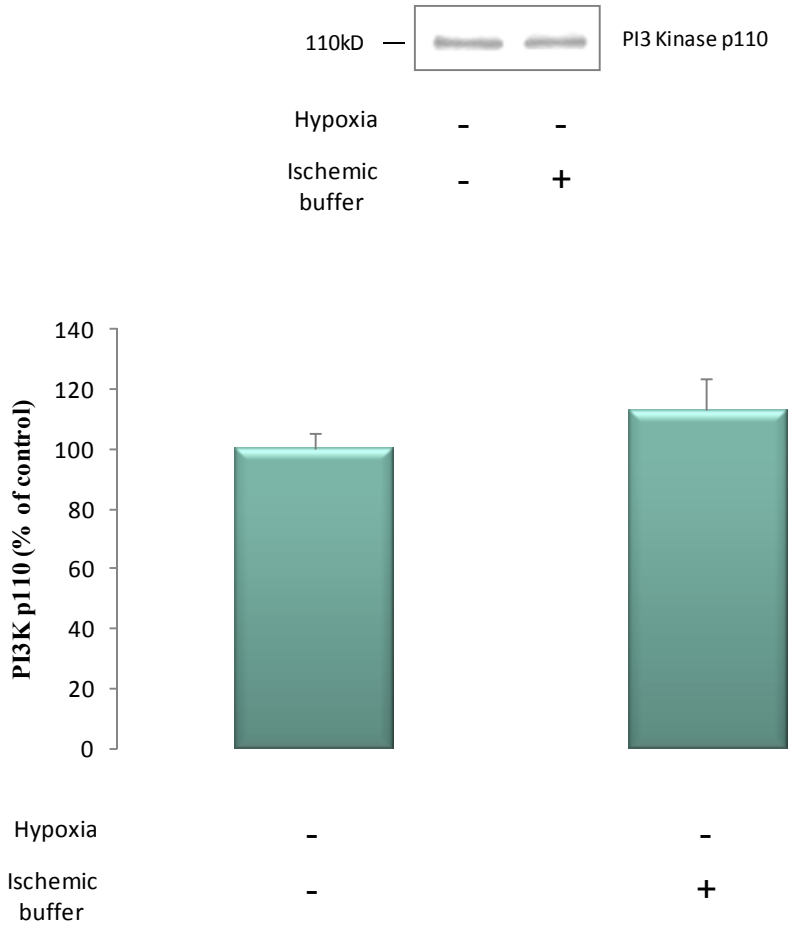

Figure 3.6B The effect of a modified Esumi buffer on protein expression of PI3K's catalytic p110 subunit. Samples were examined by Western blot analysis with antibodies recognizing the p110 catalytic subunit of PI3K. Results are presented as their mean ± S.E.M, ($n \geq 3$).

3.3.3 PI3K ELISA

Utilizing the p85 subunit of PI3K immunoprecipitated from cell extracts, a competitive PI3K ELISA was performed in order to corroborate the information gained from Western blot analysis of PI3K subunits.

We observed a similar trend to that of the Western blot data formerly obtained. From the ELISA data, it can be inferred that raised levels of active PI3Kα are present in C2C12 myotubes (Figure 3.7). Previous experiments demonstrated that acute SI led to significantly lower PI3K levels for both the p85 and p110 subunits. This is verified by the decreased, lipid catalysed production of $PI(3,4,5)P_3$ in this assay. Also, as forecast by our Western blot data, myotubes incubated in three hours hypoxia alone showed a trend towards decreased $PI(3,4,5)P_3$ generation, albeit an non-significant one.

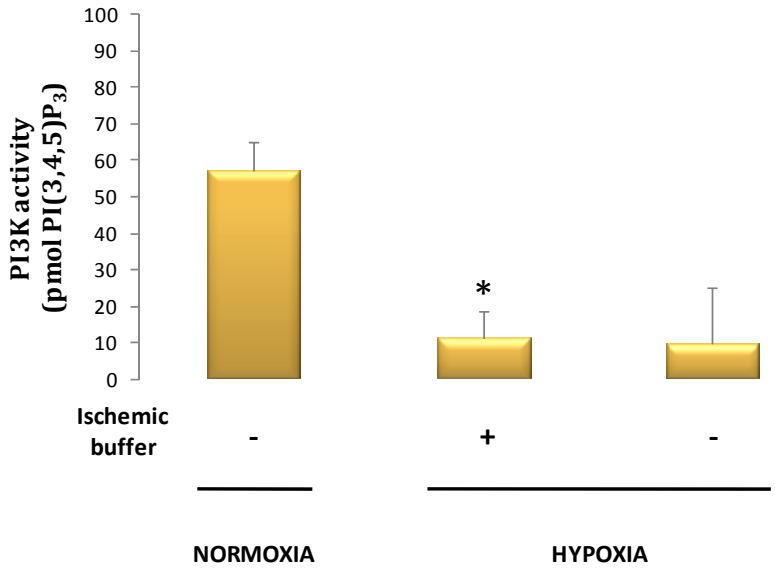

Figure 3.7 The effect of 3 hrs of hypoxia and simulated ischemia on the PI3Kα catalysed production of $PI(3,4,5)P_3$ in C2C12 myotubes. The p85 subunit of PI3K was immunoprecipitated from cell lysates using an anti-PI3K antibody before a competitive ELISA assay was used to detect the amount of $PI(2,4,5)P_3$ produced from a substrate. Results are presented as their mean ± S.E.M of true values obtained, *p<0.05 vs. untreated control ($n \geq 3$).

3.3.4 Inhibitors of the PI3K pathway (MTT cell activities)

Both of the major selective inhibitors of the PI3 kinase pathway, wortmannin and 2-(4-morpholino)-8-phenyl-4H-1-benzopyran-4-one (LY294002), were tested in this study.

3.3.4.1 Wortmannin

The addition of wortmannin (200 nM) leads to a decrease in the metabolic cell viability of C2C12 myotubes (Figure 3.8A). While cells incubated in three hours of SI, both with and without wortmannin supplementation, have significantly lower metabolic cell viabilities than those incubated in acute hypoxia alone, interestingly, the addition of 200 nM wortmannin showed no further decrease in the already decreased metabolic cell viabilities of myotubes incubated in hypoxia (Figure 3.8B). A DMSO vehicle control showed only a small, insignificant decrease in metabolic cell viability.

3.3.4.2 LY294002

The selective inhibitor LY294002 was used in concentrations up to 100 μM in this study. As expected, there was a successive decrease in the metabolic cell viabilities of C2C12 myotubes incubated in normoxic conditions with increasing concentrations of the inhibitor (Figure3.9A). In a similar trend to the results found for wortmannin, LY294002 showed no significant decrease in the metabolic cell viabilities for C2C12 myotubes incubated in acute SI (Figure 3.9B). A significant reduction in metabolic cell viability was only achieved when using the high, 100 μM, concentration of the inhibitor.

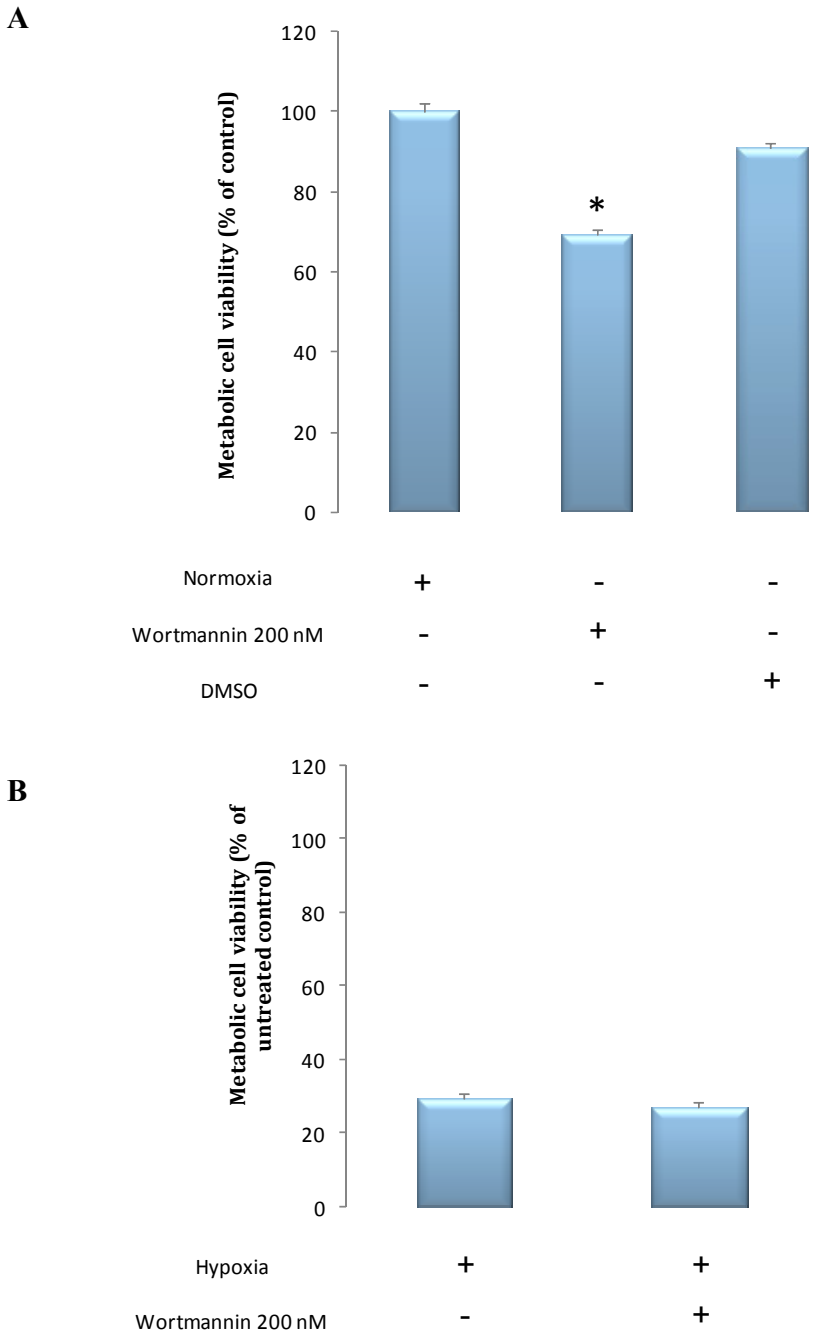

Figure 3.8 Wortmannin decreases metabolic cell viability in C2C12 myotubes incubated in normoxia but not in those incubated in 3 hrs of simulated ischemia. Wortmannin (200 nM) was added to myotube cultures 20 min prior to the incubation step. Simulated ischemia consisted of 3 hours in a modified Esumi buffer in 1.0% oxygen tension (B). Metabolic cell viability was measured using the MTT assay. Results are presented as their mean ± S.E.M, *p<0.05 vs. control (n ≥ 3).

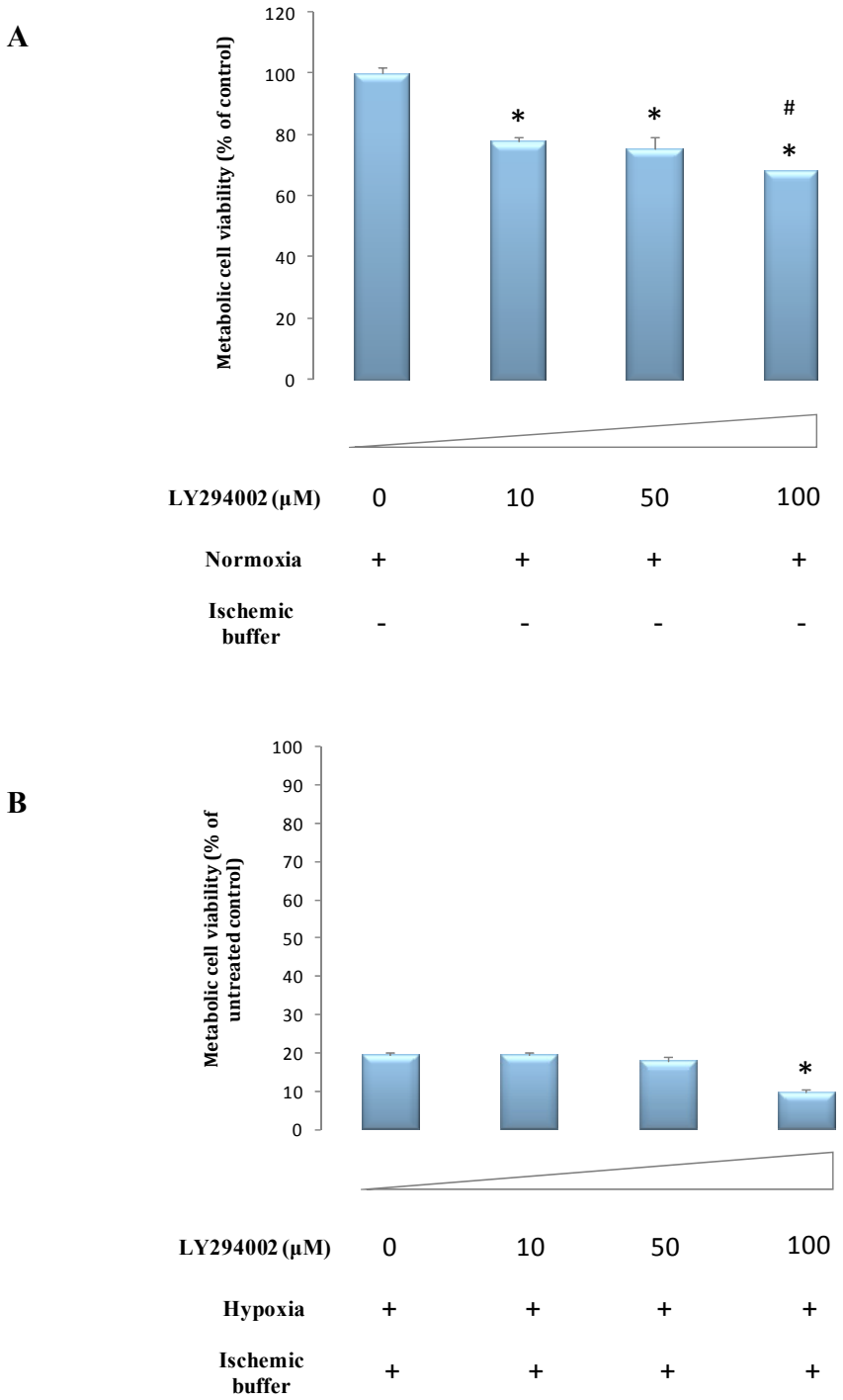

Figure 3.9 LY294002 decreases metabolic cell viability in C2C12 myotubes incubated in normoxia but not in those incubated in 3 hrs of simulated ischemia. Only a high concentration, 100 µM, of LY294002 shows decreased metabolic cell viability (B). LY294002 was added to myotube cultures 20 min prior to the incubation step. Cell activities were measured using the MTT assay. Results are presented as their mean ± S.E.M, *p<0.05 vs. control (n ≥ 3); #p<0.05 vs. 10µM inhibitor (n ≥ 3)

3.3.5 PTEN and PDK-1 (Western blots)

3.3.5.1 PTEN

Inositol phospholipids produced by the action of PI3K are key substrates of PTEN (phosphatase and tensin homologue detected on chromosome ten). PTEN is therefore a key negative regulator of PI3K, hence its consideration here.

No change in phosphorylation of PTEN at the serine 380 position was found for myotubes incubated in three hours of SI, in this study (Figure 3.10).

3.3.5.2 PDK-1

Phosphorylation of PDK-1 (Phosphoinositide-dependent protein kinase 1) at its serine 241 position is essential for its activity. PDK-1 is necessary for the phosphorylation of Akt at the threonine 308 position. PDK-1 phosphorylation is assessed here.

No change in phosphorylation of PDK-1 at the serine 241 position was found for myotubes incubated in three hours of SI or in myotubes incubated in acute hypoxia in the absence of a modified Esumi buffer (Figure 3.11).

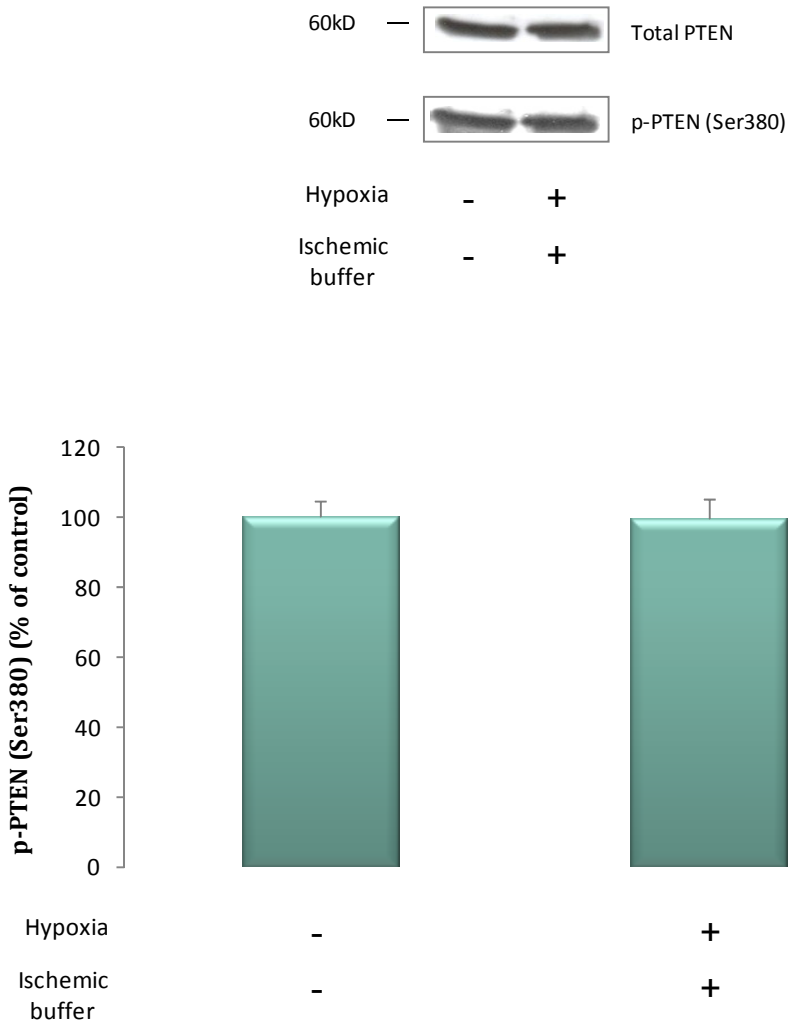

Figure 3.10 PTEN phosphorylation at serine 380 is not affected by incubation in 3 hrs of simulated ischemia. Samples were examined by Western blot analysis with antibodies recognizing PTEN only when phosphorylated at the serine 380 position. Results are presented as their mean ± S.E.M, ($n \geq 3$).

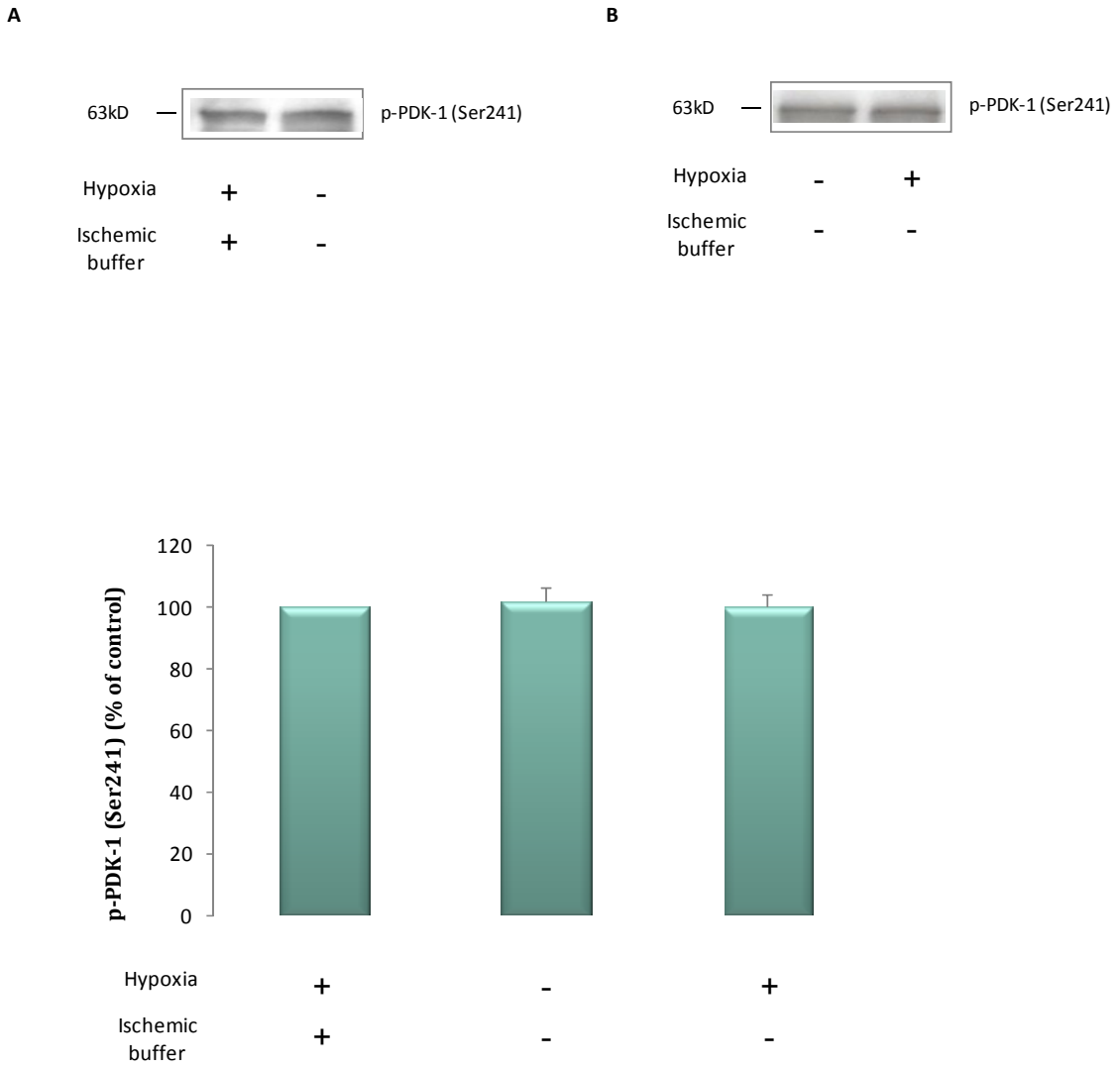

Figure 3.11 PDK-1 phosphorylation at serine 241 is not affected by incubation in 3 hrs of hypoxia or simulated ischemia. Samples were examined by Western blot analysis with antibodies recognizing PDK-1 only when phosphorylated at the serine 241 position. Results are presented as their mean ± S.E.M, ($n \geq 3$).

3.4 Akt (Western blots)

Akt (PKB) operates downstream of PI3K and has a key responsibility in the regulation of cell survival. By phosphorylating of certain proteins it can inhibit apoptosis and control protein synthesis. Important downstream effectors include CREB, FKHR, AFX and TSC2.

3.4.1 Phospho-Akt (Ser473)

The levels of phosphorylated Akt (Ser473) detected here are consistent with our previous results. As with PI3K, levels of phospho-Akt (Ser473) decreased significantly ($p<0.03$) with incubation in acute SI, compared to the normoxic controls. Myotube cultures placed in acute hypoxia in the absence of the modified Esumi buffer show a statistically insignificant tendency towards reduced phosphorylation of Akt (Ser473) compared to controls but did not differ from SI cultures (Figure 3.12).

C2C12 myotubes were incubated in the modified Esumi buffer for three hours, in the absence of hypoxia. No noticeable difference in phospho-Akt was found between these cultures and the baseline state (Figure 3.15).

3.4.1.1 Inhibitors

Myotube cultures were incubated in three hours of SI supplemented with LY294002 (Figure 3.13) or wortmannin (Figure 3.14A). Phosphorylation of Akt at the serine 473 position decreased with increasing concentrations of the inhibitors, as expected.

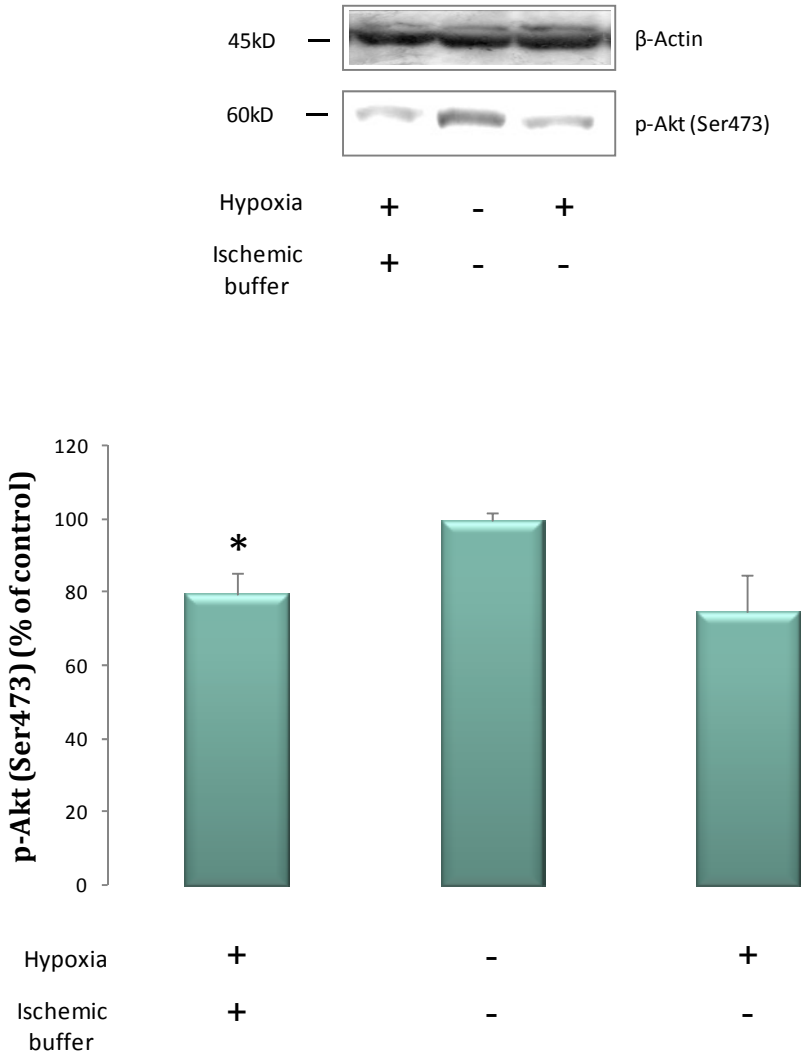

Figure 3.12 The effect of 3 hrs of hypoxia or simulated ischemia on phosphorylation of Akt (Ser473). Samples were examined by Western blot analysis with antibodies recognizing phospho-Akt (Ser473). Results are presented as their mean ± S.E.M, **p*<0.05 vs. control (n ≥ 3).

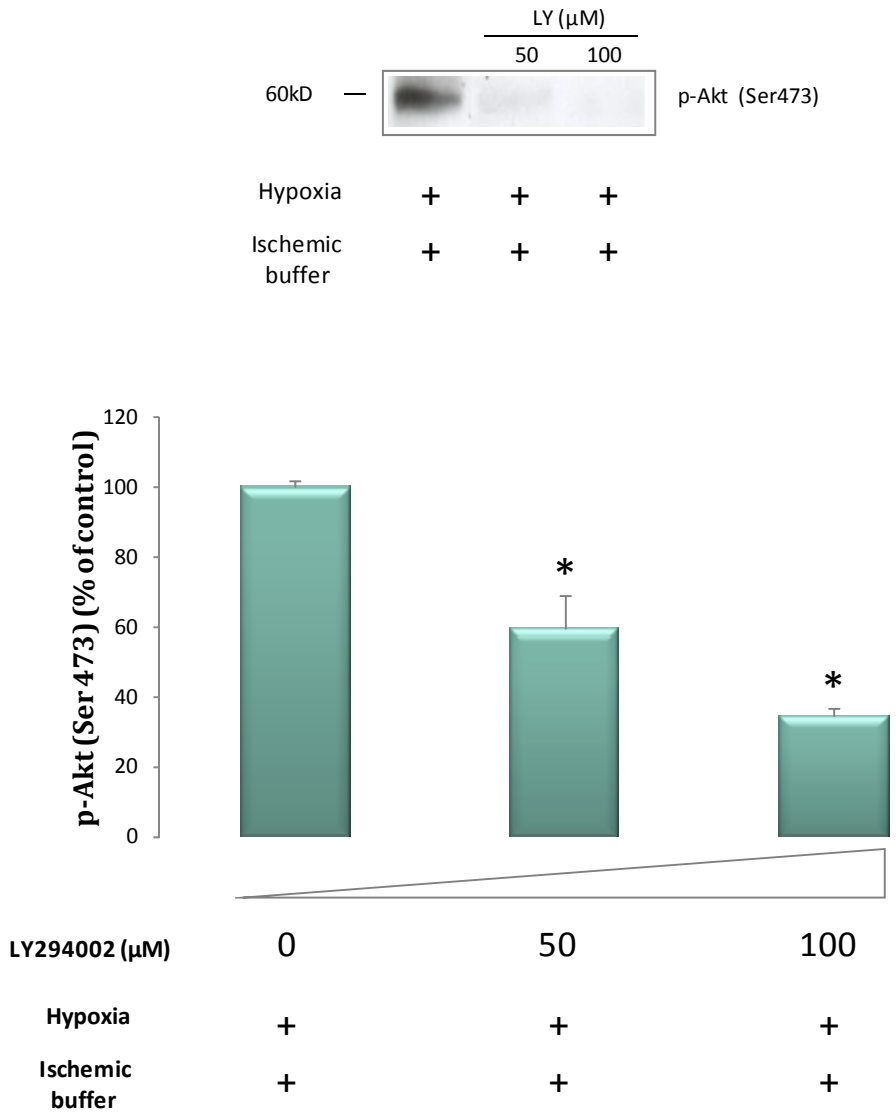

Figure 3.13 LY294002 decreases phosphorylation of Akt (Ser473) in C2C12 myotubes during 3 hrs of simulated ischemia. Samples were examined by Western blot analysis with antibodies recognizing phospho-Akt (Ser473). Results are presented as their mean ± S.E.M, *p<0.05 vs. control (n ≥ 3).

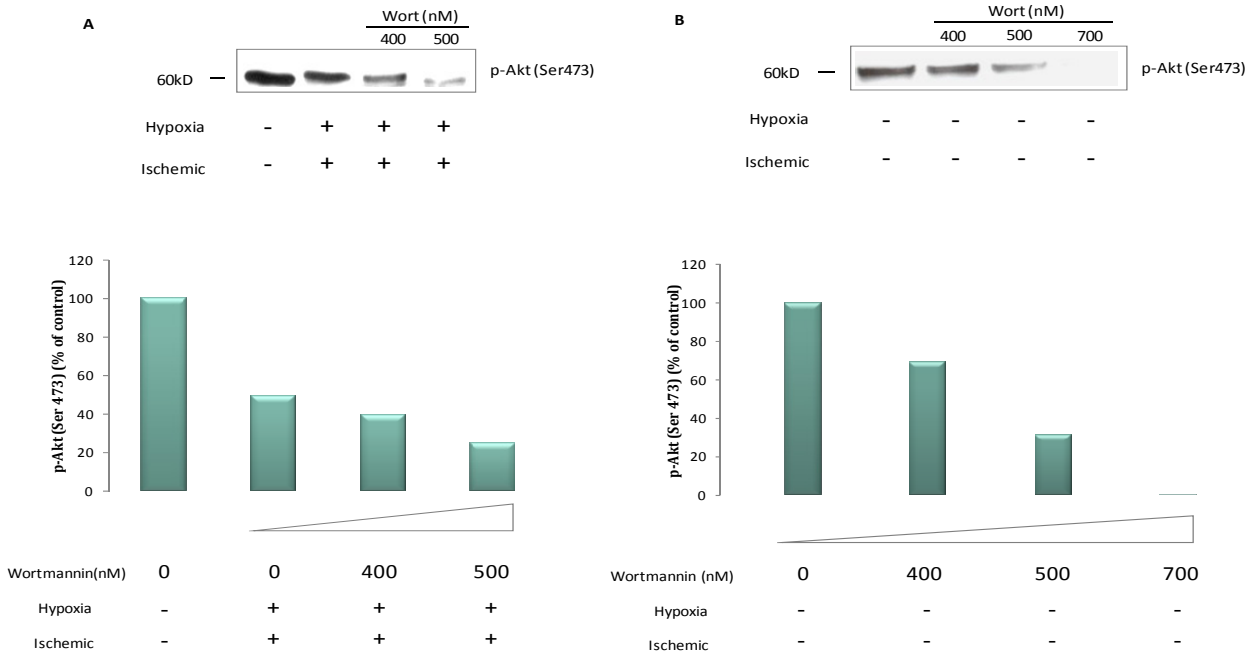

Figure 3.14 Wortmannin decreases phosphorylation of Akt (Ser473) in C2C12 myotubes during 3 hrs of simulated ischemia. Samples were examined by Western blot analysis with antibodies recognizing phospho-Akt (Ser473).

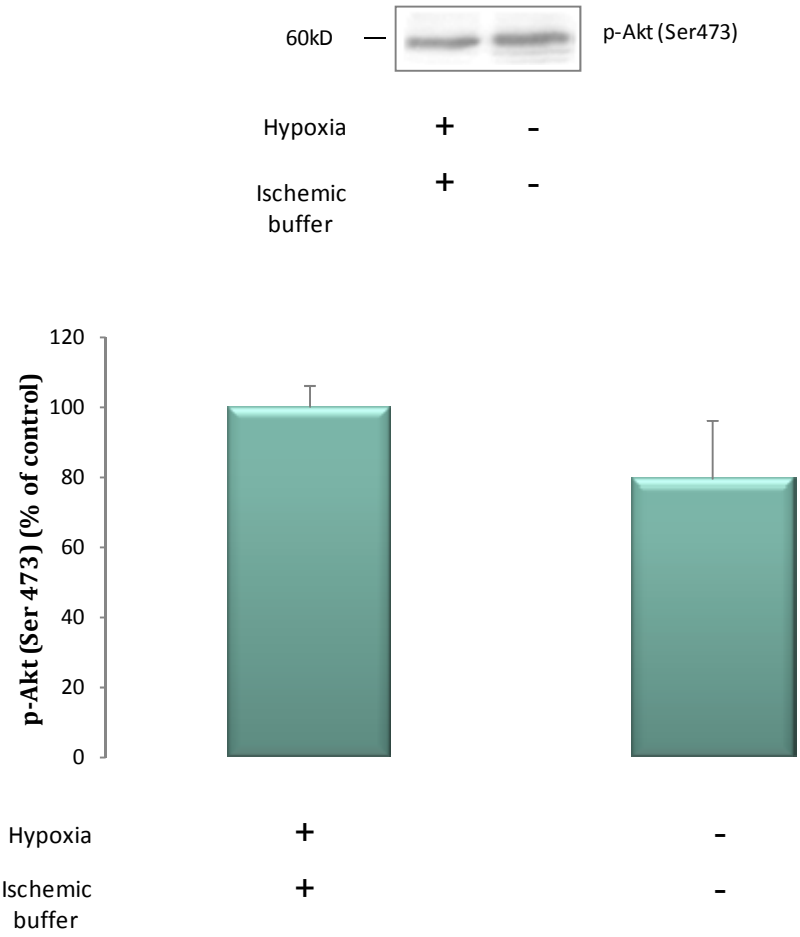

Figure 3.15 The effect of a modified Esumi buffer on phosphorylation of Akt (Ser473) in C2C12 myotubes. Samples were examined by Western blot analysis with antibodies recognizing phospho-Akt (Ser473). Results are presented as their mean ± S.E.M, ($n \geq 3$).

3.4.2 Phospho-Akt Threonine 308

The degree of Akt (Thr308) phosphorylation observed here reflects previous findings for PI3K and Akt (Ser473), and the level of phosphorylation of Akt (Thr308) dropped significantly for cultures during acute SI (Figure 3.16). C2C12s in hypoxia in the absence of the modified Esumi buffer did not differ significantly from normoxic control for phospho-Akt (Thr308).

3.4.2.1 Inhibitors

Myotubes were incubated in three hours of SI, supplemented with LY294002 (Figure 3.17) or wortmannin (Figure 3.18). Phosphorylation of Akt at the threonine 308 position showed a trend of decline for increasing concentrations of the inhibitors, as expected.

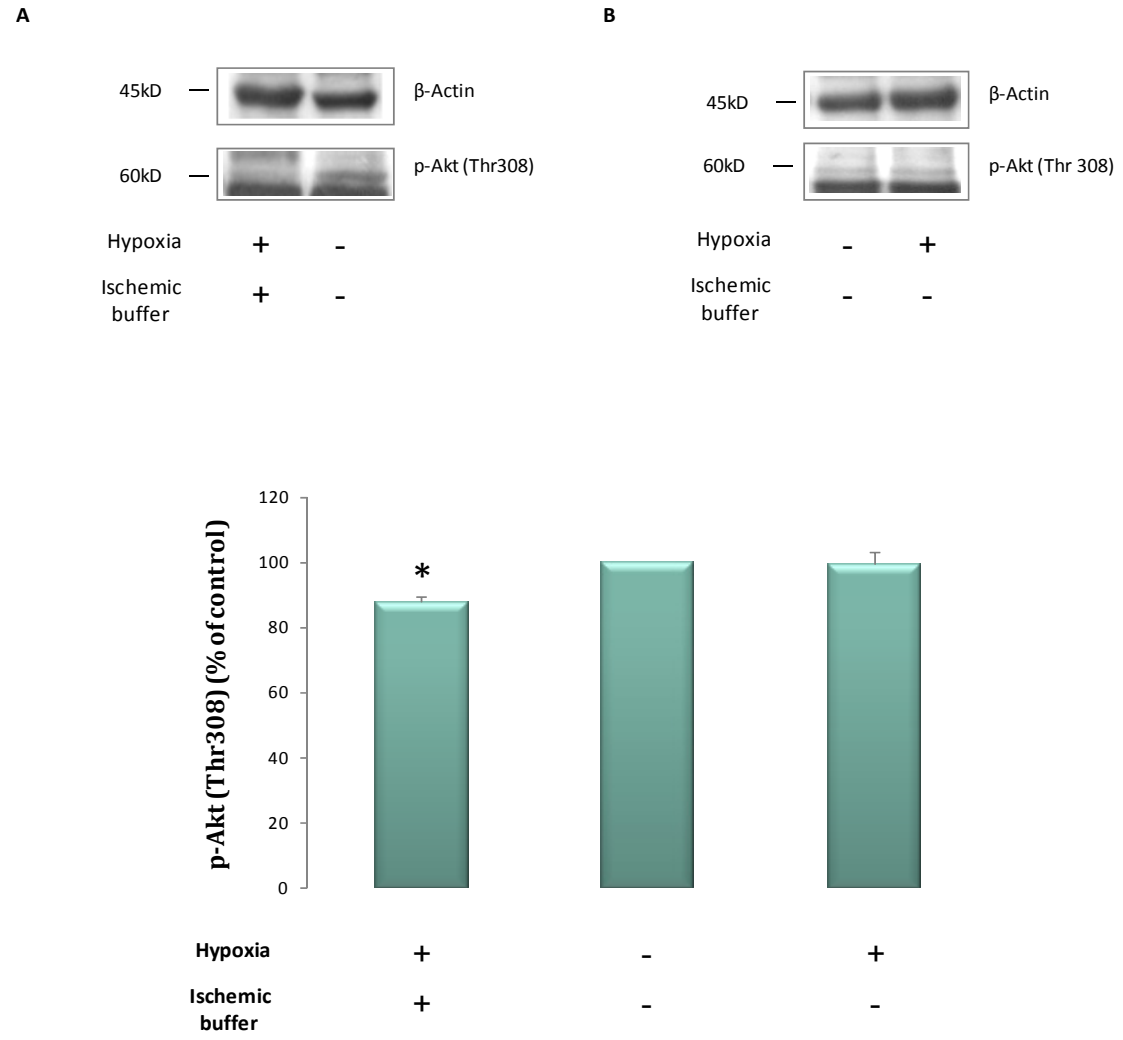

Figure 3.16 The effect of 3 hrs of hypoxia or simulated ischemia on phosphorylation of Akt (Thr308). Samples were examined by Western blot analysis with antibodies recognizing phospho-Akt (Thr308). Results are presented as their mean ± S.E.M, **p*<0.05 vs. control (n ≥ 3).

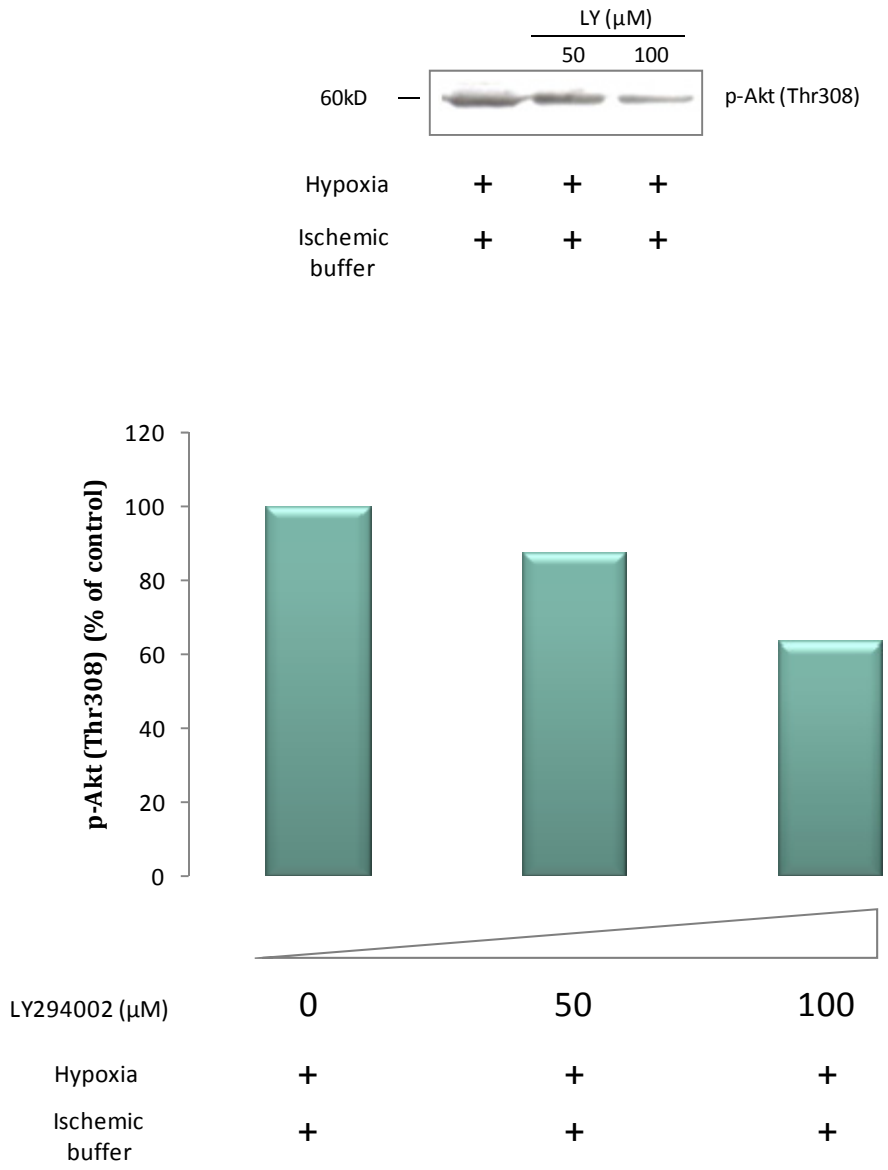

Figure 3.17 LY294002 decreases the level of phosphorylation of Akt (Thr308) in C2C12 myotubes during 3 hrs of simulated ischemia. Samples were examined by Western blot analysis with antibodies recognizing phospho-Akt (Thr308).

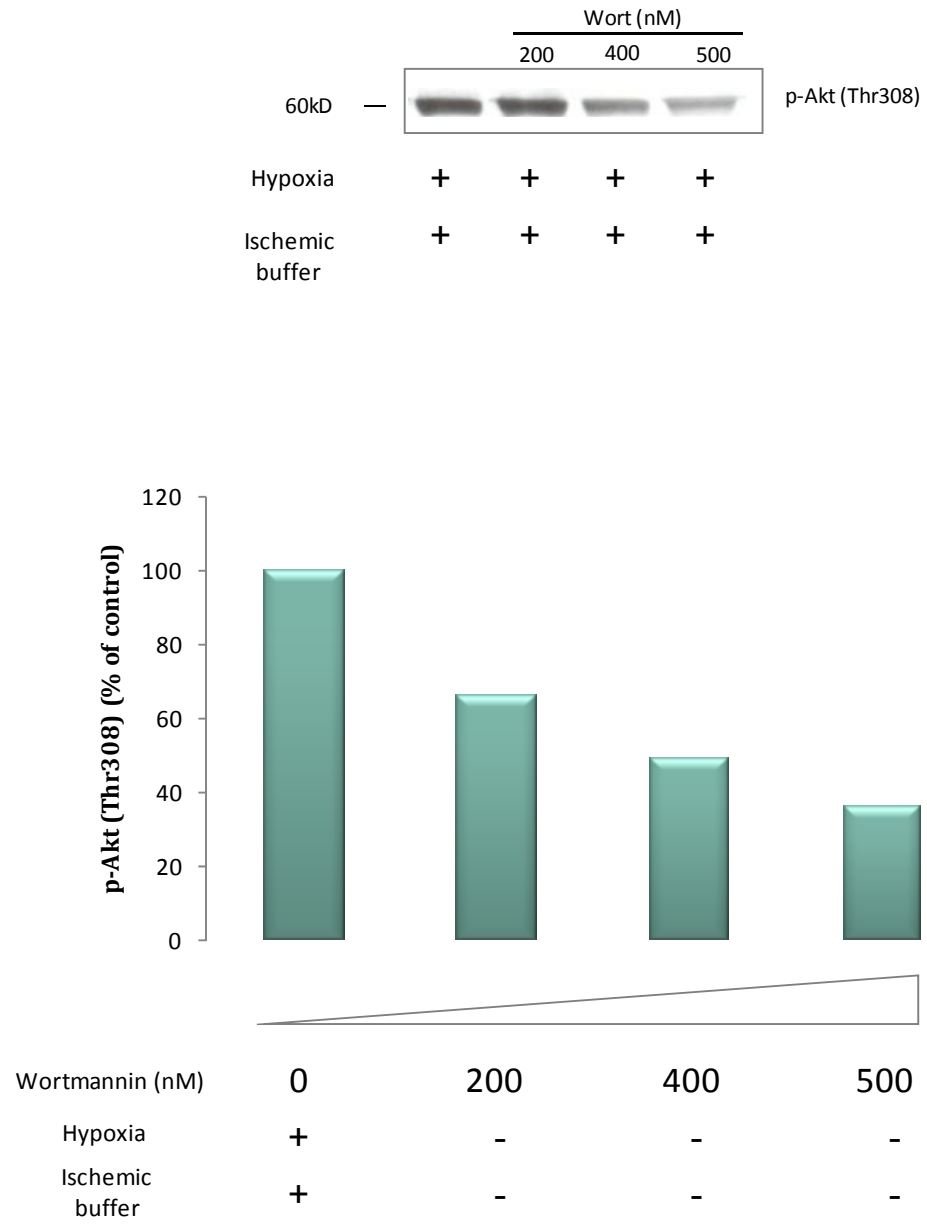

Figure 3.18 Wortmannin decreases phosphorylation of Akt (Thr308) in C2C12 myotubes during 3 hrs of simulated ischemia. Samples were examined by Western blot analysis with antibodies recognizing phospho-Akt (Thr308).

3.4.3 Effectors of phospho-Akt (Western blots)

Akt abrogates cell death through the phosphorylation of many downstream effectors. Three of these are assessed in this section.

3.4.3.1 Fox01 and Fox04

Akt is able to promote cell survival by the phosphorylation and subsequent inactivation of certain members of the forkhead transcription factor family. Two of these, namely Fox01 (FKHR) and Fox04 (AFX), are assessed here.

Phosphorylation of Fox01 and Fox04 both display a similar pattern, and they both show the trends predicted by our previous findings (Figure 3.19). The levels of phosphorylation of Fox01 and Fox04 diminished significantly for C2C12 myotubes during acute SI. Myotubes incubated in three hours of SI and supplemented with LY294002 showed a significant reduction in phosphorylation of Fox01 and Fox04, as anticipated.

3.4.3.2 CREB

Akt is able to phosphorylate and cause the activation of the CREB transcription factor. CREB is investigated here.

Phosphorylation of CREB shows results divergent from those found for Akt. Phosphorylation of CREB was shown to increase significantly for C2C12 myotubes during acute SI, whereas myotubes incubated for three hours with a modified Esumi buffer in the absence of hypoxia showed no difference from the controls (Figure 3.20).

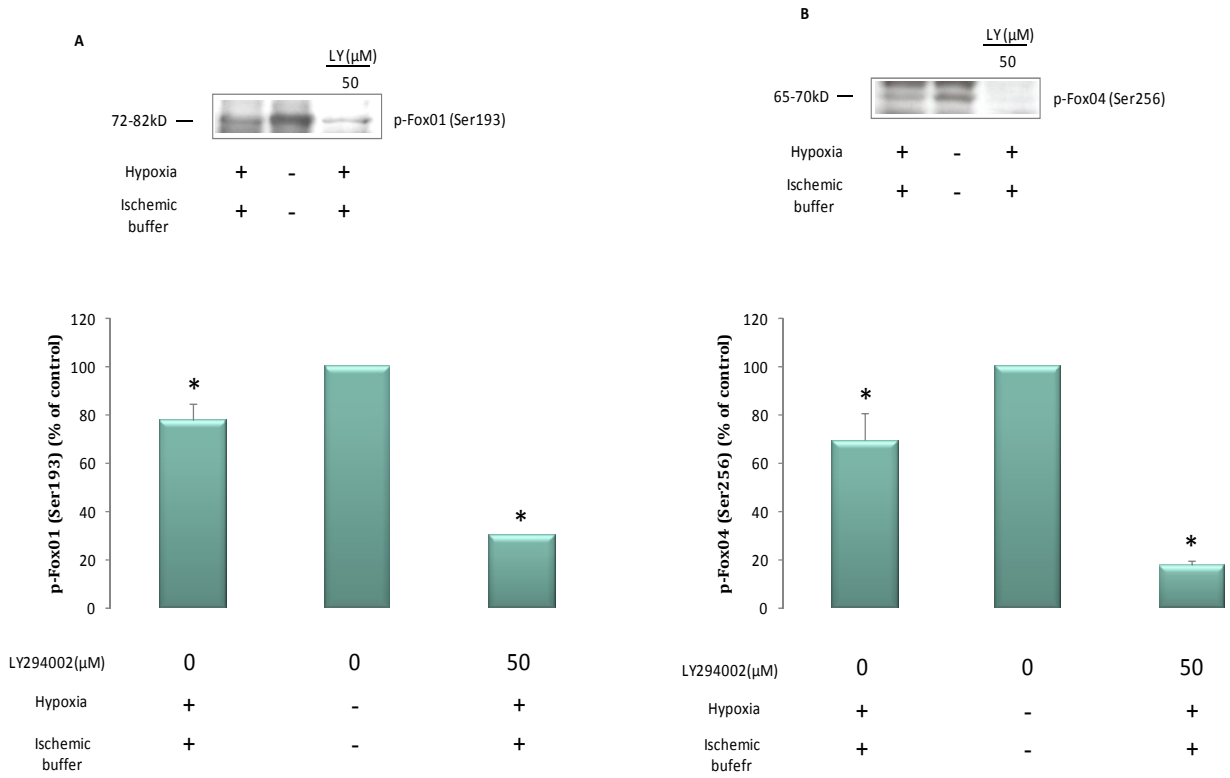

Figure 3.19 The effect of 3 hrs of simulated ischemia and LY294002 on phosphorylation of Fox01 and Fox04. Samples were examined by Western blot analysis with antibodies recognizing phospho-Fox01 (Ser193) and phospho-Fox04 (Ser256). Results are presented as their mean ± S.E.M, *p<0.05 vs. control (n ≥ 3).

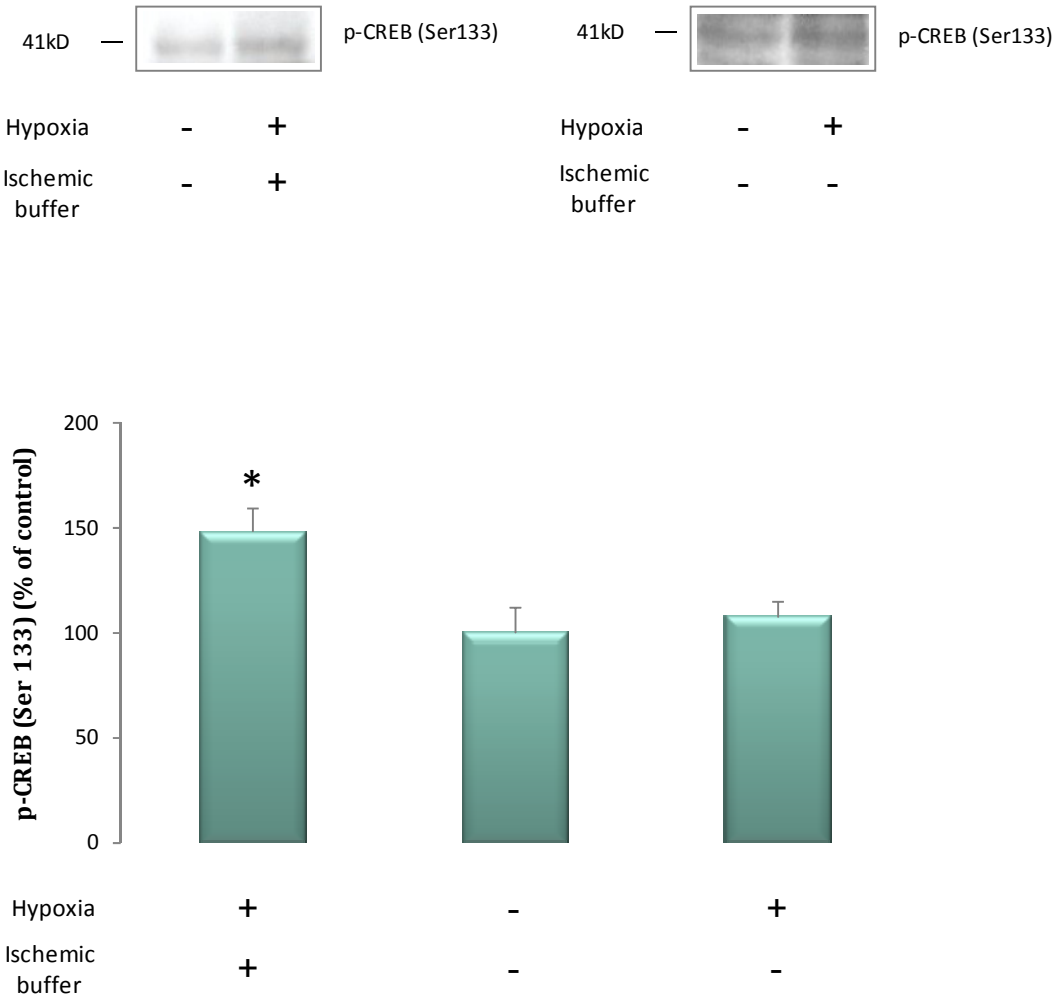

Figure 3.20 The effect of 3 hrs of hypoxia or simulated ischemia on phosphorylation of CREB. Samples were examined by Western blot analysis with antibodies recognizing phospho-CREB (Ser133). Results are presented as their mean ± S.E.M, *p<0.05 vs. control (n ≥ 3).

3.5 Cell death

Three methods are used to assess cell death in this section. That is, detection of apoptosis by Western blot analysis, vital staining using Annexin V and propidium iodide and DNA fragmentation.

3.5.1 Caspase-3 (Western blots)

Caspase-3 is one of the purported 'executioners of cell death'. It is accountable for the proteolytic cleavage of many proteins during apoptosis including poly (ADP-ribose) polymerase (PARP). Caspase-3 is activated following its cleavage into smaller active fragments.

The 19kD, cleaved fragment of caspase-3 was analysed here using Western blots. Detection of the cleaved fragment of caspase-3 increased significantly for C2C12 myotubes during acute SI (Figure 3.21). Myotubes incubated in acute hypoxia without the modified Esumi buffer showed a noticeable trend towards an increase in caspase-3 cleavage, this was not found to be statistically significant however. Three hours of SI supplemented with a high concentration of the PI3K inhibitor LY294002, showed a distinct, significant, increase in caspase-3 cleavage.

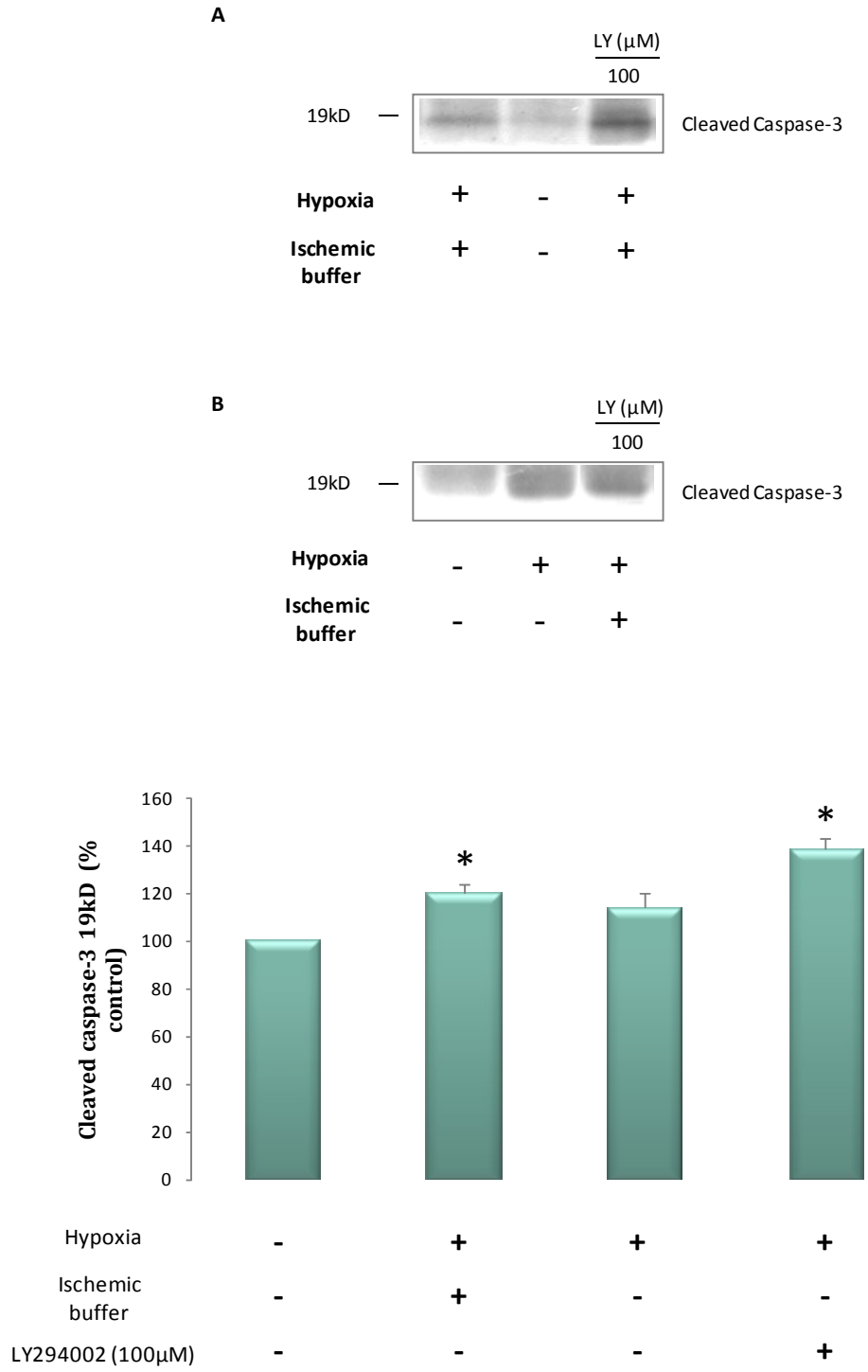

Figure 3.21 Caspase-3 cleavage in C2C12 myotubes incubated in 3 hrs of simulated ischemia. Cultures were supplemented with LY294002 20min prior to incubation. Samples were examined by Western blot analysis with antibodies recognizing caspase-3 and cleaved caspase-3. Results are presented as their mean ± S.E.M, *p<0.05 vs. control ($n \geq 3$).

3.5.2 PARP-1 (Western blots)

During apoptosis, caspase-3 becomes cleaved and in turn cleaves and inactivates PARP-1. PARP-1 is a 116kD enzyme that is cleaved into 85kD and 24kD subunits. In order to indirectly support our caspase-3 findings, the cleaved 85kD subunits are detected here using Western blot analysis.

Detection of the inactive 85kD fragment of PARP-1 increased noticeably for C2C12 myotubes during acute SI (Figure 3.22). This increase was found to be statistically significant. Myotubes incubated in three hours of hypoxia showed a clear, significant trend towards an increase in PARP-1 cleavage. Incubation in acute SI supplemented with a high concentration of the PI3K inhibitor LY294002, showed a definite, albeit insignificant, increase in the appearance of the 85kD subunit of PARP-1. Although they were not examined by means of densitometry, the un-cleaved 116kD PARP-1 units apparently complimented their cleaved subunits, as is expected.

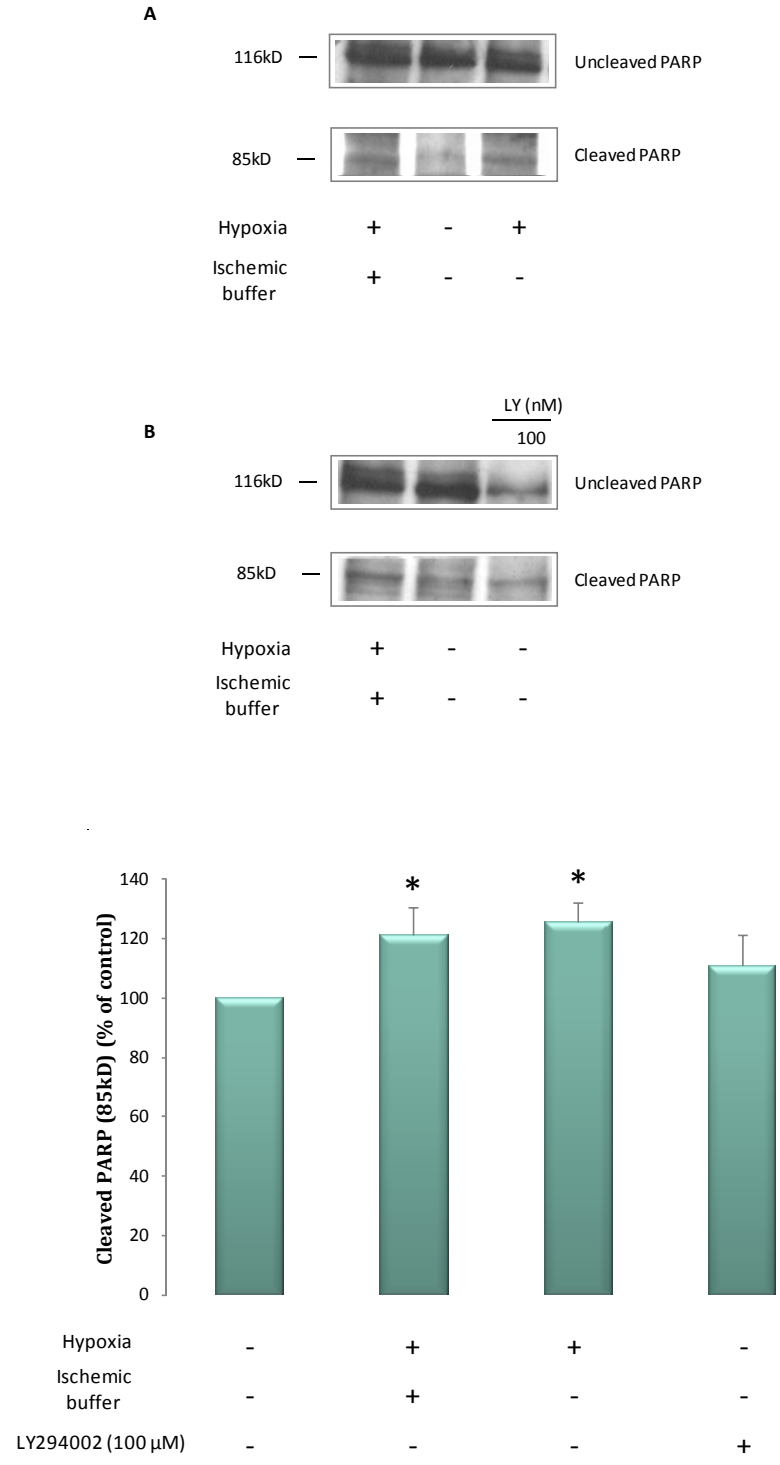

Figure 3.22 PARP-1 cleavage in C2C12 myotubes, triggered during 3 hrs of simulated ischemia. Cultures were supplemented with LY294002 20 min prior to incubation. Samples were examined by Western blot analysis with antibodies recognizing PARP-1 and the cleaved 85kD subunit of PARP-1. Results are presented as their mean ± S.E.M, *p<0.05 vs. control (n ≥ 3).

3.5.3 Assessment of changes in the cell membrane (Vital staining)

3.5.3.1 Propidium Iodide (PI) and Hoechst staining

Propidium iodide is usually excluded from healthy cells whereas Hoechst 33342 is able to diffuse through cell membranes regardless of their condition. Therefore, by co-staining cells with PI and Hoechst, healthy cells can be distinguished from those with damaged membranes. Cells with slightly permeable membranes stain with PI to a small degree. Late apoptotic and necrotic cells stain homogeneously for PI and Hoechst and appear pink when co-stained.

Compared to the normoxic controls, cultures incubated for three hours either with the modified Esumi buffer or in hypoxia showed a similar, significant increase in permeability to PI (Figure 3.24). Myotubes incubated in three hours SI showed an escalating permeability to PI. In fact, SI caused an increase in membrane permeability that was statistically significantly greater than cultures incubated with either the modified Esumi buffer or in hypoxia alone. Pink regions in co-stains of acute SI cultures indicate that some cells are in the late apoptotic or necrotic phase of cell death here (Figure 3.23).

3.5.3.1.1 Inhibitor

Myotubes were incubated in three hours of SI, supplemented with 50 μM LY294002 (Figure 3.25), and this caused a significant increase in membrane permeability in contrast to myotubes incubated in SI alone (Figure 3.26).

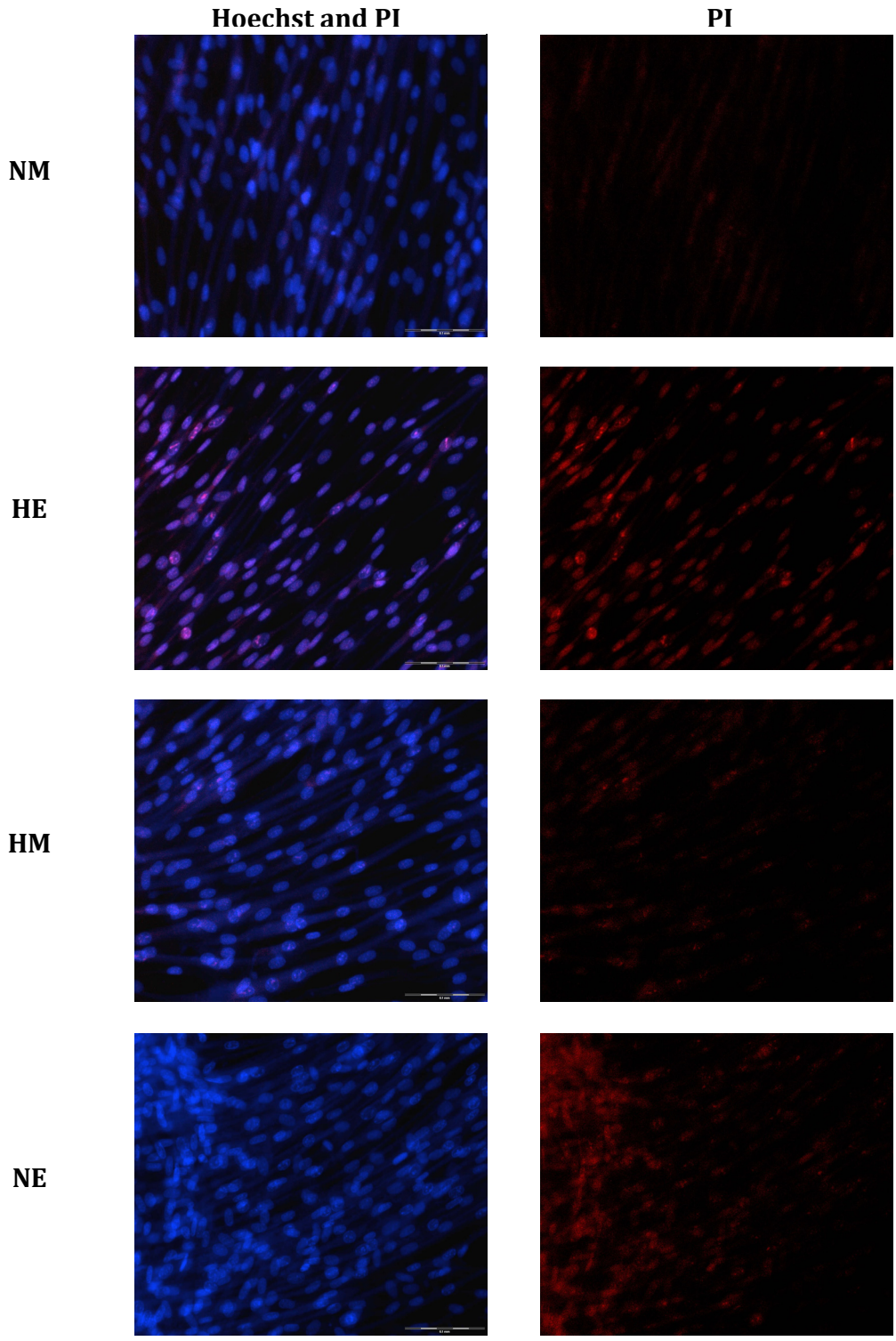

Figure 3.23 The effect of acute of simulated ischemia and hypoxia on membrane permeability of C2C12 myotubes. Cells were stained with Hoechst 33342 (blue) and PI (red) and analysed for membrane impairment using fluorescence microscopy. Healthy cells stain only for Hoechst, late apoptotic cells stain for PI and Hoechst while necrotic cells stain homogenously for PI and Hoechst (pink). NM (Normoxia), HM (Hypoxia), NE (Ischemic buffer), HE (Simulated ischemia), ($n \geq 3$).

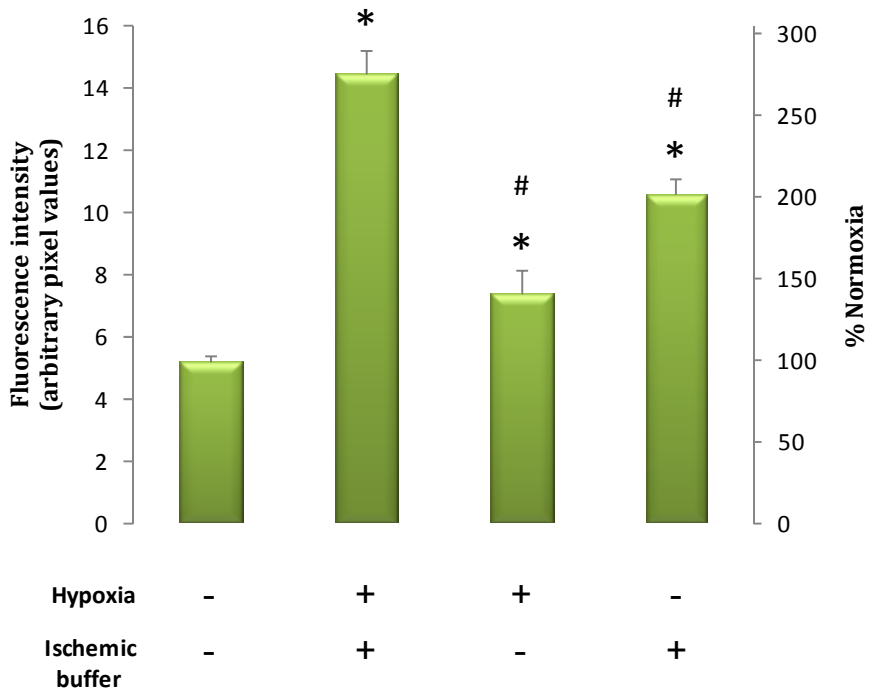

Figure 3.24 Quantification of PI intensity in myotubes incubated in acute hypoxia and with a modified Esumi buffer. Cells were stained with Hoechst 33342 (blue) and PI (red) and analysed using fluorescence microscopy. At least 250 cells were selected and assessed for the fluorescence intensity of PI. Results are presented as their mean ± S.E.M, *p<0.05 vs. control (n ≥ 3); #p<0.05 vs. SI (n ≥ 3). Normoxia refers to the untreated control.

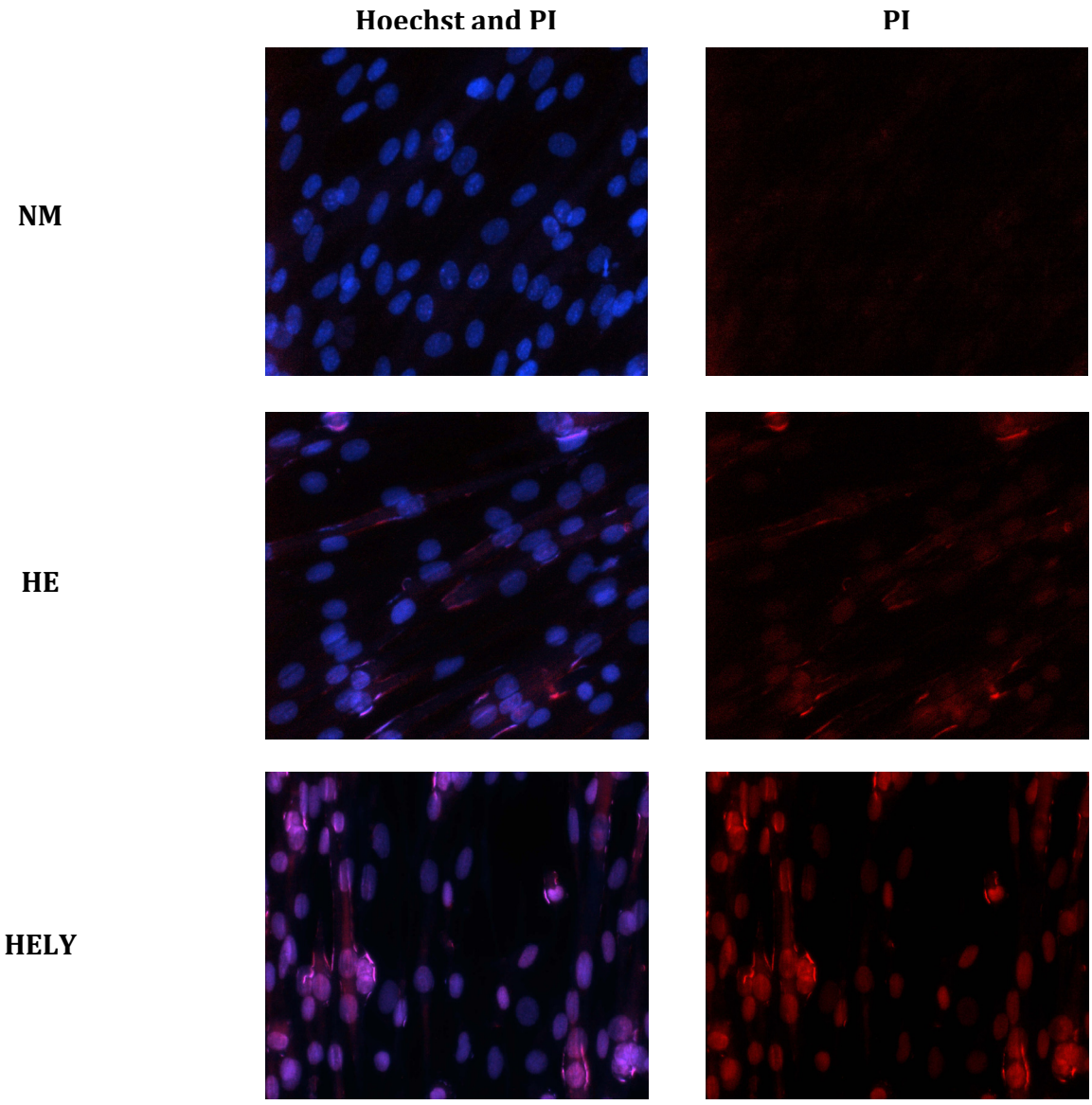

Figure 3.25 The effect of acute simulated ischemia and LY294002 on membrane permeability of C2C12 myotubes. Cells were stained with Hoechst 33342 (blue) and PI (red) and analysed for membrane impairment using fluorescence microscopy. Healthy cells stain only for Hoechst, late apoptotic cells stain for PI and Hoechst while necrotic cells stain homogenously for PI and Hoechst (pink). NM (Normoxia), HE (Simulated ischemia), HELY (Simulated ischemia + 50 μM LY294002), ($n \geq 3$).

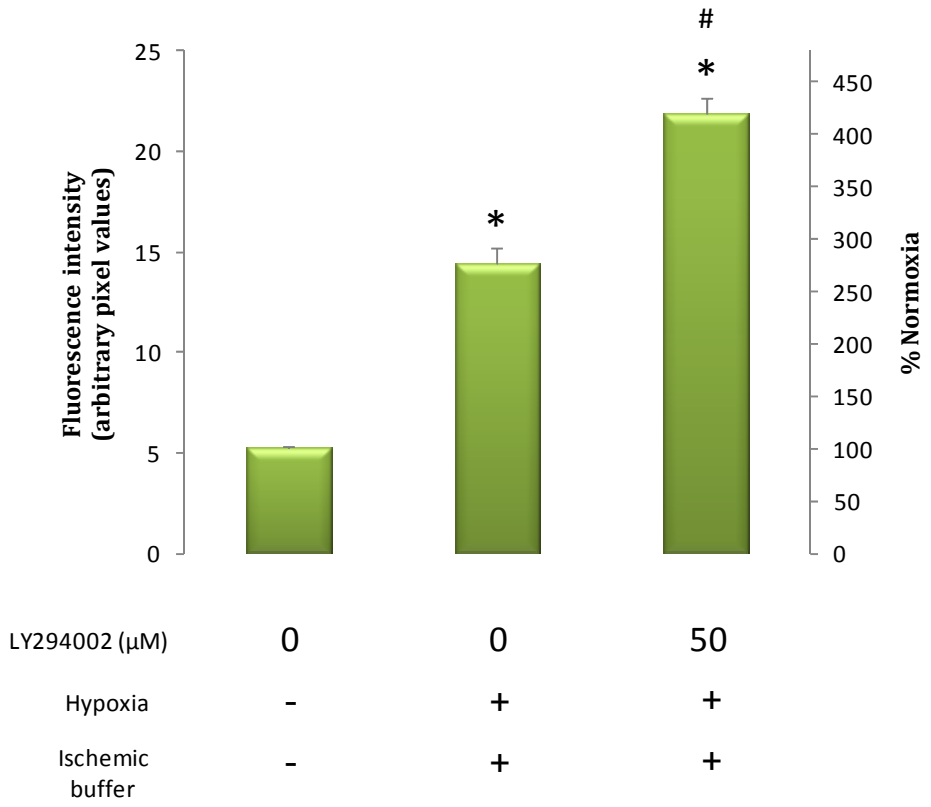

Figure 3.26 Quantification of PI intensity in myotubes incubated in acute simulated ischemia and LY294002. Cells were stained with Hoechst 33342 (blue) and PI (red) and analysed using fluorescence microscopy. At least 145 cells were selected and assessed for the fluorescence intensity of PI. Results are presented as their mean ± S.E.M, *p<0.05 vs. control (n ≥ 3). Normoxia refers to the untreated control.

3.5.3.2 Annexin V and Hoechst staining

Normal cells possess an asymmetric distribution of phospholipids in the leaflets of the cell membrane. During apoptotic cell death, this asymmetry is lost and phosphatidylserine (PS) becomes abundant in the outer leaflet of the cell membrane. Annexin V is a phospholipid binding protein that has a high affinity for PS. Here we have conjugated Annexin V to a fluorescent molecule in order to label apoptotic cells. Notably, Annexin V is known to bind at the fusion points of C2C12 myotubes, even in non-apoptotic cells.

Compared to the normoxic controls, a significant increase in Annexin V binding was observed for cultures incubated for three hours in hypoxia in normal culture medium (Figure 3.27 & 3.28). Annexin V binding was found to be 80.5% greater when myotubes were incubated in acute SI.

3.5.3.2.1 Inhibitor

Myotubes were incubated in three hours of SI, supplemented with 50 μM LY294002 (Figure 3.29), but there was no significant difference in apparent Annexin V binding between these and cultures incubated in SI alone (Figure 3.30). In fact, a slight trend towards a decrease was seen in cultures of SI with inhibitor compared to SI cultures without inhibitor

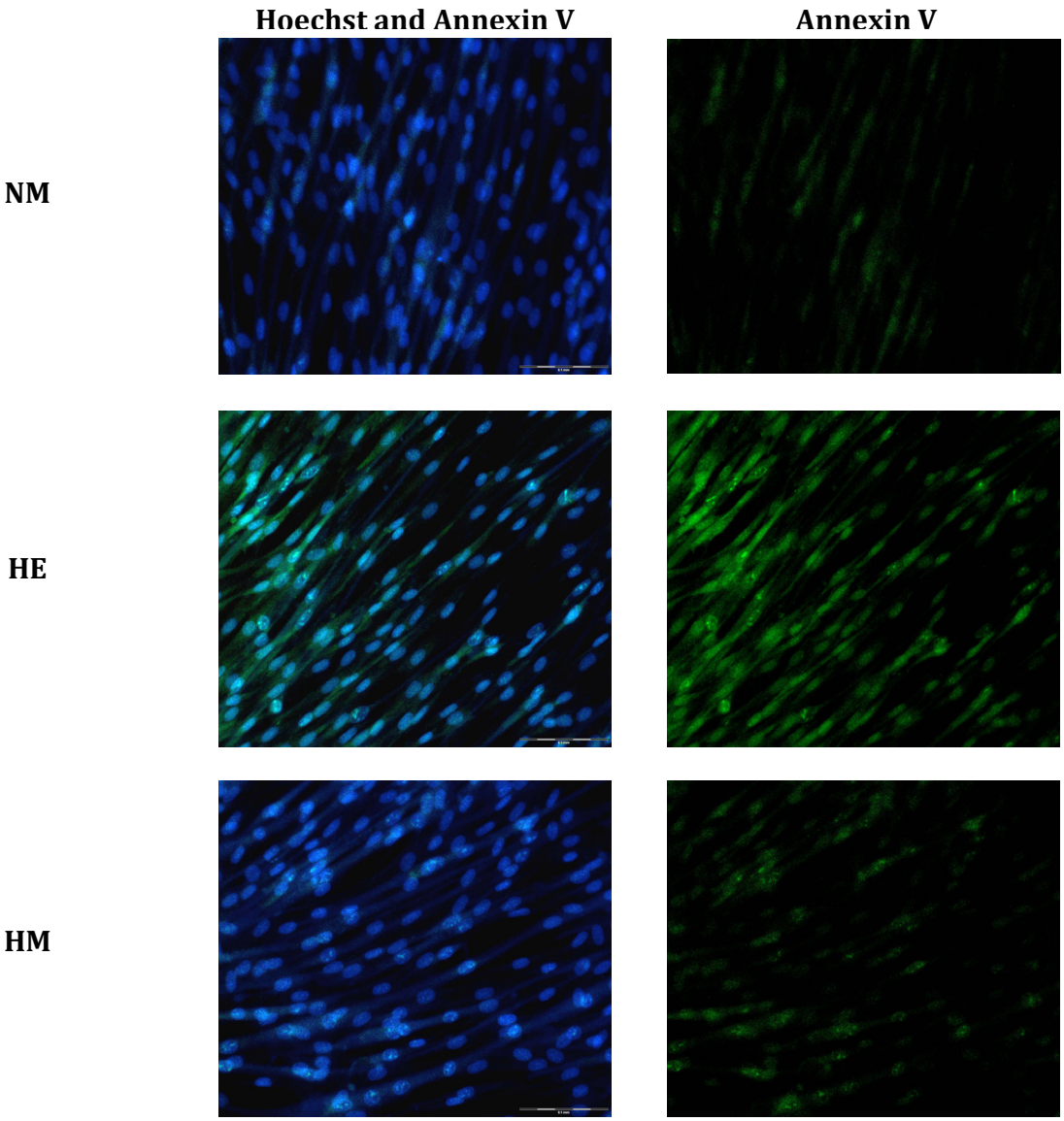

Figure 3.27 The effect of acute hypoxia and simulated ischemia on apoptosis - Annexin V binding. Cells were stained with Hoechst 33342 (blue) and Annexin V (green) and analysed for apoptosis using fluorescence microscopy. Healthy cells stain only for Hoechst whereas apoptotic cells stain for Hoechst and Annexin V. NM (Normoxia), HM (Hypoxia), HE (Simulated ischemia), ($n \geq 3$).

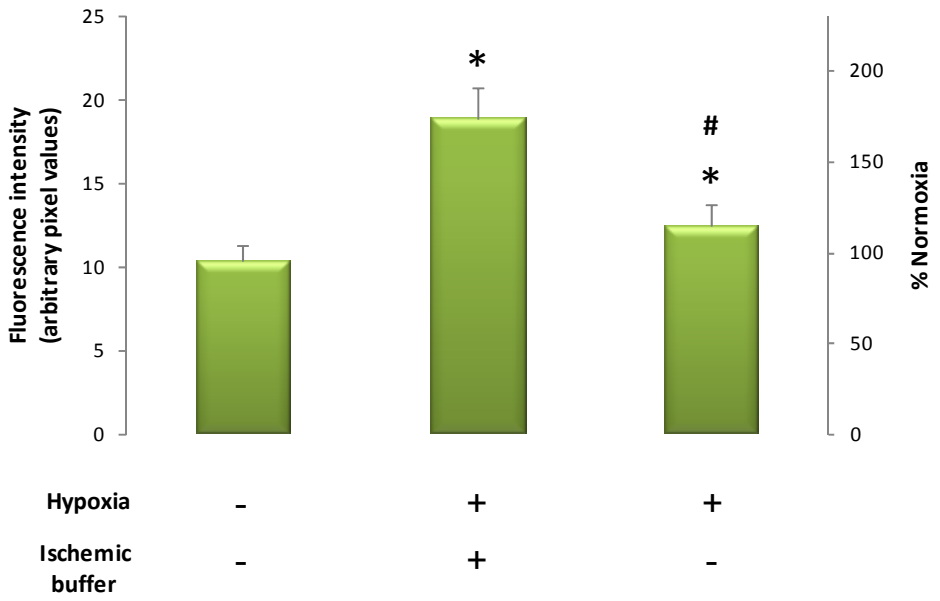

Figure 3.28 Quantification of Annexin V intensity in myotubes incubated in acute hypoxia and simulated ischemia. Cells were stained with Hoechst 33342 and Annexin V and analysed using fluorescence microscopy. At least 75 whole myotubes were selected and assessed for the fluorescence intensity of Annexin V. Results are presented as their mean ± S.E.M, *p<0.05 vs. control (n ≥ 3). Normoxia refers to the untreated control.

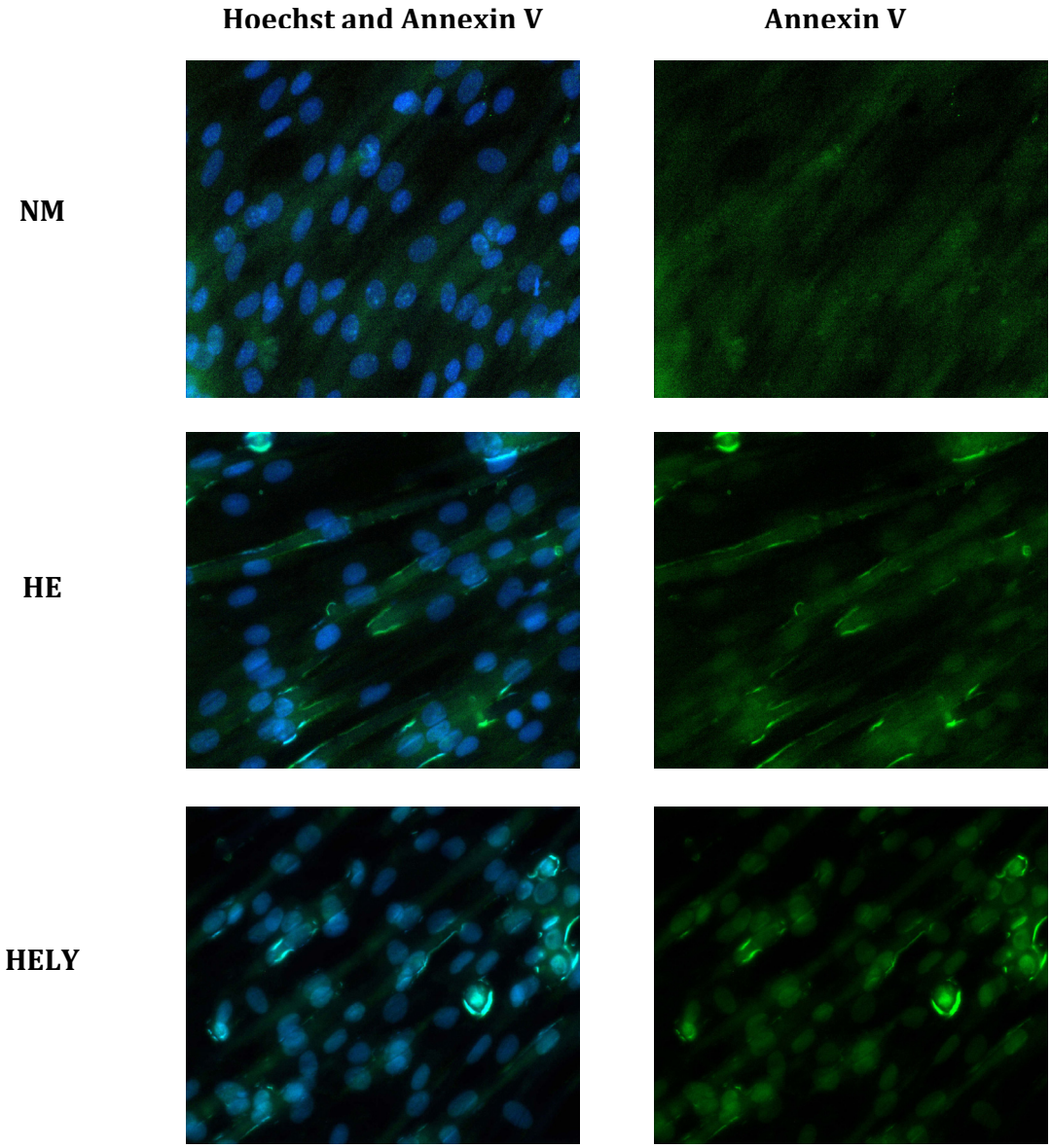

Figure 3.29 The effect of acute simulated ischemia and LY294002 on apoptosis in C2C12 myotubes - Annexin V binding. Cells were stained with Hoechst 33342 (blue) and Annexin V (green) and for analysed apoptosis using fluorescence microscopy. Healthy cells stain only for Hoechst whereas apoptotic cells stain for Hoechst and Annexin V. NM (Normoxia), HELY (Simulated ischemia + 50 μM LY294002), HE (Simulated ischemia), ($n \geq 3$).

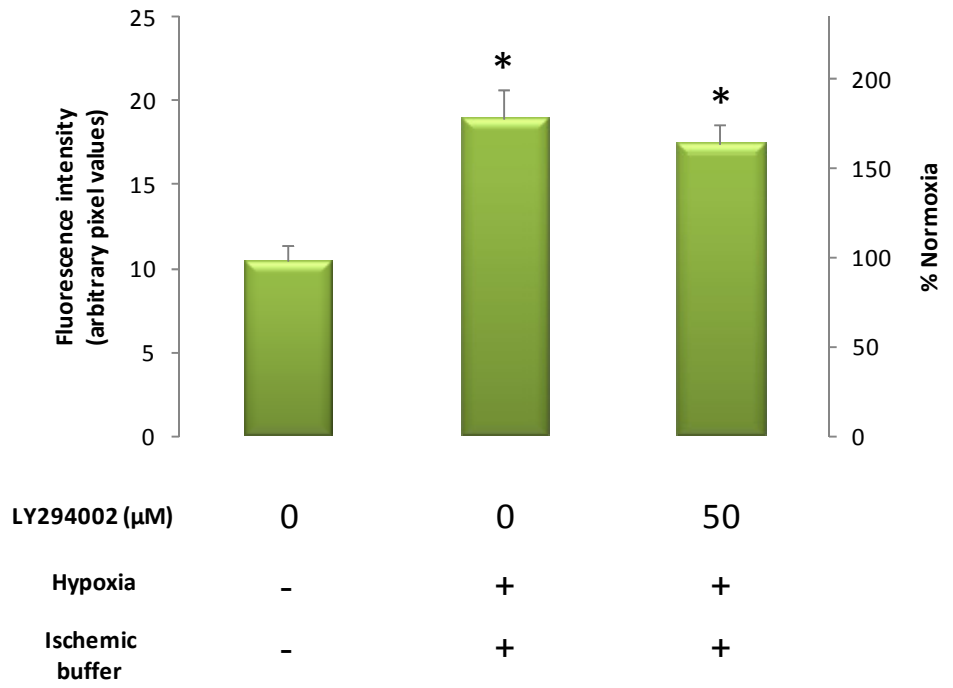

Figure 3.30 Quantification of Annexin V intensity in myotubes incubated in acute simulated ischemia supplemented with LY294002. Cells were stained with Hoechst 33342 (blue) and Annexin V (green) and analysed using fluorescence microscopy. At least 75 whole myotubes were selected and assessed for the fluorescence intensity of Annexin V. Results are presented as their mean ± S.E.M, *p<0.05 vs. control (n ≥ 3). Normoxia refers to the untreated control.

3.5.4 Detection of apoptosis using DNA fragmentation

In many cell lines, the genomic DNA of apoptotic cells is cleaved into multimers of 180-200bp long. Cleaved DNA is observed as a characteristic ladder on analysis by TAE-agarose gel electrophoresis. Although the characteristic ladder normally seen for cells undergoing apoptosis was not observed here, all of our representative experiments showed a pattern similar to the one represented below. Untreated groups gave a much weaker 'DNA smear'. While SI treated cultures gave the greatest detectable signal (Figure 3.31). Other samples consistently gave comparable 'DNA smears'.

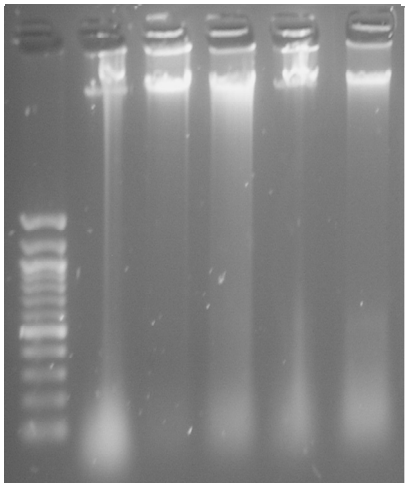

Figure 3.31 DNA fragmentation in C2C12 myotubes incubated in 3 hrs of hypoxia and simulated ischemia. Genomic DNA was extracted from cells and then run on a 1% TAE-agarose gel. DNA was detected using ethidium bromide staining. Representative image of repeats>3.

3.6 Akt-dependent regulation of mTOR (Western blots)

3.6.1 TSC1-TSC2 complex

3.6.1.1 TSC1

No change in the expression of TSC1 was found for myotubes incubated in three hours of SI compared to untreated controls (Figure 3.32).

3.6.1.2 Phospho-TSC2 (Thr1462)

Akt is able to phosphorylate TSC2 at the threonine 1462 position. There was significantly lower Akt-dependent phosphorylation of TSC2 after three hours SI, compared to untreated controls (Figure 3.33). Inhibition of the PI3K pathway with LY294002 during acute SI caused a dramatic, statistically significant decrease in Akt-dependent TSC2 phosphorylation.

3.6.2 Phospho-mTOR (Ser2448)

Akt is able to phosphorylate mTOR directly at the Ser2448 motif. Results showed significantly lower Akt-dependent phosphorylation of mTOR after three hours SI, compared to untreated controls (Figure 3.34). Inhibition of the PI3K pathway with LY294002 during acute SI also led to a statistically significant decrease in Akt-dependent mTOR phosphorylation.

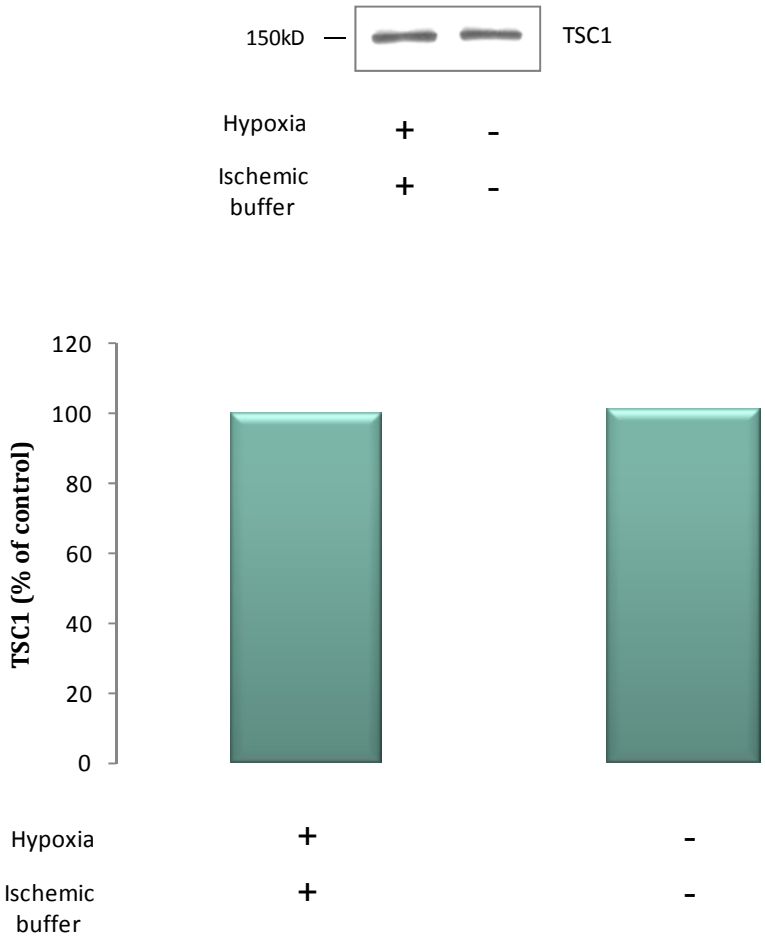

Figure 3.32 The effect of 3 hrs of simulated ischemia on the expression of TSC1 (Hamartin). Samples were examined by Western blot analysis with antibodies recognizing endogenous TSC1. Results are presented as their mean ± S.E.M, *p<0.05 vs. control (n ≥ 3).

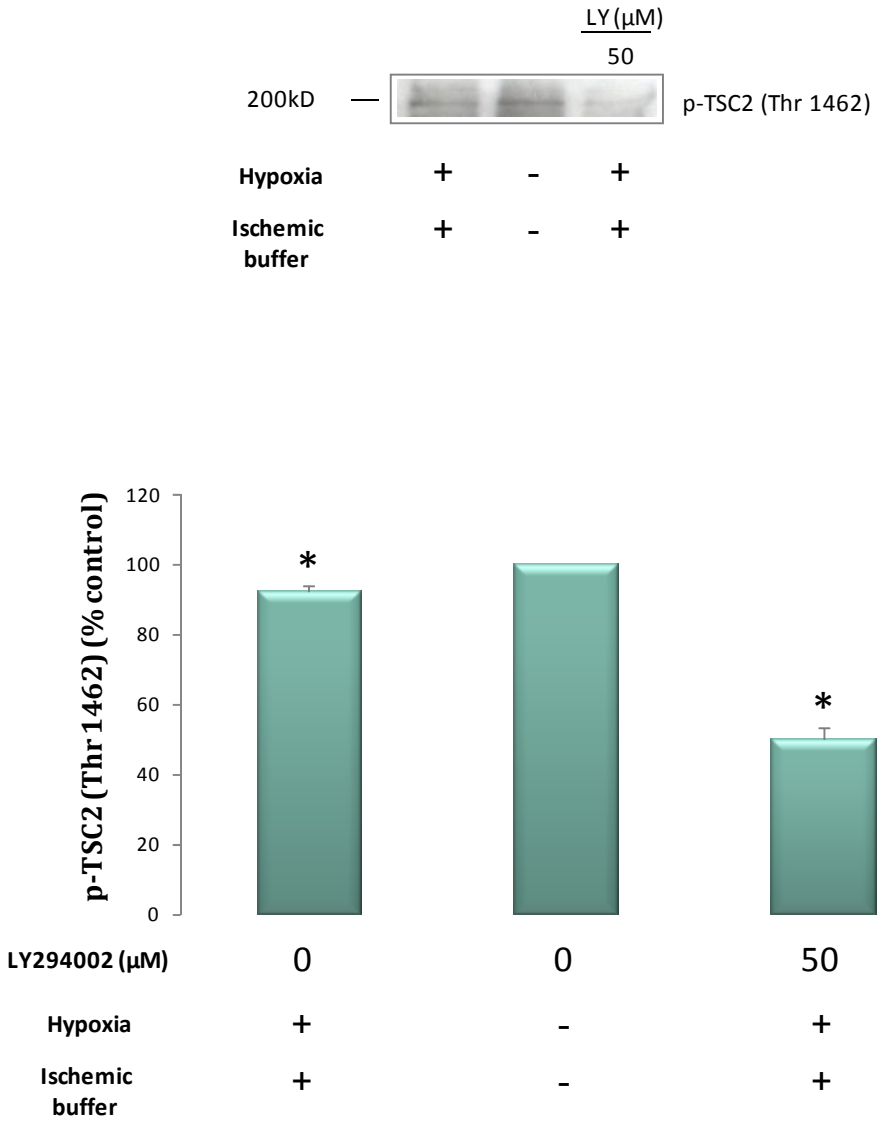

Figure 3.33 The effect of 3 hrs of simulated ischemia on Akt-dependent phosphorylation of TSC2 (Tuberin). Samples were examined by Western blot analysis with antibodies recognizing endogenous levels of TSC2 only when phosphorylated at the threonine 1462 position. Results are presented as their mean ± S.E.M, *$p<0.05$ vs. control ($n \geq 3$).

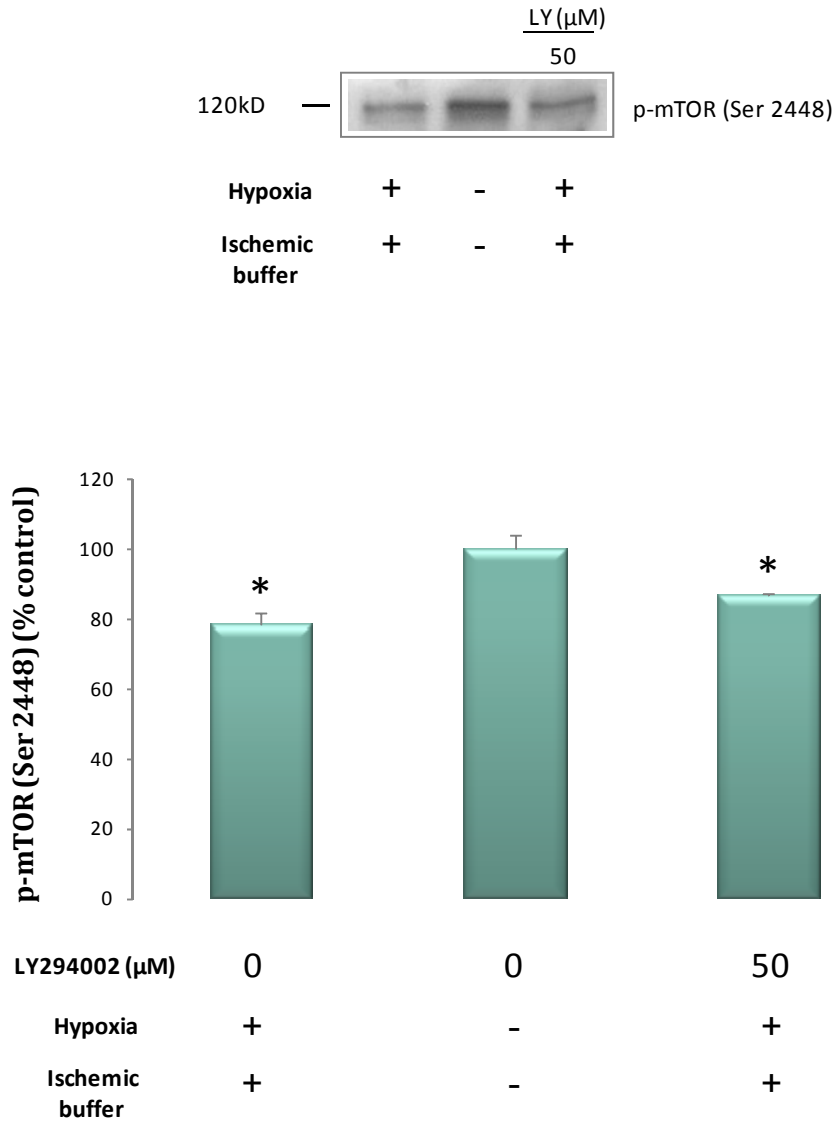

Figure 3.34 The effect of 3 hrs of simulated ischemia on the Akt-dependent phosphorylation of mTOR. Samples were examined by Western blot analysis with antibodies recognizing endogenous levels of mTOR only when phosphorylated at the serine 2448 position. Results are presented as their mean ± S.E.M, *p<0.05 vs. control (n ≥ 3).

3.7 HIF1α – REDD1 (Preliminary results)

HIF causes increased transcription of REDD1 which is thought to lead to a subsequent decrease in mTOR activity during hypoxia. Preliminary results indicate that HIF1α and REDD1 are apparent in normoxic, untreated controls (Figure 3.35). Both HIF1α and associated REDD1 levels seem to increase in acute hypoxia and simulated ischemia (Figure 3.35).

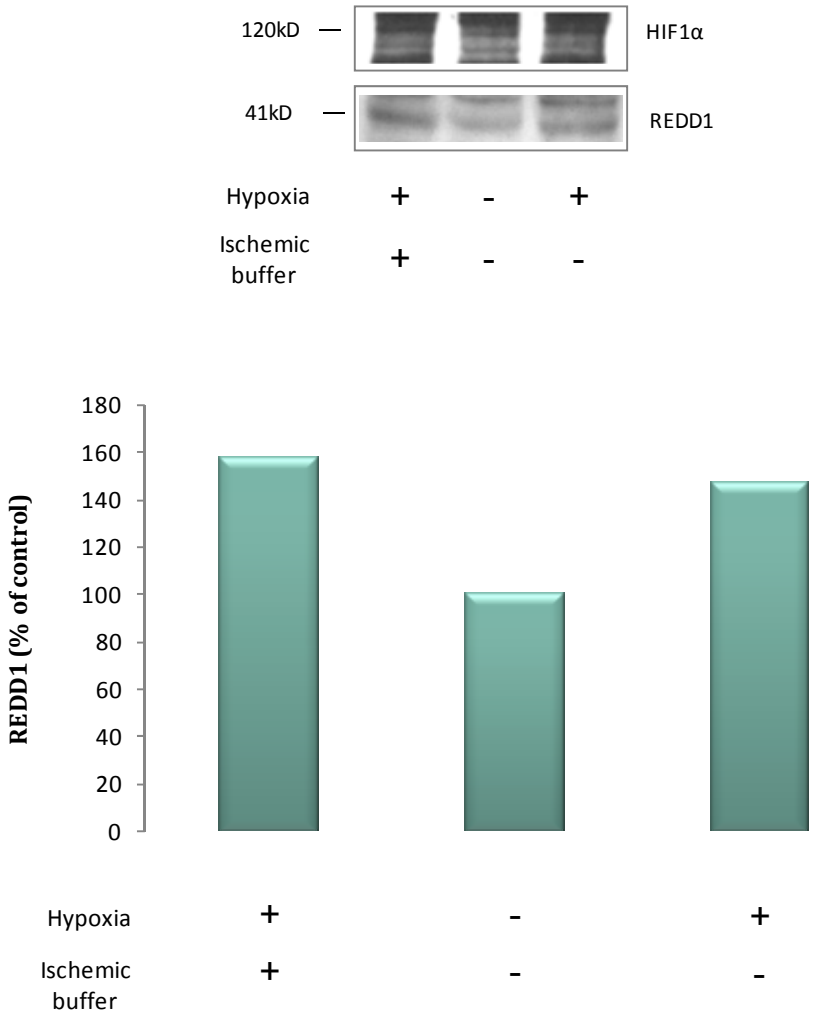

Figure 3.35 The effect of 3 hrs of hypoxia or simulated ischemia on REDD1 levels in C2C12 myotubes. Samples were examined by Western blot analysis with antibodies recognizing endogenous levels of HIF1α and REDD1. Results are presented as their mean.

Chapter 4

Discussion

It has been reported that hypoxia can elicit a direct or indirect response from more than 2% of human genes in arterial endothelial cells (Manalo *et al.*, 2005). One needn't look further than this statement to appreciate the significance of oxygen homeostasis to the cell. Nevertheless, oxygen is only one of many vital nutrients required for cells to function optimally. The reduced tissue perfusion seen during ischemia (Hockel and Vaupel, 2001) causes decreased oxygen and nutrient supply to vital organs, while the proficiency of waste product removal is simultaneously diminished (Semenza, 2000; Dirnagl *et al.*, 1999).

Chronic low oxygen tension, in conditions such as exposure to high altitudes, can result in drastically reduced muscle fibre size and mass (Hoppeler and Vogt, 2001). What's more, there are several acute and chronic pathophysiological conditions where ischemia and associated hypoxia are known to disturb standard cellular functioning and lead to cell and tissue damage (Semenza, 2000), including the manifestation of peripheral limb ischemia from acute and chronic vascular diseases (Santilli and Santilli, 1999). Cells are consequently equipped with an array of adaptive mechanisms to contest any undesirable reductions in oxygen availability. Under these conditions of diminished cellular oxygen availability, the PI3K signalling pathway is believed to initiate cell survival systems. Indeed, many studies

have suggested that there is an increase in the PI3K/Akt pathway activation during hypoxia (Barry *et al.*, 2007) and ischemia (Matsui *et al.*, 2001). How cells are able to alter their PI3K/Akt activity in response to these changes is unknown.

Adult skeletal muscle displays the incredible potential to regenerate following stresses (Aranguren *et al.*, 2008; Heemskerk *et al.*, 2007; Scholz *et al.*, 2003). In fact, ischemic muscle damage is thought to prompt the recruitment of myogenic satellite cells to injured areas. Here they rapidly proliferate before undergoing differentiation in response to distinct cues, leading to the eventual regeneration of damaged myofibers (Aranguren *et al.*, 2008; Hawke and Garry, 2001). We investigate such a model here. The C2C12 murine myogenic cell line model is popular for studying myogenesis *in vitro*, and has been used in the study of ischemic microenvironments in various unrelated studies (Loos *et al.*, 2008; Lacerda *et al.*, 2006; Yun *et al.*, 2005).

Simulated ischemic model

Nutrients, growth factors and oxygen can be deprived from cultured cells, in order to mimic the increased hypoxia and decreased blood flow seen during an acute ischemic insult (Long *et al.*, 1997). In addition to these factors, the altered ion concentrations and decreased pH also seen during physiological ischemia were replicated in our model by employing a buffer modified from the work of Esumi (Esumi *et al.*, 1991).

Together, the increased acidosis and altered ion concentrations (Yao and Haddad, 2004) as well as the increase in anaerobic glycolysis (King and Opie, 1998) are believed to be the main cause of ischemic cell death in cells. It is plausible that ‘weaker’ cells that are less equipped to handle the shock of being exposed to the harsh simulated ischemic environment

in our model would die or have their metabolic viability compromised first. Metabolic cell viability of C2C12 myotubes, as assessed using the MTT cell activity assay, was shown to decrease precipitously to 40% of the untreated controls after being incubated for one hour in simulated ischemia (SI) (Figure 3.1). Thereafter, metabolic cell viability was found to decrease linearly over a time period of seven hours spent in simulated ischemic conditions (Figure 3.2). C2C12 myoblasts, on the other hand, proved considerably less robust than their corresponding myotube counterparts when analysed over a period of five hours spent in SI (Figure 3.1). Although we are reluctant to infer decreased cell viability per se, it is clear that the functional capacity (MTT reducing capacity) of the culture populations in our model were dramatically reduced following one hour spent in SI. Thereafter, the cell populations were probably more evenly distributed and a linear trend of decreased metabolic viability was therefore observed.

Acute, three hour time point

While, compared to other studies in the literature, there is no doubt that three hours of SI can rightfully be called acute, the selection of exactly one hundred and eighty minutes as our acute time point is admittedly somewhat arbitrary. It has been found that irreversible muscle cell damage starts after three hours (Blaisdell, 2002), and this time point represented an almost 75% decrease in metabolic cell viability for myotubes incubated in SI in our model (Figure 3.3). Moreover, the apparent linear decrease in metabolic cell viabilities observed for all of the time points tested after one hour incubation in SI justifies further use of a three hour acute time point, as it fell within this linear trend.

Myotubes incubated in the modified Esumi buffer for a period of three hours at normal oxygen levels, show a drastic, significant decrease in metabolic cell viability (Figure 3.4).

Whereas, myotubes incubated in hypoxia alone (i.e. in normal culture medium) showed only a statistically insignificant trend towards a decrease (Figure 3.4). Together, these results implicate an important role for the harsh, altered cellular microenvironment in the decreasing cell function found in our experiments. Myotubes incubated in three hours SI showed a significant decrease in cell viability compared to those incubated in the buffer alone. This suggests that decreased oxygen levels certainly play a role in decreased cell functioning during acute SI. However, the exact contribution of hypoxia here is not known.

A role for PI3K

Although many studies have shown PI3K/Akt pathway activity to be increased during hypoxia (Barry *et al.*, 2007) and ischemia (Matsui *et al.*, 2001), contrasting results have been found for a few cell lines (Blancher *et al.*, 2001; Jiang *et al.*, 2002; Kwon *et al.*, 2006; Loberg *et al.*, 2002, Barillas *et al.*, 2007). We wished to establish if acute SI or hypoxia displayed any changes to PI3K activity or expression in our C2C12 myotube model, on day ten post-differentiation.

Interestingly, even after only three hours of incubation in SI, endogenous levels of the p85 regulatory subunit of PI3K were significantly lower when compared to untreated controls (Figure 3.5A). Yet, while endogenous p85 levels from whole cell extracts of myotubes incubated in hypoxia alone showed a definite trend towards a decrease, it proved to be a statistically insignificant one. Expression levels of p85 and the p110 catalytic subunit of PI3K are known to be linked (Geering *et al.*, 2007). So it was no surprise that expression levels of the p110 subunit for acute SI and hypoxia treated myotubes mirrored those seen for p85 (Figure 3.6A). As an aside, we incubated myotubes for three hours in the ischemic buffer alone (that is, in normoxia). Fascinatingly, we found no difference in levels of the p85

subunit (Figure 3.5B) or the p110 subunit (Figure 3.6B) compared to untreated controls. This indicates that the findings of decreased p85 and p110 levels in acute SI are not solely dependent on the altered microenvironment created by ischemia, but seem to be linked to changes in oxygen tension as well. Actually, decreased oxygen appears to be an important component of the decreased protein levels found for both subunits.

To determine if these findings translated into a decreased capacity to generate lipid second messengers during acute SI and hypoxia, we examined the relative ability of our treated groups to produce PIP_3 when compared to untreated controls (Figure 3.7). As the activation of PI3K during C2C12 differentiation is now commonly understood to be owing to the increased autocrine expression of IGF-II acting through IGF-I receptors (Bach *et al.*, 1995), we utilized the class IA subset PI3Kα isoform immunoprecipitated from our cell extracts. A competitive PI3K ELISA was performed in order to corroborate the information gained from the Western blot analysis.

From the ELISA data, it can be inferred that PI3K enzyme activity is constitutively active in our C2C12 myotubes in normoxia (Figure 3.7). It seems as though the significantly lower PI3K levels for both the p85 and p110 subunits in acute SI treated cultures (previously demonstrated) may translate as decreased lipid catalysed production of PIP_3. This statement is further substantiated by the fact that we found only an insignificant trend towards decreased PIP_3 generating capacity for acute hypoxia treated cultures (Figure 3.7). Results also forecast by our Western blot data.

Our findings are not unprecedented however. Interestingly, in contrast to other studies, models exhibiting a constitutively expressed PI3K/Akt pathway have also shown a decrease

in their PI3K/Akt activity during hypoxia (Mottet *et al.*, 2003) and ischemia (Noshita *et al.*, 2003). In further support of our findings, differentiating C2C12s may too, in fact, display such a constitutively activated PI3K/Akt pathway during myogensis (Yoshiko *et al.*, 2002). In conditions favourable for differentiation of C2C12 myoblasts, PI3K lipids become greatly accumulated at the plasma membrane in an unconventional manner (Mandl *et al.*, 2007), and the induction of Akt becomes considerably enhanced (Fujio *et al.*, 1999). This has been shown to be sustained in terminally differentiated cells, even after serum re-stimulation (Fujio *et al.*, 1999; Rommel *et al.*, 1999). This activation of PI3K during differentiation is probably a symptom of increased expression of IGF-II (Bach *et al.*, 1995).

What do these decreases in PI3K activity during acute ischemia and hypoxia signify for our model? By simply supplementing skeletal muscle cultures with inhibitors of the PI3K pathway, significant decreases in metabolic cell viability were observed (Figures 3.8A & 3.9A). Two of the most widely used PI3K inhibitors, namely wortmannin and LY294002, were employed for these tests. Wortmannin for it's purported higher potency (Ui *et al.*, 1995) and LY294002 for the benefits of it's extended half-life (Vanhaesebroeck *et al.*, 2001). Both yielded similar results. The significantly decreased metabolic cell viability observed following administration of wortmannin (Figure 3.8A) or escalating concentrations of LY294002 (Figure 3.9A) indicate that the PI3K pathway could have a protective role in our model. The lack of a similar, significant response for myotubes incubated in acute SI in conjunction with the inhibitors (Figures 3.8B & 3.9B) suggests that the protective effect of the PI3K pathway may have been lost here.

When the profile of growth factors in culture medium changes and there is decreased expression of growth factors and a concomitant increase in IGF-II expression (Yoshiko *et al.*,

2002), there is an associated increased in PI3K/Akt pathway activity as well. This is essential to myoblast differentiation and is thought to promote cell survival (Florini *et al.*, 1991; Stewart and Rotwein, 1996). The precise mechanisms by which this occurs are not yet known. Were the pro-survival effects of high basal PI3K pathway activity lost or weakened during acute SI and hypoxia then this could explain, at least in part, the results seen here.

Akt

Akt operates downstream of PI3K and has a key responsibility in regulating signalling pathways concerning cell survival (Song *et al.*, 2005). It is believed that an increase in PI3K/Akt activation during myotube development is mainly responsible for the relatively apoptotic resistant phenotype of differentiated C2C12 myotubes (Fujio *et al.*, 1999).

The high basal activity of PI3K, witnessed in normoxia in our C2C12 model, is reflected again here in our results for PI3K-dependent Akt phosphorylation (Figures 3.12 & 3.15). Phosphorylation at both the serine 473 and threonine 308 motifs of Akt is thought to be necessary for the complete activation of Akt and its downstream targets (Sarbassov *et al.*, 2005b). The significant decrease in levels of phospho-Akt at both serine 473 (Figure 3.12) and threonine 308 (Figure 3.15), observed for myotubes incubated in acute SI, echoed our previous findings of decreased PI3K activity in similar experiments. This indicates that acute SI does indeed lead to decreased activity downstream of PI3K in C2C12 myotubes. In addition, and as expected, results of decreased Akt activity in myotube cultures incubated in three hours of hypoxia are reflective of our previous findings as well. However, while levels of phospho-Akt (serine 473) displayed a similar trend towards a decrease, levels of phospho-Akt (threonine 308) showed no change compared to untreated controls (Figure 3.15). It is tempting to imagine that hypoxia is somehow favouring one Akt phosphorylation site over

another, but we believe that this finding may merely be an artefact of the disparately regulated Akt activity in differentiating versus proliferating C2C12s (Yun and Matts, 2005). It is thought that, after being activated, subsequent phosphorylation of Akt (threonine 308) is not required for Akt activity (Gonzalez *et al.*, 2004), and that it is Akt (serine 473) that is mainly phosphorylated in differentiating C2C12s (Yun and Matts, 2005). Therefore, less of a change in phospho-Akt (threonine 308) levels is seen. However, to confirm that phospho-Akt levels are not being differently manipulated upstream of Akt, we evaluated PDK1 activity. PDK1 leads to the full activation of Akt by means of a phosphorylation event that takes place at the Akt threonine 308 motif within the activation loop in the kinase domain (Stephens *et al.*, 1998). Yet, no change in phosphorylation of PDK-1 (serine 241) was found for myotubes incubated in acute SI or in hypoxia alone (Figure 3.11).

We also decided to evaluate phospho-PTEN, as it is a major negative regulator of PI3K that lies upstream of Akt (Vanhaesebroeck *et al.*, 2001). No change in phosphorylation of PTEN (serine 380) was found for myotubes incubated in acute SI or in hypoxia alone (Figure 3.10). Together, our results suggest that the decreases in Akt activity in our model are PI3K-dependent, and that this works independently of PTEN and PDK-1.

The decline in Akt phosphorylation when acute SI and untreated cultures were inhibited with wortmannin (Figures 3.14 and 3.18) or LY294002 (Figures 3.13 and 3.17) confirm that Akt phosphorylation is indeed being regulated upstream by PI3K in our model. Notably, Akt phosphorylation was not abolished through inhibition. This may be due to the high basal levels to which PI3K activity had risen during myogenesis.

Downstream effectors of Akt

Akt abrogates cell death through the phosphorylation of many downstream effectors, and the regulation of various transcription factors by Akt has also been shown (Song *et al.*, 2005). FoxO1 (FKHR)) and FoxO4 (AFX) are both thought to induce apoptosis, as their target genes include the apoptosis inducing Fas and TRADD ligands as well as members of the pro-apoptotic Bcl-2 family (Burgering and Medema, 2003). By phosphorylating and inactivating its members, PI3K/Akt inhibits the transcriptional activity of the FoxO family and promotes cell survival (Reagan-Shaw and Ahmad, 2007). Phosphorylation of the FoxO family is also believed to be essential for C2C12 myotube formation (Hribal *et al.*, 2003), and FoxO1 has recently been shown to inhibit C2C12 myogenesis by degrading mTOR pathway components (Wu *et al.*, 2008).

The significantly diminished Akt-dependent phosphorylation for both FoxO1 and FoxO4 (Figure 3.19) was predicted by our previous findings for C2C12 myotubes incubated in SI. These decreased levels of phospho-FoxO1 and phospho-FoxO4 indicate that effectors downstream of Akt are being influenced by upstream signals from the PI3K/Akt pathway. A constitutively high activity of PI3K/Akt is important for the suppression of FoxO mediated inhibition of C2C12 myogenesis. At the same time, another consequence of a high PI3K/Akt activity is an increased resistance to apoptosis through suppression of FoxO transcription. It is reasonable therefore to conceive that the decreased phospho-FoxO levels seen in our experimental model of acute SI could lead to increased apoptosis, and that this occurs indirectly as a result of decreased PI3K/Akt activity.

Akt governs cell survival through several other transcription factors as well, including the c-AMP response element binding protein (CREB). Phosphorylation of CREB by Akt causes an

increase in its transcriptional activity leading to the increased expression of anti-apoptotic factors (Pugazhenthi *et al.*, 2000). Intriguingly, results obtained for phosphorylation of CREB at the serine 133 motif showed divergent results to those of Akt. Compared to untreated controls, levels of phospho-CREB (serine 133) rose significantly during SI incubation (Figure 3.20). If CREB phosphorylation was being controlled by PI3K/Akt then a decreased phosphorylation would be in line with our previous results. Hypoxic incubation of myotubes yielded a definite trend towards increased levels of phospho-CREB as well, albeit a statistically insignificant one. CREB phosphorylation has been shown to be caused by many stimuli, including hypoxia (Johannessen *et al.*, 2004). In fact, it has been demonstrated (in PC12 cells) that CREB phosphorylation increases in hypoxia in an Akt-independent manner (Beitner-Johnson *et al.*, 2001). Another study (also using PC12s), showed that this hypoxia dependent increase in phospho-CREB (serine 133) was not activated by the usual upstream mechanisms such as the PKA or calcium/calmodulin PKC-dependent pathways (Beitner-Johnson and Millhorn, 1998). Although increased phosphorylation of CREB is generally believed to lead to increased transcription of pro-survival genes, correlations to the transcription of both increased pro-survival (Kitagawa, 2007) and pro-apoptotic (Mishra *et al.*, 2002) targets have been seen in ischemia. We are unsure whether the increased levels of phospho-CREB found here lead to increased cell survival or increased apoptosis, but it does seem as if CREB is responding to hypoxia and SI in an Akt-independent manner through some other sensing mechanism.

Does decreased PI3K/Akt activity lead to increased apoptosis in our model?

The activation of Akt has been shown to protect against hypoxia induced apoptosis during ischemia and hypoxia (Matsui *et al.*, 1999; Matsui *et al.*, 2001). We aimed to establish if the

decreased Akt activity observed for cultures incubated in three hours SI or hypoxia would lead to increased levels of apoptosis.

Numerous proteins have been described as suitable detectors of apoptosis. Caspase-3 is one such 'executioner of cell death'. Caspase-3 is activated following its cleavage into smaller active fragments (Nunez *et al.*, 1998), and we chose to detect the active 19kD fragment of caspase-3 as a signal for apoptosis in our experiments. By inhibiting the PI3K pathway in cultures incubated in acute SI, we were able to cause increased cleavage of caspase-3 (Figure 3.21). This signifies that resident PI3K pathway activity is preventing the cleavage of caspase-3 downstream, under normal conditions. The significantly increased levels of cleaved caspase-3 in cultures incubated in acute SI (Figure 3.21) provide strong evidence that there is increased apoptosis in our model of acute ischemia. There is also a definite trend towards increased caspase-3 cleavage during acute hypoxia as well (Figure 3.21). This pattern is similar to previous results and gives additional support to the theory that decreased PI3K/Akt activity is producing increased apoptosis during three hours of hypoxia and SI in cultured C2C12 myotubes.

Although Akt does not prevent caspase-3 cleavage directly, decreased Akt activity does trigger increased caspase-3 cleavage through pathways upstream of caspase-3 (Nicholson and Thornberry, 1997), including via the decreased phosphorylation of the FoxO family (Burgering and Medema, 2003). Our data gives us confidence that decreased Akt activity is relaying a corresponding message to the apoptotic machinery of the cell. Caspase-3 is purported to be responsible wholly or in part for the proteolytic cleavage of many important proteins (Nunez *et al.*, 1998), and next we wished to test whether active caspase-3 is communicating this message by catalysing protein cleavage downstream. PARP-1 undergoes

distinct cleavage in a caspase-3 dependent manner (Soldani and Scovassi, 2002), and is a good indicator that cells are undergoing apoptosis.

Immunodetection of PARP-1 cleavage produced a comparable pattern to that of caspase-3 cleavage. Notably, inhibition of PI3K produced only a trend towards increased PARP-1 cleavage (Figure 3.22). Nevertheless, we remain confident that further testing would produce statistically significant results, due to the high level of statistical variance in our existing tests for this group. As in our caspase-3 experiments, acute SI lead to significantly increased levels of cleaved PARP-1. Interestingly, even higher levels of cleaved PARP-1 were found for cultures incubated in three hours of hypoxia (Figure 3.22). It is feasible that the amount of cleaved caspase-3 seen previously is enough to initiate the degree of PARP-1 cleavage seen here. As we isolated and treated the control and test samples in exactly the same way for all groups, it is unlikely that cleavage of PARP-1 resulted independently of apoptosis in all of our hypoxic repeats. Nonetheless, it does appear as though apoptosis downstream of caspase-3 is significantly increased after three hours SI as well as three hours of hypoxia.

Divergent results have been reported in studies investigating hypoxia induced cell death (Long *et al.*, 1997; Webster *et al.*, 1999; Santore *et al.*, 2002), and the mechanism by which decreases in oxygen might lead to cell death remains a controversial subject (Webster *et al.*, 2005). It has been proposed that cell death might not even be triggered directly by a decrease in oxygen as such, but that it is initiated indirectly by secondary mechanisms instead (Webster *et al.*, 1999). Still, Akt has been implicated in protection against apoptosis during ischemia and hypoxia (Matsui *et al.*, 1999; Matsui *et al.*, 2001) and levels of the Bcl-2 protein have also been shown to decline in some animal models of ischemia (Webster *et al.*, 2005).

These findings, in concert with our results, do indicate a protective role for the PI3K/Akt pathway in hypoxia and ischemia induced apoptosis.

Next, to substantiate these findings further, we sought to assess changes in cell morphology using vital staining (Figure 3.23). Propidium iodide is usually excluded from healthy cells whereas Hoechst 33342 is able to diffuse through cell membranes regardless of their condition. So, when co-staining cells with PI and Hoechst, healthy cells can be distinguished from those with damaged membranes. The significant increase in membrane permeability found for cells incubated in acute hypoxia alone is a sign that membrane impairment is caused by low oxygen conditions in C2C12 cultures (Figure 3.24). Furthermore, it is clear from our findings that changes in the cellular microenvironment caused by ischemia can give rise to a greater amount of membrane impairment and cell death than hypoxia alone does. Interestingly, acute SI produced a greater significant increase in membrane permeability than either acute hypoxia or the modified Esumi buffer alone (Figure 3.24). This signifies roles for both hypoxia and the ischemic microenvironment in increased cell death. In addition, the pink regions seen in cells that stained homogeneously for PI and Hoechst are indicative of late apoptotic or necrotic cells found after acute SI only (Figure 3.23). Furthermore, inhibiting the PI3K pathway during acute SI leads to considerable, statistically significant increases in membrane permeability with signs of late apoptosis (pink co-staining) (Figures 3.25 and 3.26). This signifies that the PI3K/Akt pathway does participate in protecting C2C12 myotubes from membrane impairment, and possibly apoptosis, caused by acute SI. This, together with our previous results, leads us to conclude that the increased levels of membrane damage seen during acute hypoxia and SI (as assessed by PI staining) are caused, at least partially, by decreased PI3K/Akt activity.

To further demonstrate increased apoptosis during acute SI and hypoxia, we treated our cells with annexin V bound to a green fluorescent probe (Figure 3.27). Normal cells possess an asymmetric distribution of phospholipids in the leaflets of the cell membrane, but this asymmetry is lost during apoptosis and phosphatidylserine (PS) becomes abundant on the cell membrane's outer leaflet. Annexin V is a phospholipid binding protein that has a high affinity for the PS exposed on cells undergoing apoptosis. We can deduce from our findings that there is increased apoptosis in myotubes incubated in acute hypoxia, and that acute SI causes an even greater degree of apoptosis still (Figure 3.28). The fact that inhibiting the PI3K pathway during acute SI lead to no statistically significant increases compared to those cultures incubated in three hours of SI alone is troubling (Figures 3.29 and 3.30). Since results for SI and for SI and inhibitor together were statistically insignificant when compared, we cannot conclude from this data that the PI3K/Akt pathway is participating in protecting C2C12 myotubes from apoptosis caused by acute SI. Having said this, we cannot rule out this possibility either, as it is feasible that inhibiting the PI3K pathway is just unable to cause any further increased apoptosis in this experiment. It is also plausible that the sensitivity (of statistical software) needed to distinguish the degree of annexin V binding at these levels is merely too fine. Additional tests are needed. It should also be noted, that moderate annexin V binding was seen in untreated controls as well (Figure 3.29). It has been found that annexin V binds at the fusion points of C2C12 myotubes (van den Eijnde *et al.*, 2001), but this should not skew our findings due to the fact that all results are compared to an untreated control.

DNA extracts from our culture samples failed to present a typical ladder characteristic of the small cleaved multimers of genomic DNA normally seen during apoptosis. Even so, a clear difference between untreated and treated groups was evident, with treated groups giving a noticeable DNA 'smear' pattern (Figure 3.31). We deemed this to be adequate evidence for

both an increased apoptosis during acute SI and hypoxia as well as a protective role for the PI3K/Akt pathway, when accompanied with previous findings.

Mechanism of decreased PI3K/Akt activity

It is likely that the decreased perfusion found during ischemia leads to reduced nutrients and supply of RTK agonists, a situation mimicked by our model design. This could lead to an initial drop in PI3K pathway activity. PI3K/Akt activity is known to be elevated due to the increased autocrine/paracrine expression of IFG-II functioning through IGF-I receptors (Bach *et al.*, 1995). This IGF-II expression has been found to be tightly regulated by mTOR (Erbay *et al.*, 2003), a key controller of protein synthesis in the cell. After the initial drop in available IGF-II levels it would be expected that autocrine/paracrine IGF expression would rapidly compensate for this, thereby preventing apoptosis. However, mTOR activity is also firmly regulated by the level of available nutrients and amino acids. A situation of decreased nutrients and amino acids might occur during the decreased blood flow observed in ischemic diseases (Zhou *et al.*, 2008; Sarbassov *et al.*, 2005a; Vaupel *et al.*, 1989), and again our study design compensates for these inevitable changes to the cellular microenvironment. Decreased amino acids have been shown to diminish mTOR dependent IGF-II expression in C2C12 myogenesis (Erbay *et al.*, 2003), and the dearth of available amino acids in SI could explain, in part, the decreased PI3K/Akt activity seen in our experiments.

We provide evidence that Akt-dependent mTOR activity may be decreased during acute SI as well (Figures 3.33 and 3.34). mTOR functioning is negatively regulated by a heterodimer made up of the tubular sclerosis proteins TSC1 (hamartin) and TSC2 (tuberin) (Tee *et al.*, 2002), and TSC2 has been identified as the target for Akt phosphorylation *in vivo* and *in vitro* (Manning *et al.*, 2002). Our results show that the decreased Akt activity witnessed after acute

SI caused a concomitant, Akt-dependent decrease in phospho-TSC2 (Figure 3.33) and phospho-mTOR (Figure 3.34) levels. Supplementation with a PI3K inhibitor confirmed a role for PI3K control at these motifs.

However, this does not explain the drop in PI3K/Akt activity for the cells incubated in normal culture medium in hypoxic conditions, nor does it describe why cultures incubated in a modified Esumi buffer in normoxic conditions displayed no significant decrease in PI3K/Akt activity either (Figure 3.15 & Figure 5B). A possible explanation for these results is that mTOR is known to be sensitive to hypoxia and decreased energy levels as well. In fact, energy depletion has been shown to decrease flux through the PI3K/Akt pathway (Tzatsos and Tsichlis, 2007). Lowered energy levels lead to an increasing AMP/ATP ratio which is thought to result in the phosphorylation of TSC2 and subsequent inhibition of mTOR (Inoki *et al.*, 2003). The decreasing energy levels seen during hypoxia interact with mTOR signalling through the AMPK/mTOR pathway. Moreover, it was found that, increased HIF-1α stability during hypoxia increases expression of REDD-1 which is thought to lead to TSC1/TSC2-dependent inhibition of mTOR signalling (Brugarolas *et al.*, 2004).

However, during myogenesis, many of the signalling cascades that participate in the regulation of cell proliferation and growth are up-regulated. PI3K/Akt is one of these pathways and is important for the proliferation, differentiation and survival in differentiating myoblasts (Jiang *et al.*, 1998). HIFs interact with a multitude of angiogenic and metabolic genes as well. This powerful resource has been shrewdly employed by differentiating cells with the intention of using HIFs remodelling capabilities in normoxic conditions (Ono *et al.*, 2006). As such, HIF1α is thought to be vital for normal C2C12 myotube development, albeit in non-hypoxic conditions. AMPK, the other aforementioned sensing molecule, is also up-

regulated and is also a vital element of C2C12 differentiation (Niesler *et al.*, 2007). Therefore, it seems as though the pro-differentiation effects of PI3K/Akt, HIF1α and AMPK have been commandeered, and they are all up-regulated during C2C12 differentiation.

This raises some interesting questions. Does this mean that differentiating cells are more vulnerable to hypoxic and ischemic insults, and is their capacity to detect these changes diminished if these detection systems are being employed for another purpose, namely differentiation?

Are differentiated C2C12s more vulnerable to apoptosis during acute hypoxia and ischemia?

Our preliminary testing indicates that, although the HIF1α and REDD-1 proteins are apparent during normoxia, there seems to be a visible increase in REDD-1 levels during both acute hypoxia and acute SI (Figure 3.35). Although further testing is required, this provides evidence of an oxygen sensing mechanism for C2C12 myotubes in culture. Importantly though, it has also been shown that the effects of hypoxia on myogenesis of C2C12 cells can operate independently of HIF1 (Yun *et al.*, 2005). In addition, our finding that CREB phosphorylation is increased in an Akt-independent manner (Figure 3.20) demonstrates another method by which decreased oxygen levels and an acute SI insult could lead to enhanced activity at a transcriptional level. It is difficult to speculate as to the method of oxygen sensing by CREB, but ROS or the decreased calcium regulation during hypoxia and ischemia are obvious candidates.

Whether or not C2C12 myotubes have a diminished capacity to detect changes in oxygen levels is an open question at this point.

Based on our results and evidence from the literature, we have proposed a mechanism of how decreased PI3K/Akt activity might occur during acute SI and hypoxia (Figure 4.1). A drop in amino acid, nutrient and oxygen levels during ischemia and reduced oxygen in hypoxia could be sensed at the level of the TSC2/TSC1 complex thereby causing reduced expression of IGF-II by mTOR. Prolonged, diminished IGF-II availability could lead to decreased receptor demand and a shrinking pool of PI3K lipids at the cell membrane. At the same time, decreased Akt activation might lead to decreased mTOR activity through lessened phosphorylation of TSC2 and mTOR. This in turn could cause a further drop in IGF-II expression and exacerbate the decreased flux through PI3K/Akt even more. Ultimately, the protective effect of PI3K/Akt could be lost and an increase in apoptosis could occur. This could also explain a rapid decrease in PI3K/Akt activity in acute SI.

Another more tentative conjecture is that this pathway could even be interpreted as a survival mechanism of sorts. In times of stress and decreased nutrients, cells need to conserve valuable energy stores. mTOR ensures that protein synthesis and its associated energy consumption remain in equilibrium with nutrient supply (Wullschleger *et al.*, 2006). Shutting down protein synthesis pathways in response to ischemia and hypoxia might also lead increased cell death of C2C12 myotubes too. In this way ‘less fit’ cells perish leaving what meagre resources are available for ‘fitter’ cells, lest the stress event comes to an end in time for them to survive. Autophagy (type II cell death), which is inhibited by mTOR (Meijer and Codogno, 2004), is in fact thought to save cells by cannibalizing cell constituents and freeing up energy during stressful times. So, decreased PI3K/Akt activity during acute hypoxia or ischemia could inadvertently allow ‘fitter’ myotubes to survive at the expense of their weaker neighbours.

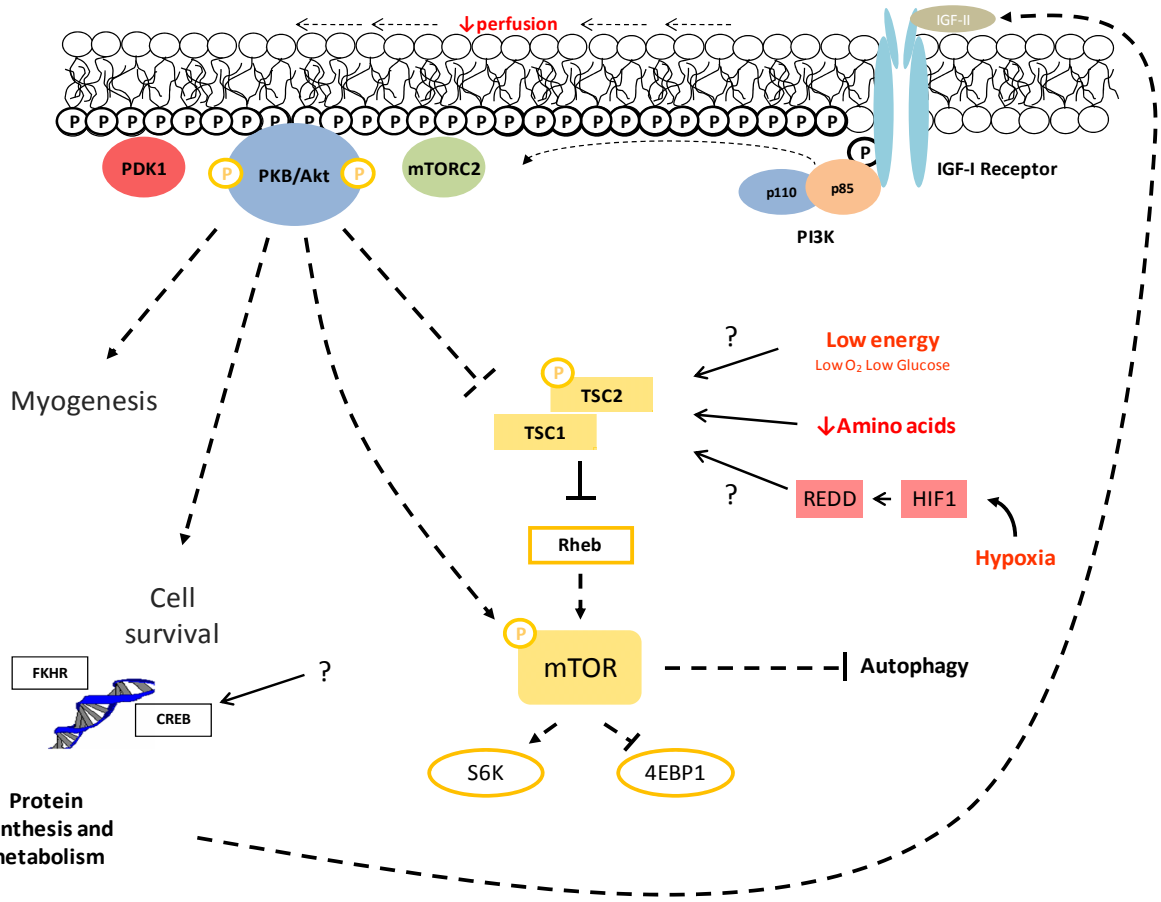

Figure 4.1 Proposed mechanism of decreased PI3K/Akt activity during acute SI and hypoxia in C2C12 myotubes on day ten post-differentiation. Explained in detail in the text - - - indicates decreased activity.

Future recommendations and limitations of our study

In the ever changing climate of scientific ethics, cell culture studies are becoming increasingly valuable as precursors and, in some cases, alternatives to animal studies. Although it is our contention that animal models are the logical conclusion for most studies starting in cell culture, more information on popular, relevant cell lines such as the one used here is needed in order to better design and understand the implications of future work.

C2C12 myotubes are generally used on day seven to day ten post-differentiation, but it is not uncommon to see studies that treat them as 'myotubes' on much earlier days into

differentiation. It is clear from our results that an acute ischemic or hypoxic insult leads to perturbations in the activity of the key signalling node that is PI3K, at day ten post-differentiation in C2C12s. The activity status of PI3K is presumed to be high during early myogenesis as well (Yoshiko *et al.*, 2002), and future studies using C2C12s in different experimental conditions should bear in mind the high basal PI3K/Akt activity and consequences of its inhibition or decreased function.

Although our study was designed with the intention to have as few limitations as possible, scope and time constraints mean that limitations are of course encountered. Larger sample sizes would allow for more accurate statistical analysis and could cause some of the trends seen in our work to reach statistical significance.

Better, more sophisticated methods of cell death analysis (such as appropriate flow cytometry and more refined imagining techniques) as well as closer investigation of transcriptional modifications that are caused by decreased PI3K/Akt activity could help further elucidate which cell survival targets are being effected in our model.

Analysis of more time points would certainly help in our understanding of how the profile of PI3K/Akt activity is changing during acute ischemia and acute hypoxia. Time points simulating chronic ischemia and hypoxia could also reveal if C2C12s are able to rectify this decrease in PI3K/Akt activity over time. Future experiments simulating cellular reperfusion post-ischemia/hypoxia could also divulge interesting information about the PI3K/Akt activity profile in our model.

Finally, as whole cell lysates were employed in our experiments, it would be desirable to separate our protein samples into cytoplasmic, nuclear and membrane fractions and evaluate,

in particular, levels of HIF1α as well as the cellular localization of the constituents of PI3K studied here.

Chapter 5

Summary and conclusions

In this study, we established that high basal levels of PI3K activity exist in C2C12 myotubes on day ten post-differentiation. Muscle ischemia is characterized by changes in pH and in ion concentrations and a diminished nutrient and amino acid supply. Using models that mimic these changes as well as the reduced oxygen levels found in hypoxic muscle, we showed that both three hours of simulated ischemia (SI) and three hours of hypoxia (1.0% oxygen) led to decreases in the endogenous levels of the p85 and p110 subunits of PI3K. We then went on to provide convincing evidence that these changes were translated as decreased PI3K activity. In addition, we demonstrated that, although the harsh environment seen during ischemia is what is mostly responsible for the observed decrease in metabolic cell viability, the inextricably associated hypoxia is a vital component in decreased cell activity during simulated ischemia in our model.

Thereafter, we presented persuasive findings that PI3K has a protective role in our model and that this protective shield may be lost or lowered during SI. We revealed that the activity of the major downstream effector of PI3K, namely Akt, is concurrently decreased during acute SI and acute hypoxia in a PI3K-dependent manner that is independent of PDK-1 and PTEN. The PI3K/Akt pathway is known to produce an apoptosis resistant phenotype in C2C12 cells during myogenesis, and we provided compelling evidence that this resistance is

at least partially lost during acute SI and acute hypoxia due to decreases in PI3K/Akt pathway activity. It was shown that decreases in the PI3K/Akt pathway in our model produces a knock-on effect to downstream signalling transcription factors, such as Fox01 and Fox04, and that apoptosis downstream of one of the main executioners of cell death, namely caspase-3, is indeed increased during acute hypoxia and acute SI. These increases in apoptosis were found to be related, at least in part, to the decreased PI3K/Akt pathway activity. Furthermore, we generated additional data to support the suggestion that decreased PI3K/Akt pathway activity in our model causes increased cell death via apoptosis, by illustrating cell membrane impairment during acute ischemia and acute hypoxia and linking these changes to decreased PI3K/Akt pathway activity in our C2C12 model. We then showed increased Annexin V binding as well as evidence of increased DNA fragmentation during acute hypoxia and acute ischemia, both states indicative of increased late stage apoptosis.

After completing the study aims and confirming that decreased PI3K/Akt activity does indeed lead to decreased downstream signalling, and substantiating the suggestion that this leads to decreased cell survival, we went on to produce evidence that mTOR activity may be impaired due to decreased Akt-dependent phosphorylation at the level of TSC2 and mTOR directly, during acute hypoxia and acute SI in our model. Finally, we speculated as to an oxygen sensing mechanism for C2C12 myotubes in culture and provided preliminary findings indicating that, although the HIF1α and REDD-1 proteins are apparent during normoxia, their levels seem to increase during both acute hypoxia and acute SI. Together with these and our findings of increased CREB phosphorylation during hypoxia and SI, we provided a platform for further investigation into the oxygen sensing mechanism in C2C12 cells during myogenesis. Finally, based on our results and evidence from the literature, we propose a

mechanism of how decreased PI3K/Akt activity might occur during the three hours of acute SI and hypoxia in our model.

References

(1973) Glossary on respiration and gas exchange. *J Appl Physiol,* 34**,** 549-58.

ACKER, T., FANDREY, J. & ACKER, H. (2006) The good, the bad and the ugly in oxygen-sensing: ROS, cytochromes and prolyl-hydroxylases. *Cardiovasc Res,* 71**,** 195-207.

AFFORD, S. & RANDHAWA, S. (2000) Apoptosis. *Mol Pathol,* 53**,** 55-63.

ALISON, M. R., POULSOM, R., FORBES, S. & WRIGHT, N. A. (2002) An introduction to stem cells. *J Pathol,* 197**,** 419-23.

ALLEN, D. G. & XIAO, X. H. (2003) Role of the cardiac Na+/H+ exchanger during ischemia and reperfusion. *Cardiovasc Res,* 57**,** 934-41.

ANASTASI, S., GIORDANO, S., STHANDIER, O., GAMBAROTTA, G., MAIONE, R., COMOGLIO, P. & AMATI, P. (1997) A natural hepatocyte growth factor/scatter factor autocrine loop in myoblast cells and the effect of the constitutive Met kinase activation on myogenic differentiation. *J Cell Biol,* 137**,** 1057-68.

ARANGUREN, X. L., MCCUE, J. D., HENDRICKX, B., ZHU, X. H., DU, F., CHEN, E., PELACHO, B., PENUELAS, I., ABIZANDA, G., URIZ, M., FROMMER, S. A., ROSS, J. J., SCHROEDER, B. A., SEABORN, M. S., ADNEY, J. R., HAGENBROCK, J., HARRIS, N. H., ZHANG, Y., ZHANG, X., NELSON-HOLTE, M. H., JIANG, Y., BILLIAU, A. D., CHEN, W., PROSPER, F., VERFAILLIE, C. M. & LUTTUN, A. (2008) Multipotent adult progenitor cells sustain function of ischemic limbs in mice. *J Clin Invest,* 118**,** 505-14.

ARSHAM, A. M., PLAS, D. R., THOMPSON, C. B. & SIMON, M. C. (2002) Phosphatidylinositol 3-kinase/Akt signaling is neither required for hypoxic stabilization of HIF-1 alpha nor sufficient for HIF-1-dependent target gene transcription. *J Biol Chem,* 277**,** 15162-70.

ASSUNCAO GUIMARAES, C. & LINDEN, R. (2004) Programmed cell deaths. Apoptosis and alternative deathstyles. *Eur J Biochem,* 271**,** 1638-50.

BACH, L. A., SALEMI, R. & LEEDING, K. S. (1995) Roles of insulin-like growth factor (IGF) receptors and IGF-binding proteins in IGF-II-induced proliferation and differentiation of L6A1 rat myoblasts. *Endocrinology,* 136**,** 5061-9.

BAE, Y. S., KANG, S. W., SEO, M. S., BAINES, I. C., TEKLE, E., CHOCK, P. B. & RHEE, S. G. (1997) Epidermal growth factor (EGF)-induced generation of hydrogen peroxide. Role in EGF receptor-mediated tyrosine phosphorylation. *J Biol Chem,* 272**,** 217-21.

BANASIAK, K. J., XIA, Y. & HADDAD, G. G. (2000) Mechanisms underlying hypoxia-induced neuronal apoptosis. *Prog Neurobiol,* 62**,** 215-49.

BARBAZETTO, I. A., LIANG, J., CHANG, S., ZHENG, L., SPECTOR, A. & DILLON, J. P. (2004) Oxygen tension in the rabbit lens and vitreous before and after vitrectomy. *Exp Eye Res,* 78**,** 917-24.

BARILLAS, R., FRIEHS, I., CAO-DANH, H., MARTINEZ, J. F. & DEL NIDO, P. J. (2007) Inhibition of glycogen synthase kinase-3beta improves tolerance to ischemia in hypertrophied hearts. *Ann Thorac Surg,* 84**,** 126-33.

BARKETT, M. & GILMORE, T. D. (1999) Control of apoptosis by Rel/NF-kappaB transcription factors. *Oncogene,* 18**,** 6910-24.

BARRY, R. E., ALLAN, B. B., CUMMINS, E. P., KATTLA, J. J., GIBLIN, A., SCALLY, N., TAYLOR, C. T. & BRAZIL, D. P. (2007) Enhanced sensitivity of protein kinase B/Akt to insulin in hypoxia is independent of HIF1alpha and promotes cell viability. *Eur J Cell Biol,* 86**,** 393-403.

BEITNER-JOHNSON, D. & MILLHORN, D. E. (1998) Hypoxia induces phosphorylation of the cyclic AMP response element-binding protein by a novel signaling mechanism. *J Biol Chem,* 273**,** 19834-9.

BEITNER-JOHNSON, D., RUST, R. T., HSIEH, T. C. & MILLHORN, D. E. (2001) Hypoxia activates Akt and induces phosphorylation of GSK-3 in PC12 cells. *Cell Signal,* 13**,** 23-7.

BELAIBA, R. S., BONELLO, S., ZAHRINGER, C., SCHMIDT, S., HESS, J., KIETZMANN, T. & GORLACH, A. (2007) Hypoxia up-regulates hypoxia-inducible factor-1alpha transcription by involving phosphatidylinositol 3-kinase and nuclear factor kappaB in pulmonary artery smooth muscle cells. *Mol Biol Cell,* 18**,** 4691-7.

BLAISDELL, F. W. (2002) The pathophysiology of skeletal muscle ischemia and the reperfusion syndrome: a review. *Cardiovasc Surg,* 10**,** 620-30.

BLANCHER, C., MOORE, J. W., ROBERTSON, N. & HARRIS, A. L. (2001) Effects of ras and von Hippel-Lindau (VHL) gene mutations on hypoxia-inducible factor (HIF)-1alpha, HIF-2alpha, and vascular endothelial growth factor expression and their regulation by the phosphatidylinositol 3'-kinase/Akt signaling pathway. *Cancer Res,* 61**,** 7349-55.

BOGOYEVITCH, M. A., NG, D. C., COURT, N. W., DRAPER, K. A., DHILLON, A. & ABAS, L. (2000) Intact mitochondrial electron transport function is essential for signalling by hydrogen peroxide in cardiac myocytes. *J Mol Cell Cardiol,* 32**,** 1469-80.

BRADFORD, M. M. (1976) A rapid and sensitive method for the quantitation of microgram quantities of protein utilizing the principle of protein-dye binding. *Anal Biochem,* 72**,** 248-54.

BREVETTI, L. S., CHANG, D. S., TANG, G. L., SARKAR, R. & MESSINA, L. M. (2003) Overexpression of endothelial nitric oxide synthase increases skeletal muscle blood flow and oxygenation in severe rat hind limb ischemia. *J Vasc Surg,* 38**,** 820-6.

BRUGAROLAS, J., LEI, K., HURLEY, R. L., MANNING, B. D., REILING, J. H., HAFEN, E., WITTERS, L. A., ELLISEN, L. W. & KAELIN, W. G., JR. (2004) Regulation of mTOR function in response to hypoxia by REDD1 and the TSC1/TSC2 tumor suppressor complex. *Genes Dev,* 18**,** 2893-904.

BRUICK, R. K. & MCKNIGHT, S. L. (2001) A conserved family of prolyl-4-hydroxylases that modify HIF. *Science,* 294**,** 1337-40.

BRUNELLE, J. K., BELL, E. L., QUESADA, N. M., VERCAUTEREN, K., TIRANTI, V., ZEVIANI, M., SCARPULLA, R. C. & CHANDEL, N. S. (2005) Oxygen sensing requires mitochondrial ROS but not oxidative phosphorylation. *Cell Metab,* 1**,** 409-14.

BUDAS, G. R., SUKHODUB, A., ALESSI, D. R. & JOVANOVIC, A. (2006) 3'Phosphoinositide-dependent kinase-1 is essential for ischemic preconditioning of the myocardium. *Faseb J,* 20**,** 2556-8.

BURGERING, B. M. & MEDEMA, R. H. (2003) Decisions on life and death: FOXO Forkhead transcription factors are in command when PKB/Akt is off duty. *J Leukoc Biol,* 73**,** 689-701.

CANTLEY, L. C. (2002) The phosphoinositide 3-kinase pathway. *Science,* 296**,** 1655-7.

CANTLEY, L. C. & NEEL, B. G. (1999) New insights into tumor suppression: PTEN suppresses tumor formation by restraining the phosphoinositide 3-kinase/AKT pathway. *Proc Natl Acad Sci U S A,* 96**,** 4240-5.

CANTRELL, D. A. (2001) Phosphoinositide 3-kinase signalling pathways. *J Cell Sci,* 114**,** 1439-45.

CARDONE, M. H., ROY, N., STENNICKE, H. R., SALVESEN, G. S., FRANKE, T. F., STANBRIDGE, E., FRISCH, S. & REED, J. C. (1998) Regulation of cell death protease caspase-9 by phosphorylation. *Science,* 282**,** 1318-21.

CHAI, J., DU, C., WU, J. W., KYIN, S., WANG, X. & SHI, Y. (2000) Structural and biochemical basis of apoptotic activation by Smac/DIABLO. *Nature,* 406**,** 855-62.

CHANDEL, N. S., MCCLINTOCK, D. S., FELICIANO, C. E., WOOD, T. M., MELENDEZ, J. A., RODRIGUEZ, A. M. & SCHUMACKER, P. T. (2000) Reactive oxygen species generated at mitochondrial complex III stabilize hypoxia-inducible factor-1alpha during hypoxia: a mechanism of O2 sensing. *J Biol Chem,* 275**,** 25130-8.

CHARGE, S. B. & RUDNICKI, M. A. (2004) Cellular and molecular regulation of muscle regeneration. *Physiol Rev,* 84**,** 209-38.

CHEN, C., PORE, N., BEHROOZ, A., ISMAIL-BEIGI, F. & MAITY, A. (2001) Regulation of glut1 mRNA by hypoxia-inducible factor-1. Interaction between H-ras and hypoxia. *J Biol Chem,* 276**,** 9519-25.

CHEN, G. & GOEDDEL, D. V. (2002) TNF-R1 signaling: a beautiful pathway. *Science,* 296**,** 1634-5.

CHIARUGI, P., CIRRI, P., TADDEI, M. L., TALINI, D., DORIA, L., FIASCHI, T., BURICCHI, F., GIANNONI, E., CAMICI, G., RAUGEI, G. & RAMPONI, G. (2002) New perspectives in PDGF receptor downregulation: the main role of phosphotyrosine phosphatases. *J Cell Sci,* 115**,** 2219-32.

CLANTON, T. (2005) Yet another oxygen paradox. *J Appl Physiol,* 99**,** 1245-6.

CLANTON, T. L. (2007) Hypoxia-induced reactive oxygen species formation in skeletal muscle. *J Appl Physiol,* 102**,** 2379-88.

COHEN, G. M. (1997) Caspases: the executioners of apoptosis. *Biochem J,* 326 (Pt 1)**,** 1-16.

COLEMAN, C. N., MITCHELL, J. B. & CAMPHAUSEN, K. (2002) Tumor hypoxia: chicken, egg, or a piece of the farm? *J Clin Oncol,* 20**,** 610-5.

CONEJO, R. & LORENZO, M. (2001) Insulin signaling leading to proliferation, survival, and membrane ruffling in C2C12 myoblasts. *J Cell Physiol,* 187**,** 96-108.

COOLICAN, S. A., SAMUEL, D. S., EWTON, D. Z., MCWADE, F. J. & FLORINI, J. R. (1997) The mitogenic and myogenic actions of insulin-like growth factors utilize distinct signaling pathways. *J Biol Chem,* 272**,** 6653-62.

CREGAN, S. P., DAWSON, V. L. & SLACK, R. S. (2004) Role of AIF in caspase-dependent and caspase-independent cell death. *Oncogene,* 23**,** 2785-96.

CROSS, D. A., ALESSI, D. R., COHEN, P., ANDJELKOVICH, M. & HEMMINGS, B. A. (1995) Inhibition of glycogen synthase kinase-3 by insulin mediated by protein kinase B. *Nature,* 378**,** 785-9.

DATTA, S. R., DUDEK, H., TAO, X., MASTERS, S., FU, H., GOTOH, Y. & GREENBERG, M. E. (1997) Akt phosphorylation of BAD couples survival signals to the cell-intrinsic death machinery. *Cell,* 91**,** 231-41.

DENKO, N., SCHINDLER, C., KOONG, A., LADEROUTE, K., GREEN, C. & GIACCIA, A. (2000) Epigenetic regulation of gene expression in cervical cancer cells by the tumor microenvironment. *Clin Cancer Res,* 6**,** 480-7.

DIRNAGL, U., IADECOLA, C. & MOSKOWITZ, M. A. (1999) Pathobiology of ischaemic stroke: an integrated view. *Trends Neurosci,* 22**,** 391-7.

ENGELMAN, J. A., LUO, J. & CANTLEY, L. C. (2006) The evolution of phosphatidylinositol 3-kinases as regulators of growth and metabolism. *Nat Rev Genet,* 7**,** 606-19.

ERBAY, E. & CHEN, J. (2001) The mammalian target of rapamycin regulates C2C12 myogenesis via a kinase-independent mechanism. *J Biol Chem,* 276**,** 36079-82.

ERBAY, E., PARK, I. H., NUZZI, P. D., SCHOENHERR, C. J. & CHEN, J. (2003) IGF-II transcription in skeletal myogenesis is controlled by mTOR and nutrients. *J Cell Biol,* 163**,** 931-6.

ERZURUM, S. C., GHOSH, S., JANOCHA, A. J., XU, W., BAUER, S., BRYAN, N. S., TEJERO, J., HEMANN, C., HILLE, R., STUEHR, D. J., FEELISCH, M. & BEALL, C. M. (2007) Higher blood flow and circulating NO products offset high-altitude hypoxia among Tibetans. *Proc Natl Acad Sci U S A,* 104**,** 17593-8.

ESSOP, M. F. (2007) Cardiac metabolic adaptations in response to chronic hypoxia. *J Physiol,* 584**,** 715-26.

ESUMI, K., NISHIDA, M., SHAW, D., SMITH, T. W. & MARSH, J. D. (1991) NADH measurements in adult rat myocytes during simulated ischemia. *Am J Physiol,* 260**,** H1743-52.

FELDSER, D., AGANI, F., IYER, N. V., PAK, B., FERREIRA, G. & SEMENZA, G. L. (1999) Reciprocal positive regulation of hypoxia-inducible factor 1alpha and insulin-like growth factor 2. *Cancer Res,* 59**,** 3915-8.

FLORINI, J. R., MAGRI, K. A., EWTON, D. Z., JAMES, P. L., GRINDSTAFF, K. & ROTWEIN, P. S. (1991) "Spontaneous" differentiation of skeletal myoblasts is dependent upon autocrine secretion of insulin-like growth factor-II. *J Biol Chem,* 266**,** 15917-23.

FLOSS, T., ARNOLD, H. H. & BRAUN, T. (1997) A role for FGF-6 in skeletal muscle regeneration. *Genes Dev,* 11**,** 2040-51.

FORMAN, H. J., FUKUTO, J. M. & TORRES, M. (2004) Redox signaling: thiol chemistry defines which reactive oxygen and nitrogen species can act as second messengers. *Am J Physiol Cell Physiol,* 287**,** C246-56.

FOSTER, F. M., TRAER, C. J., ABRAHAM, S. M. & FRY, M. J. (2003) The phosphoinositide (PI) 3-kinase family. *J Cell Sci,* 116**,** 3037-40.

FUJIO, Y., GUO, K., MANO, T., MITSUUCHI, Y., TESTA, J. R. & WALSH, K. (1999) Cell cycle withdrawal promotes myogenic induction of Akt, a positive modulator of myocyte survival. *Mol Cell Biol,* 19**,** 5073-82.

FUKUNAGA, K. & KAWANO, T. (2003) Akt is a molecular target for signal transduction therapy in brain ischemic insult. *J Pharmacol Sci,* 92**,** 317-27.

GAO, T., FURNARI, F. & NEWTON, A. C. (2005) PHLPP: a phosphatase that directly dephosphorylates Akt, promotes apoptosis, and suppresses tumor growth. *Mol Cell,* 18**,** 13-24.

GEERING, B., CUTILLAS, P. R. & VANHAESEBROECK, B. (2007) Regulation of class IA PI3Ks: is there a role for monomeric PI3K subunits? *Biochem Soc Trans,* 35**,** 199-203.

GERASIMOVSKAYA, E. V., TUCKER, D. A. & STENMARK, K. R. (2005) Activation of phosphatidylinositol 3-kinase, Akt, and mammalian target of rapamycin is necessary for hypoxia-induced pulmonary artery adventitial fibroblast proliferation. *J Appl Physiol,* 98**,** 722-31.

GERMANI, A., DI CARLO, A., MANGONI, A., STRAINO, S., GIACINTI, C., TURRINI, P., BIGLIOLI, P. & CAPOGROSSI, M. C. (2003) Vascular endothelial growth factor modulates skeletal myoblast function. *Am J Pathol,* 163**,** 1417-28.

GLEADLE, J. M., MOLE, D. R. & PUGH, C. W. (2006) Hypoxia-inducible factors: where, when and why? *Kidney Int,* 69**,** 15-7.

GONZALEZ, I., TRIPATHI, G., CARTER, E. J., COBB, L. J., SALIH, D. A., LOVETT, F. A., HOLDING, C. & PELL, J. M. (2004) Akt2, a novel functional link between p38 mitogen-activated protein kinase and phosphatidylinositol 3-kinase pathways in myogenesis. *Mol Cell Biol,* 24**,** 3607-22.

GORT, E. H., GROOT, A. J., DERKS VAN DE VEN, T. L., VAN DER GROEP, P., VERLAAN, I., VAN LAAR, T., VAN DIEST, P. J., VAN DER WALL, E. & SHVARTS, A. (2006) Hypoxia-inducible factor-1alpha expression requires PI 3-kinase activity and correlates with Akt1 phosphorylation in invasive breast carcinomas. *Oncogene,* 25**,** 6123-7.

GOTTLIEB, R. A., GIESING, H. A., ZHU, J. Y., ENGLER, R. L. & BABIOR, B. M. (1995) Cell acidification in apoptosis: granulocyte colony-stimulating factor delays programmed cell death in neutrophils by up-regulating the vacuolar H(+)-ATPase. *Proc Natl Acad Sci U S A,* 92**,** 5965-8.

GREIJER, A. E., VAN DER GROEP, P., KEMMING, D., SHVARTS, A., SEMENZA, G. L., MEIJER, G. A., VAN DE WIEL, M. A., BELIEN, J. A., VAN DIEST, P. J. & VAN DER WALL, E. (2005) Up-regulation of gene expression by hypoxia is mediated predominantly by hypoxia-inducible factor 1 (HIF-1). *J Pathol,* 206**,** 291-304.

GROUNDS, M. D. (1998) Age-associated changes in the response of skeletal muscle cells to exercise and regeneration. *Ann N Y Acad Sci,* 854**,** 78-91.

GUYTON, A. C., HALL, J.E. (2006) *Textbook of medical physiology,* Philadelphia, Elsevier Saunders.

GUZY, R. D., HOYOS, B., ROBIN, E., CHEN, H., LIU, L., MANSFIELD, K. D., SIMON, M. C., HAMMERLING, U. & SCHUMACKER, P. T. (2005) Mitochondrial complex III is required for hypoxia-induced ROS production and cellular oxygen sensing. *Cell Metab,* 1**,** 401-8.

HAHN-WINDGASSEN, A., NOGUEIRA, V., CHEN, C. C., SKEEN, J. E., SONENBERG, N. & HAY, N. (2005) Akt activates the mammalian target of rapamycin by regulating cellular ATP level and AMPK activity. *J Biol Chem,* 280**,** 32081-9.

HANCOCK, J. T., DESIKAN, R. & NEILL, S. J. (2001) Role of reactive oxygen species in cell signalling pathways. *Biochem Soc Trans,* 29**,** 345-50.

HARRINGTON, L. S., FINDLAY, G. M. & LAMB, R. F. (2005) Restraining PI3K: mTOR signalling goes back to the membrane. *Trends Biochem Sci,* 30**,** 35-42.

HARRIS, A. L. (2002) Hypoxia--a key regulatory factor in tumour growth. *Nat Rev Cancer,* 2**,** 38-47.

HAWKE, T. J. & GARRY, D. J. (2001) Myogenic satellite cells: physiology to molecular biology. *J Appl Physiol,* 91**,** 534-51.

HAY, N. & SONENBERG, N. (2004) Upstream and downstream of mTOR. *Genes Dev,* 18**,** 1926-45.

HEEMSKERK, A. M., STRIJKERS, G. J., DROST, M. R., VAN BOCHOVE, G. S. & NICOLAY, K. (2007) Skeletal muscle degeneration and regeneration after femoral artery ligation in mice: monitoring with diffusion MR imaging. *Radiology,* 243**,** 413-21.

HOCKEL, M. & VAUPEL, P. (2001) Tumor hypoxia: definitions and current clinical, biologic, and molecular aspects. *J Natl Cancer Inst,* 93**,** 266-76.

HOLLERAN, J. L., EGORIN, M. J., ZUHOWSKI, E. G., PARISE, R. A., MUSSER, S. M. & PAN, S. S. (2003) Use of high-performance liquid chromatography to characterize the rapid decomposition of wortmannin in tissue culture media. *Anal Biochem,* 323**,** 19-25.

HOPPELER, H. & VOGT, M. (2001) Muscle tissue adaptations to hypoxia. *J Exp Biol,* 204**,** 3133-9.

HOPPELER, H., VOGT, M., WEIBEL, E. R. & FLUCK, M. (2003) Response of skeletal muscle mitochondria to hypoxia. *Exp Physiol,* 88**,** 109-19.

HOWALD, H. & HOPPELER, H. (2003) Performing at extreme altitude: muscle cellular and subcellular adaptations. *Eur J Appl Physiol,* 90**,** 360-4.

HRIBAL, M. L., NAKAE, J., KITAMURA, T., SHUTTER, J. R. & ACCILI, D. (2003) Regulation of insulin-like growth factor-dependent myoblast differentiation by Foxo forkhead transcription factors. *J Cell Biol,* 162**,** 535-41.

HUANG, L. E., GU, J., SCHAU, M. & BUNN, H. F. (1998) Regulation of hypoxia-inducible factor 1alpha is mediated by an O2-dependent degradation domain via the ubiquitin-proteasome pathway. *Proc Natl Acad Sci U S A,* 95**,** 7987-92.

HUR, E., CHANG, K. Y., LEE, E., LEE, S. K. & PARK, H. (2001) Mitogen-activated protein kinase kinase inhibitor PD98059 blocks the trans-activation but not the stabilization or DNA binding ability of hypoxia-inducible factor-1alpha. *Mol Pharmacol,* 59**,** 1216-24.

HUXLEY, A. F. (2000) Mechanics and models of the myosin motor. *Philos Trans R Soc Lond B Biol Sci,* 355**,** 433-40.

INOKI, K., OUYANG, H., LI, Y. & GUAN, K. L. (2005) Signaling by target of rapamycin proteins in cell growth control. *Microbiol Mol Biol Rev,* 69**,** 79-100.

INOKI, K., ZHU, T. & GUAN, K. L. (2003) TSC2 mediates cellular energy response to control cell growth and survival. *Cell,* 115**,** 577-90.

JIANG, B. H., AOKI, M., ZHENG, J. Z., LI, J. & VOGT, P. K. (1999) Myogenic signaling of phosphatidylinositol 3-kinase requires the serine-threonine kinase Akt/protein kinase B. *Proc Natl Acad Sci U S A,* 96**,** 2077-81.

JIANG, B. H., ZHENG, J. Z. & VOGT, P. K. (1998) An essential role of phosphatidylinositol 3-kinase in myogenic differentiation. *Proc Natl Acad Sci U S A,* 95**,** 14179-83.

JIANG, X. & WANG, X. (2004) Cytochrome C-mediated apoptosis. *Annu Rev Biochem,* 73**,** 87-106.

JIANG, Z., ZHANG, Y., CHEN, X., LAM, P. Y., YANG, H., XU, Q. & YU, A. C. (2002) Activation of Erk1/2 and Akt in astrocytes under ischemia. *Biochem Biophys Res Commun,* 294**,** 726-33.

JIN, K. L., MAO, X. O., NAGAYAMA, T., GOLDSMITH, P. C. & GREENBERG, D. A. (2000) Induction of vascular endothelial growth factor receptors and phosphatidylinositol 3'-kinase/Akt signaling by global cerebral ischemia in the rat. *Neuroscience,* 100**,** 713-7.

JOHANNESSEN, M., DELGHANDI, M. P. & MOENS, U. (2004) What turns CREB on? *Cell Signal,* 16**,** 1211-27.

JOZA, N., SUSIN, S. A., DAUGAS, E., STANFORD, W. L., CHO, S. K., LI, C. Y., SASAKI, T., ELIA, A. J., CHENG, H. Y., RAVAGNAN, L., FERRI, K. F., ZAMZAMI, N., WAKEHAM, A., HAKEM, R., YOSHIDA, H., KONG, Y. Y., MAK, T. W., ZUNIGA-PFLUCKER, J. C., KROEMER, G. & PENNINGER, J. M. (2001) Essential role of the mitochondrial apoptosis-inducing factor in programmed cell death. *Nature,* 410**,** 549-54.

KALIMAN, P., VINALS, F., TESTAR, X., PALACIN, M. & ZORZANO, A. (1996) Phosphatidylinositol 3-kinase inhibitors block differentiation of skeletal muscle cells. *J Biol Chem,* 271**,** 19146-51.

KALLIO, P. J., PONGRATZ, I., GRADIN, K., MCGUIRE, J. & POELLINGER, L. (1997) Activation of hypoxia-inducible factor 1alpha: posttranscriptional regulation and conformational change by recruitment of the Arnt transcription factor. *Proc Natl Acad Sci U S A,* 94**,** 5667-72.

KATAGIRI, T., YAMAGUCHI, A., KOMAKI, M., ABE, E., TAKAHASHI, N., IKEDA, T., ROSEN, V., WOZNEY, J. M., FUJISAWA-SEHARA, A. & SUDA, T. (1994) Bone morphogenetic protein-2 converts the differentiation pathway of C2C12 myoblasts into the osteoblast lineage. *J Cell Biol,* 127**,** 1755-66.

KAYSER, B., HOPPELER, H., CLAASSEN, H. & CERRETELLI, P. (1991) Muscle structure and performance capacity of Himalayan Sherpas. *J Appl Physiol,* 70**,** 1938-42.

KIETZMANN, T., FANDREY, J. & ACKER, H. (2000) Oxygen Radicals as Messengers in Oxygen-Dependent Gene Expression. *News Physiol Sci,* 15**,** 202-208.

KIM, A. H., KHURSIGARA, G., SUN, X., FRANKE, T. F. & CHAO, M. V. (2001) Akt phosphorylates and negatively regulates apoptosis signal-regulating kinase 1. *Mol Cell Biol,* 21**,** 893-901.

KING, L. M. & OPIE, L. H. (1998) Glucose and glycogen utilisation in myocardial ischemia--changes in metabolism and consequences for the myocyte. *Mol Cell Biochem,* 180**,** 3-26.

KITAGAWA, K. (2007) CREB and cAMP response element-mediated gene expression in the ischemic brain. *Febs J,* 274**,** 3210-7.

KRISTIAN, T. & SIESJO, B. K. (1998) Calcium in ischemic cell death. *Stroke,* 29**,** 705-18.

KRYSKO, D. V., D'HERDE, K. & VANDENABEELE, P. (2006) Clearance of apoptotic and necrotic cells and its immunological consequences. *Apoptosis,* 11**,** 1709-26.

KRYSTAL, G., DAMEN, J. E., HELGASON, C. D., HUBER, M., HUGHES, M. R., KALESNIKOFF, J., LAM, V., ROSTEN, P., WARE, M. D., YEW, S. & HUMPHRIES, R. K. (1999) SHIPs ahoy. *Int J Biochem Cell Biol,* 31**,** 1007-10.

KULISZ, A., CHEN, N., CHANDEL, N. S., SHAO, Z. & SCHUMACKER, P. T. (2002) Mitochondrial ROS initiate phosphorylation of p38 MAP kinase during hypoxia in cardiomyocytes. *Am J Physiol Lung Cell Mol Physiol,* 282**,** L1324-9.

KWON, D. S., KWON, C. H., KIM, J. H., WOO, J. S., JUNG, J. S. & KIM, Y. K. (2006) Signal transduction of MEK/ERK and PI3K/Akt activation by hypoxia/reoxygenation in renal epithelial cells. *Eur J Cell Biol,* 85**,** 1189-99.

LACERDA, L., SMITH, R. M., OPIE, L. & LECOUR, S. (2006) TNFalpha-induced cytoprotection requires the production of free radicals within mitochondria in C2C12 myotubes. *Life Sci,* 79**,** 2194-201.

LANDO, D., PEET, D. J., GORMAN, J. J., WHELAN, D. A., WHITELAW, M. L. & BRUICK, R. K. (2002) FIH-1 is an asparaginyl hydroxylase enzyme that regulates the transcriptional activity of hypoxia-inducible factor. *Genes Dev,* 16**,** 1466-71.

LAUGHNER, E., TAGHAVI, P., CHILES, K., MAHON, P. C. & SEMENZA, G. L. (2001) HER2 (neu) signaling increases the rate of hypoxia-inducible factor 1alpha (HIF-1alpha) synthesis: novel mechanism for HIF-1-mediated vascular endothelial growth factor expression. *Mol Cell Biol,* 21**,** 3995-4004.

LAWEN, A. (2003) Apoptosis-an introduction. *Bioessays,* 25**,** 888-96.

LEE, K. & ESSELMAN, W. J. (2002) Inhibition of PTPs by H(2)O(2) regulates the activation of distinct MAPK pathways. *Free Radic Biol Med,* 33**,** 1121-32.

LEE, K., ROTH, R. A. & LAPRES, J. J. (2007) Hypoxia, drug therapy and toxicity. *Pharmacol Ther,* 113**,** 229-46.

LI, Y., INOKI, K., YEUNG, R. & GUAN, K. L. (2002) Regulation of TSC2 by 14-3-3 binding. *J Biol Chem,* 277**,** 44593-6.

LIN, C. F., CHEN, C. L., CHIANG, C. W., JAN, M. S., HUANG, W. C. & LIN, Y. S. (2007) GSK-3beta acts downstream of PP2A and the PI 3-kinase-Akt pathway, and upstream of caspase-2 in ceramide-induced mitochondrial apoptosis. *J Cell Sci,* 120**,** 2935-43.

LOBERG, R. D., VESELY, E. & BROSIUS, F. C., 3RD (2002) Enhanced glycogen synthase kinase-3beta activity mediates hypoxia-induced apoptosis of vascular smooth muscle cells and is prevented by glucose transport and metabolism. *J Biol Chem,* 277**,** 41667-73.

LOCKSHIN, R. A. & ZAKERI, Z. (2004) Apoptosis, autophagy, and more. *Int J Biochem Cell Biol,* 36**,** 2405-19.

LONG, X., BOLUYT, M. O., HIPOLITO, M. L., LUNDBERG, M. S., ZHENG, J. S., O'NEILL, L., CIRIELLI, C., LAKATTA, E. G. & CROW, M. T. (1997) p53 and the hypoxia-induced apoptosis of cultured neonatal rat cardiac myocytes. *J Clin Invest,* 99**,** 2635-43.

LOOS, B., SMITH, R. & ENGELBRECHT, A. M. (2008) Ischaemic preconditioning and TNF-alpha-mediated preconditioning is associated with a differential cPLA2 translocation pattern in early ischaemia. *Prostaglandins Leukot Essent Fatty Acids,* 78**,** 403-13.

LUO, J., MANNING, B. D. & CANTLEY, L. C. (2003) Targeting the PI3K-Akt pathway in human cancer: rationale and promise. *Cancer Cell,* 4**,** 257-62.

MAHON, P. C., HIROTA, K. & SEMENZA, G. L. (2001) FIH-1: a novel protein that interacts with HIF-1alpha and VHL to mediate repression of HIF-1 transcriptional activity. *Genes Dev,* 15**,** 2675-86.

MANALO, D. J., ROWAN, A., LAVOIE, T., NATARAJAN, L., KELLY, B. D., YE, S. Q., GARCIA, J. G. & SEMENZA, G. L. (2005) Transcriptional regulation of vascular endothelial cell responses to hypoxia by HIF-1. *Blood,* 105**,** 659-69.

MANDL, A., SARKES, D., CARRICABURU, V., JUNG, V. & RAMEH, L. (2007) Serum withdrawal-induced accumulation of phosphoinositide 3-kinase lipids in differentiating 3T3-L6 myoblasts: distinct roles for Ship2 and PTEN. *Mol Cell Biol,* 27**,** 8098-112.

MANNING, B. D., TEE, A. R., LOGSDON, M. N., BLENIS, J. & CANTLEY, L. C. (2002) Identification of the tuberous sclerosis complex-2 tumor suppressor gene product tuberin as a target of the phosphoinositide 3-kinase/akt pathway. *Mol Cell,* 10**,** 151-62.

MARTINET, W., DE MEYER, G. R., HERMAN, A. G. & KOCKX, M. M. (2005) Amino acid deprivation induces both apoptosis and autophagy in murine C2C12 muscle cells. *Biotechnol Lett,* 27**,** 1157-63.

MASSON, N., WILLAM, C., MAXWELL, P. H., PUGH, C. W. & RATCLIFFE, P. J. (2001) Independent function of two destruction domains in hypoxia-inducible factor-alpha chains activated by prolyl hydroxylation. *Embo J,* 20**,** 5197-206.

MATSUI, T., LI, L., DEL MONTE, F., FUKUI, Y., FRANKE, T. F., HAJJAR, R. J. & ROSENZWEIG, A. (1999) Adenoviral gene transfer of activated phosphatidylinositol 3'-kinase and Akt inhibits apoptosis of hypoxic cardiomyocytes in vitro. *Circulation,* 100**,** 2373-9.

MATSUI, T., TAO, J., DEL MONTE, F., LEE, K. H., LI, L., PICARD, M., FORCE, T. L., FRANKE, T. F., HAJJAR, R. J. & ROSENZWEIG, A. (2001) Akt activation preserves cardiac function and prevents injury after transient cardiac ischemia in vivo. *Circulation,* 104**,** 330-5.

MATTIASSON, G. (2004) Analysis of mitochondrial generation and release of reactive oxygen species. *Cytometry A,* 62**,** 89-96.

MAURO, A. (1961) Satellite cell of skeletal muscle fibers. *J Biophys Biochem Cytol,* 9**,** 493-5.

MEIJER, A. J. & CODOGNO, P. (2004) Regulation and role of autophagy in mammalian cells. *Int J Biochem Cell Biol,* 36**,** 2445-62.

MILLER, K. J., THALOOR, D., MATTESON, S. & PAVLATH, G. K. (2000) Hepatocyte growth factor affects satellite cell activation and differentiation in regenerating skeletal muscle. *Am J Physiol Cell Physiol,* 278**,** C174-81.

MISHRA, O. P., ASHRAF, Q. M. & DELIVORIA-PAPADOPOULOS, M. (2002) Phosphorylation of cAMP response element binding (CREB) protein during hypoxia in cerebral cortex of newborn piglets and the effect of nitric oxide synthase inhibition. *Neuroscience,* 115**,** 985-91.

MO, F. M. & BALLARD, H. J. (2005) Acute systemic hypoxia elevates venous but not interstitial potassium of dog skeletal muscle. *Am J Physiol Heart Circ Physiol,* 289**,** H1710-8.

MOTTET, D., DUMONT, V., DECCACHE, Y., DEMAZY, C., NINANE, N., RAES, M. & MICHIELS, C. (2003) Regulation of hypoxia-inducible factor-1alpha protein level during hypoxic conditions by the phosphatidylinositol 3-kinase/Akt/glycogen synthase kinase 3beta pathway in HepG2 cells. *J Biol Chem,* 278**,** 31277-85.

NAVE, B. T., OUWENS, M., WITHERS, D. J., ALESSI, D. R. & SHEPHERD, P. R. (1999) Mammalian target of rapamycin is a direct target for protein kinase B: identification of a convergence point for opposing effects of insulin and amino-acid deficiency on protein translation. *Biochem J,* 344 Pt 2**,** 427-31.

NEELY, J. R. & GROTYOHANN, L. W. (1984) Role of glycolytic products in damage to ischemic myocardium. Dissociation of adenosine triphosphate levels and recovery of function of reperfused ischemic hearts. *Circ Res,* 55**,** 816-24.

NEMOTO, S., TAKEDA, K., YU, Z. X., FERRANS, V. J. & FINKEL, T. (2000) Role for mitochondrial oxidants as regulators of cellular metabolism. *Mol Cell Biol,* 20**,** 7311-8.

NICHOLSON, D. W. & THORNBERRY, N. A. (1997) Caspases: killer proteases. *Trends Biochem Sci,* 22**,** 299-306.

NIESLER, C. U., MYBURGH, K. H. & MOORE, F. (2007) The changing AMPK expression profile in differentiating mouse skeletal muscle myoblast cells helps confer increasing resistance to apoptosis. *Exp Physiol,* 92**,** 207-17.

NOBUKUNI, T., JOAQUIN, M., ROCCIO, M., DANN, S. G., KIM, S. Y., GULATI, P., BYFIELD, M. P., BACKER, J. M., NATT, F., BOS, J. L., ZWARTKRUIS, F. J. & THOMAS, G. (2005) Amino acids mediate mTOR/raptor signaling through activation of class 3 phosphatidylinositol 3OH-kinase. *Proc Natl Acad Sci U S A,* 102**,** 14238-43.

NOSHITA, N., SUGAWARA, T., LEWEN, A., HAYASHI, T. & CHAN, P. H. (2003) Copper-zinc superoxide dismutase affects Akt activation after transient focal cerebral ischemia in mice. *Stroke,* 34**,** 1513-8.

NUNEZ, G., BENEDICT, M. A., HU, Y. & INOHARA, N. (1998) Caspases: the proteases of the apoptotic pathway. *Oncogene,* 17**,** 3237-45.

OLSON, E. N. (1990) MyoD family: a paradigm for development? *Genes Dev,* 4**,** 1454-61.

ONO, Y., SENSUI, H., SAKAMOTO, Y. & NAGATOMI, R. (2006) Knockdown of hypoxia-inducible factor-1alpha by siRNA inhibits C2C12 myoblast differentiation. *J Cell Biochem,* 98**,** 642-9.

OZAKI, H., YU, A. Y., DELLA, N., OZAKI, K., LUNA, J. D., YAMADA, H., HACKETT, S. F., OKAMOTO, N., ZACK, D. J., SEMENZA, G. L. & CAMPOCHIARO, P. A. (1999) Hypoxia inducible factor-1alpha is increased in ischemic retina: temporal and spatial correlation with VEGF expression. *Invest Ophthalmol Vis Sci,* 40**,** 182-9.

PAPANDREOU, I., POWELL, A., LIM, A. L. & DENKO, N. (2005) Cellular reaction to hypoxia: sensing and responding to an adverse environment. *Mutat Res,* 569**,** 87-100.

PLAS, D. R. & THOMPSON, C. B. (2005) Akt-dependent transformation: there is more to growth than just surviving. *Oncogene,* 24**,** 7435-42.

POTTER, C. J., PEDRAZA, L. G. & XU, T. (2002) Akt regulates growth by directly phosphorylating Tsc2. *Nat Cell Biol,* 4**,** 658-65.

POUYSSEGUR, J., DAYAN, F. & MAZURE, N. M. (2006) Hypoxia signalling in cancer and approaches to enforce tumour regression. *Nature,* 441**,** 437-43.

PUGAZHENTHI, S., NESTEROVA, A., SABLE, C., HEIDENREICH, K. A., BOXER, L. M., HEASLEY, L. E. & REUSCH, J. E. (2000) Akt/protein kinase B up-regulates Bcl-2 expression through cAMP-response element-binding protein. *J Biol Chem,* 275**,** 10761-6.

PUGH, C. W. & RATCLIFFE, P. J. (2003) Regulation of angiogenesis by hypoxia: role of the HIF system. *Nat Med,* 9**,** 677-84.

RAMEH, L. E. & CANTLEY, L. C. (1999) The role of phosphoinositide 3-kinase lipid products in cell function. *J Biol Chem,* 274**,** 8347-50.

RASSIER, D. E., MACINTOSH, B. R. & HERZOG, W. (1999) Length dependence of active force production in skeletal muscle. *J Appl Physiol,* 86**,** 1445-57.

REAGAN-SHAW, S. & AHMAD, N. (2007) The role of Forkhead-box Class O (FoxO) transcription factors in cancer: a target for the management of cancer. *Toxicol Appl Pharmacol,* 224**,** 360-8.

REYNAFARJE, B. (1962) Myoglobin content and enzymatic activity of muscle and altitude adaptation. *J Appl Physiol,* 17**,** 301-5.

RICHARD, D. E., BERRA, E. & POUYSSEGUR, J. (2000) Nonhypoxic pathway mediates the induction of hypoxia-inducible factor 1alpha in vascular smooth muscle cells. *J Biol Chem,* 275**,** 26765-71.

ROCCHI, S., TARTARE-DECKERT, S., MURDACA, J., HOLGADO-MADRUGA, M., WONG, A. J. & VAN OBBERGHEN, E. (1998) Determination of Gab1 (Grb2-associated binder-1) interaction with insulin receptor-signaling molecules. *Mol Endocrinol,* 12**,** 914-23.

ROMMEL, C., CLARKE, B. A., ZIMMERMANN, S., NUNEZ, L., ROSSMAN, R., REID, K., MOELLING, K., YANCOPOULOS, G. D. & GLASS, D. J. (1999) Differentiation stage-specific inhibition of the Raf-MEK-ERK pathway by Akt. *Science,* 286**,** 1738-41.

ROY, S., KHANNA, S., BICKERSTAFF, A. A., SUBRAMANIAN, S. V., ATALAY, M., BIERL, M., PENDYALA, S., LEVY, D., SHARMA, N., VENOJARVI, M., STRAUCH, A., OROSZ, C. G. & SEN, C. K. (2003) Oxygen sensing by primary cardiac fibroblasts: a key role of p21(Waf1/Cip1/Sdi1). *Circ Res,* 92**,** 264-71.

SABOURIN, L. A., GIRGIS-GABARDO, A., SEALE, P., ASAKURA, A. & RUDNICKI, M. A. (1999) Reduced differentiation potential of primary MyoD-/- myogenic cells derived from adult skeletal muscle. *J Cell Biol,* 144**,** 631-43.

SALCEDA, S. & CARO, J. (1997) Hypoxia-inducible factor 1alpha (HIF-1alpha) protein is rapidly degraded by the ubiquitin-proteasome system under normoxic conditions. Its stabilization by hypoxia depends on redox-induced changes. *J Biol Chem,* 272**,** 22642-7.

SANG, N., STIEHL, D. P., BOHENSKY, J., LESHCHINSKY, I., SRINIVAS, V. & CARO, J. (2003) MAPK signaling up-regulates the activity of hypoxia-inducible factors by its effects on p300. *J Biol Chem,* 278**,** 14013-9.

SANTILLI, J. D. & SANTILLI, S. M. (1999) Chronic critical limb ischemia: diagnosis, treatment and prognosis. *Am Fam Physician,* 59**,** 1899-908.

SANTORE, M. T., MCCLINTOCK, D. S., LEE, V. Y., BUDINGER, G. R. & CHANDEL, N. S. (2002) Anoxia-induced apoptosis occurs through a mitochondria-dependent pathway in lung epithelial cells. *Am J Physiol Lung Cell Mol Physiol,* 282**,** L727-34.

SARBASSOV, D. D., ALI, S. M. & SABATINI, D. M. (2005a) Growing roles for the mTOR pathway. *Curr Opin Cell Biol,* 17**,** 596-603.

SARBASSOV, D. D., GUERTIN, D. A., ALI, S. M. & SABATINI, D. M. (2005b) Phosphorylation and regulation of Akt/PKB by the rictor-mTOR complex. *Science,* 307**,** 1098-101.

SCHOLZ, D., THOMAS, S., SASS, S. & PODZUWEIT, T. (2003) Angiogenesis and myogenesis as two facets of inflammatory post-ischemic tissue regeneration. *Mol Cell Biochem,* 246**,** 57-67.

SEALE, P., ASAKURA, A. & RUDNICKI, M. A. (2001) The potential of muscle stem cells. *Dev Cell,* 1**,** 333-42.

SEMENZA, G. L. (1998) Hypoxia-inducible factor 1: master regulator of O2 homeostasis. *Curr Opin Genet Dev,* 8**,** 588-94.

SEMENZA, G. L. (1999) Perspectives on oxygen sensing. *Cell,* 98**,** 281-4.

SEMENZA, G. L. (2000) HIF-1 and human disease: one highly involved factor. *Genes Dev,* 14**,** 1983-91.

SEMENZA, G. L. (2001) HIF-1 and mechanisms of hypoxia sensing. *Curr Opin Cell Biol,* 13**,** 167-71.

SEMENZA, G. L., NEJFELT, M. K., CHI, S. M. & ANTONARAKIS, S. E. (1991) Hypoxia-inducible nuclear factors bind to an enhancer element located 3' to the human erythropoietin gene. *Proc Natl Acad Sci U S A,* 88**,** 5680-4.

SHAO, Z., BHATTACHARYA, K., HSICH, E., PARK, L., WALTERS, B., GERMANN, U., WANG, Y. M., KYRIAKIS, J., MOHANLAL, R., KUIDA, K., NAMCHUK, M., SALITURO, F., YAO, Y. M., HOU, W. M., CHEN, X., ARONOVITZ, M., TSICHLIS, P. N., BHATTACHARYA, S., FORCE, T. & KILTER, H. (2006) c-Jun N-terminal kinases mediate reactivation of Akt and cardiomyocyte survival after hypoxic injury in vitro and in vivo. *Circ Res,* 98**,** 111-8.

SHAW, R. J. & CANTLEY, L. C. (2006) Ras, PI(3)K and mTOR signalling controls tumour cell growth. *Nature,* 441**,** 424-30.

SHEN, W. H., BOYLE, D. W., WISNIOWSKI, P., BADE, A. & LIECHTY, E. A. (2005) Insulin and IGF-I stimulate the formation of the eukaryotic initiation factor 4F complex and protein synthesis in C2C12 myotubes independent of availability of external amino acids. *J Endocrinol,* 185**,** 275-89.

SHIOJIMA, I. & WALSH, K. (2002) Role of Akt signaling in vascular homeostasis and angiogenesis. *Circ Res,* 90**,** 1243-50.

SIMON, A. R., RAI, U., FANBURG, B. L. & COCHRAN, B. H. (1998) Activation of the JAK-STAT pathway by reactive oxygen species. *Am J Physiol,* 275**,** C1640-52.

SOLDANI, C. & SCOVASSI, A. I. (2002) Poly(ADP-ribose) polymerase-1 cleavage during apoptosis: an update. *Apoptosis,* 7**,** 321-8.

SONG, G., OUYANG, G. & BAO, S. (2005) The activation of Akt/PKB signaling pathway and cell survival. *J Cell Mol Med,* 9**,** 59-71.

SONG, J. J. & LEE, Y. J. (2005) Dissociation of Akt1 from its negative regulator JIP1 is mediated through the ASK1-MEK-JNK signal transduction pathway during metabolic oxidative stress: a negative feedback loop. *J Cell Biol,* 170**,** 61-72.

STEPHENS, L., ANDERSON, K., STOKOE, D., ERDJUMENT-BROMAGE, H., PAINTER, G. F., HOLMES, A. B., GAFFNEY, P. R., REESE, C. B., MCCORMICK, F., TEMPST, P., COADWELL, J. & HAWKINS, P. T. (1998) Protein kinase B kinases that mediate phosphatidylinositol 3,4,5-trisphosphate-dependent activation of protein kinase B. *Science,* 279**,** 710-4.

STEWART, C. E. & ROTWEIN, P. (1996) Insulin-like growth factor-II is an autocrine survival factor for differentiating myoblasts. *J Biol Chem,* 271**,** 11330-8.

STROMHAUG, P. E. & KLIONSKY, D. J. (2001) Approaching the molecular mechanism of autophagy. *Traffic,* 2**,** 524-31.

SUTTER, C. H., LAUGHNER, E. & SEMENZA, G. L. (2000) Hypoxia-inducible factor 1alpha protein expression is controlled by oxygen-regulated ubiquitination that is disrupted by deletions and missense mutations. *Proc Natl Acad Sci U S A,* 97**,** 4748-53.

SUZUKI, J., YAMAZAKI, Y., LI, G., KAZIRO, Y. & KOIDE, H. (2000) Involvement of Ras and Ral in chemotactic migration of skeletal myoblasts. *Mol Cell Biol,* 20**,** 4658-65.

TAKADA, Y., HASHIMOTO, M., KASAHARA, J., AIHARA, K. & FUKUNAGA, K. (2004) Cytoprotective effect of sodium orthovanadate on ischemia/reperfusion-induced injury in the rat heart involves Akt activation and inhibition of fodrin breakdown and apoptosis. *J Pharmacol Exp Ther,* 311**,** 1249-55.

TAKAHASHI, A., KUREISHI, Y., YANG, J., LUO, Z., GUO, K., MUKHOPADHYAY, D., IVASHCHENKO, Y., BRANELLEC, D. & WALSH, K. (2002) Myogenic Akt signaling regulates blood vessel recruitment during myofiber growth. *Mol Cell Biol,* 22**,** 4803-14.

TEBOUL, L., GAILLARD, D., STACCINI, L., INADERA, H., AMRI, E. Z. & GRIMALDI, P. A. (1995) Thiazolidinediones and fatty acids convert myogenic cells into adipose-like cells. *J Biol Chem,* 270**,** 28183-7.

TEE, A. R., FINGAR, D. C., MANNING, B. D., KWIATKOWSKI, D. J., CANTLEY, L. C. & BLENIS, J. (2002) Tuberous sclerosis complex-1 and -2 gene products function together to inhibit mammalian target of rapamycin (mTOR)-mediated downstream signaling. *Proc Natl Acad Sci U S A,* 99**,** 13571-6.

TERRADOS, N., JANSSON, E., SYLVEN, C. & KAIJSER, L. (1990) Is hypoxia a stimulus for synthesis of oxidative enzymes and myoglobin? *J Appl Physiol,* 68**,** 2369-72.

THANNICKAL, V. J. & FANBURG, B. L. (2000) Reactive oxygen species in cell signaling. *Am J Physiol Lung Cell Mol Physiol,* 279**,** L1005-28.

THORNBERRY, N. A. & LAZEBNIK, Y. (1998) Caspases: enemies within. *Science,* 281**,** 1312-6.

TOKUNAGA, C., YOSHINO, K. & YONEZAWA, K. (2004) mTOR integrates amino acid- and energy-sensing pathways. *Biochem Biophys Res Commun,* 313**,** 443-6.

TSANG, A., HAUSENLOY, D. J., MOCANU, M. M., CARR, R. D. & YELLON, D. M. (2005) Preconditioning the diabetic heart: the importance of Akt phosphorylation. *Diabetes,* 54**,** 2360-4.

TSUJIMOTO, Y. & SHIMIZU, S. (2005) Another way to die: autophagic programmed cell death. *Cell Death Differ,* 12 Suppl 2**,** 1528-34.

TZATSOS, A. & TSICHLIS, P. N. (2007) Energy depletion inhibits phosphatidylinositol 3-kinase/Akt signaling and induces apoptosis via AMP-activated protein kinase-dependent phosphorylation of IRS-1 at Ser-794. *J Biol Chem,* 282**,** 18069-82.

UI, M., OKADA, T., HAZEKI, K. & HAZEKI, O. (1995) Wortmannin as a unique probe for an intracellular signalling protein, phosphoinositide 3-kinase. *Trends Biochem Sci,* 20**,** 303-7.

VAN DEN EIJNDE, S. M., VAN DEN HOFF, M. J., REUTELINGSPERGER, C. P., VAN HEERDE, W. L., HENFLING, M. E., VERMEIJ-KEERS, C., SCHUTTE, B., BORGERS, M. & RAMAEKERS, F. C. (2001) Transient expression of phosphatidylserine at cell-cell contact areas is required for myotube formation. *J Cell Sci,* 114**,** 3631-42.

VANHAESEBROECK, B., LEEVERS, S. J., AHMADI, K., TIMMS, J., KATSO, R., DRISCOLL, P. C., WOSCHOLSKI, R., PARKER, P. J. & WATERFIELD, M. D. (2001) Synthesis and function of 3-phosphorylated inositol lipids. *Annu Rev Biochem,* 70**,** 535-602.

VAUPEL, P., KALLINOWSKI, F. & OKUNIEFF, P. (1989) Blood flow, oxygen and nutrient supply, and metabolic microenvironment of human tumors: a review. *Cancer Res,* 49**,** 6449-65.

VAUPEL, P. & MAYER, A. (2007) Hypoxia in cancer: significance and impact on clinical outcome. *Cancer Metastasis Rev,* 26**,** 225-39.

VLAHOS, C. J., MATTER, W. F., HUI, K. Y. & BROWN, R. F. (1994) A specific inhibitor of phosphatidylinositol 3-kinase, 2-(4-morpholinyl)-8-phenyl-4H-1-benzopyran-4-one (LY294002). *J Biol Chem,* 269**,** 5241-8.

VOGT, M., PUNTSCHART, A., GEISER, J., ZULEGER, C., BILLETER, R. & HOPPELER, H. (2001) Molecular adaptations in human skeletal muscle to endurance training under simulated hypoxic conditions. *J Appl Physiol,* 91**,** 173-82.

WADA, T. & PENNINGER, J. M. (2004) Mitogen-activated protein kinases in apoptosis regulation. *Oncogene,* 23**,** 2838-49.

WAJANT, H. (2002) The Fas signaling pathway: more than a paradigm. *Science,* 296**,** 1635-6.

WANG, G. L., JIANG, B. H., RUE, E. A. & SEMENZA, G. L. (1995) Hypoxia-inducible factor 1 is a basic-helix-loop-helix-PAS heterodimer regulated by cellular O2 tension. *Proc Natl Acad Sci U S A,* 92**,** 5510-4.

WEBSTER, K. A., DISCHER, D. J., KAISER, S., HERNANDEZ, O., SATO, B. & BISHOPRIC, N. H. (1999) Hypoxia-activated apoptosis of cardiac myocytes requires reoxygenation or a pH shift and is independent of p53. *J Clin Invest,* 104**,** 239-52.

WEBSTER, K. A., GRAHAM, R. M. & BISHOPRIC, N. H. (2005) BNip3 and signal-specific programmed death in the heart. *J Mol Cell Cardiol,* 38**,** 35-45.

WILSON, E. M., TURECKOVA, J. & ROTWEIN, P. (2004) Permissive roles of phosphatidyl inositol 3-kinase and Akt in skeletal myocyte maturation. *Mol Biol Cell,* 15**,** 497-505.

WU, A. L., KIM, J. H., ZHANG, C., UNTERMAN, T. G. & CHEN, J. (2008) Forkhead box protein O1 negatively regulates skeletal myocyte differentiation through degradation of mammalian target of rapamycin pathway components. *Endocrinology,* 149**,** 1407-14.

WU, H., YAN, Y. & BACKER, J. M. (2007) Regulation of class IA PI3Ks. *Biochem Soc Trans,* 35**,** 242-4.

WU, W. S. (2006) The signaling mechanism of ROS in tumor progression. *Cancer Metastasis Rev,* 25**,** 695-705.

WU, X., SENECHAL, K., NESHAT, M. S., WHANG, Y. E. & SAWYERS, C. L. (1998) The PTEN/MMAC1 tumor suppressor phosphatase functions as a negative regulator of the phosphoinositide 3-kinase/Akt pathway. *Proc Natl Acad Sci U S A,* 95**,** 15587-91.

WULLSCHLEGER, S., LOEWITH, R. & HALL, M. N. (2006) TOR signaling in growth and metabolism. *Cell,* 124**,** 471-84.

YANG, Z. Z., TSCHOPP, O., BAUDRY, A., DUMMLER, B., HYNX, D. & HEMMINGS, B. A. (2004) Physiological functions of protein kinase B/Akt. *Biochem Soc Trans,* 32**,** 350-4.

YAO, H. & HADDAD, G. G. (2004) Calcium and pH homeostasis in neurons during hypoxia and ischemia. *Cell Calcium,* 36**,** 247-55.

YOSHIKO, Y., HIRAO, K. & MAEDA, N. (2002) Differentiation in C(2)C(12) myoblasts depends on the expression of endogenous IGFs and not serum depletion. *Am J Physiol Cell Physiol,* 283**,** C1278-86.

YU, F., WHITE, S. B., ZHAO, Q. & LEE, F. S. (2001) HIF-1alpha binding to VHL is regulated by stimulus-sensitive proline hydroxylation. *Proc Natl Acad Sci U S A,* 98**,** 9630-5.

YU, S. W., ANDRABI, S. A., WANG, H., KIM, N. S., POIRIER, G. G., DAWSON, T. M. & DAWSON, V. L. (2006) Apoptosis-inducing factor mediates poly(ADP-ribose) (PAR) polymer-induced cell death. *Proc Natl Acad Sci U S A,* 103**,** 18314-9.

YUN, B. G. & MATTS, R. L. (2005) Hsp90 functions to balance the phosphorylation state of Akt during C2C12 myoblast differentiation. *Cell Signal,* 17**,** 1477-85.

YUN, Z., LIN, Q. & GIACCIA, A. J. (2005) Adaptive myogenesis under hypoxia. *Mol Cell Biol,* 25**,** 3040-55.

YUNG, H. W., KOROLCHUK, S., TOLKOVSKY, A. M., CHARNOCK-JONES, D. S. & BURTON, G. J. (2007) Endoplasmic reticulum stress exacerbates ischemia-reperfusion-induced apoptosis through attenuation of Akt protein synthesis in human choriocarcinoma cells. *Faseb J,* 21**,** 872-84.

ZHANG, R., LUO, D., MIAO, R., BAI, L., GE, Q., SESSA, W. C. & MIN, W. (2005) Hsp90-Akt phosphorylates ASK1 and inhibits ASK1-mediated apoptosis. *Oncogene,* 24**,** 3954-63.

ZHONG, H., CHILES, K., FELDSER, D., LAUGHNER, E., HANRAHAN, C., GEORGESCU, M. M., SIMONS, J. W. & SEMENZA, G. L. (2000) Modulation of hypoxia-inducible factor 1alpha expression by the epidermal growth factor/phosphatidylinositol 3-kinase/PTEN/AKT/FRAP pathway in human prostate cancer cells: implications for tumor angiogenesis and therapeutics. *Cancer Res,* 60**,** 1541-5.

ZHOU, H., LI, X. M., MEINKOTH, J. & PITTMAN, R. N. (2000) Akt regulates cell survival and apoptosis at a postmitochondrial level. *J Cell Biol,* 151**,** 483-94.

ZHOU, J., HARA, K., INOUE, M., HAMADA, S., YASUDA, H., MORIYAMA, H., ENDO, H., HIROTA, K., YONEZAWA, K., NAGATA, M. & YOKONO, K. (2008) Regulation of hypoxia-inducible factor 1 by glucose availability under hypoxic conditions. *Kobe J Med Sci,* 53**,** 283-96.

ZHUANG, S. & SCHNELLMANN, R. G. (2006) A death-promoting role for extracellular signal-regulated kinase. *J Pharmacol Exp Ther,* 319**,** 991-7.

ZUO, L. & CLANTON, T. L. (2005) Reactive oxygen species formation in the transition to hypoxia in skeletal muscle. *Am J Physiol Cell Physiol,* 289**,** C207-16.

Appendix A

Protocol 1 – Cell culture

Murine myogenic cell line (C2C12)

Growth medium

Component	Final percentage
DMEM 500 ml	
Penicillin/streptomycin (PS) 5.84 ml	1%
FCS 58.4 ml	10%
Glutamine 20 ml (*re-suspend ±50 times*)	

Differentiation medium

Component	Final percentage
DMEM 500 ml	
Penicillin/streptomycin (PS) 5.31 ml	1%
Heat-inactivated horse serum (HS) 5.31 ml	1%
Glutamine 20 ml	

Thaw the medium constituents listed above in the water bath at 37°C. Under sterile conditions, add the volumes as specified above. Note that, before adding, FCS may need to be filtered, HS *must* be filtered and the L-Glutamine will need to be re-suspended until clear.

Cracking a vile

1. Remove a vile of C2C12 cells from the liquid N_2 tank and warm in the water bath at 37°C. (*be careful not to wet the lid of the cryovile*)
2. Grow the C2C12 cells, in growth medium, in a T_{25} at 37°C and 5% CO_2
3. Wash the cells in warm PBS, and replace the medium everyday until the cells reach ~70% confluence

Once 70% confluent, cells are ready to be split or differentiated

Splitting and seeding cells

1. Warm trypsin, PBS and growth medium in the water bath at 37°C
2. Decant old medium and carefully rinse the cell monolayer with warm PBS
3. Decant PBS and add trypsin (1.5 ml in T_{25}) incubate at 37°C for 4 min
4. Tap the side of the flask gently then examine under a microscope to verify that cells have loosened
5. Now add double the amount of warm medium (3 ml in T_{25}) and transfer to a falcon tube before centrifuging at 1500 rmp for 3 min
6. Decant the supernatant leaving just the pellet
7. Add 5 ml of warm medium and re-suspend the pellet ±50 times. (*use 1000 µl pipette*)
8. Count re-suspended cells using a haemocytometer (*keep all solutions warm in the meantime*). Re-seed cells at the following densities:
    a. 300 000 cells for a T_{25}
    b. 100 000 cells for a 35mm Petri

- After splitting and re-seeding, incubate for 24 hrs (or until ~70% confluence is reached) before inducing differentiation

---

Cell Differentiation

- The differentiation of C2C12 myoblasts is induced by replacing the growth medium with differentiation medium (DM)
- After replacing with DM it is Day_{00}
- The cells are washed with warm PBS and the medium is replaced with fresh differentiation medium (DM) after every 48 hrs during differentiation.
- The cells should be fully differentiated and ready to treat on $Day_{10.}$

Maintaining cells

A routine for the maintenance and passaging of cells will need to be established. Generally, the medium needs to be replaced every one to two days in order to maintain healthy culture conditions. Cell maintenance should remain consistent at all times

Protocol 2

MTT cell activity assay

Solutions and reagents

Solution A

Component	Final percentage
Isopropanol (propan-2-ol)	99%
conce. HCl	1%

Solution B

Component	Final percentage
Triton-X-100	0.1%
dH_2O	99.9%

Procedure

1. Prepare a 1% MTT working solution in PBS (0.01 g MTT/ml PBS)
2. Remove culture medium from cells. *Do not rinse with PBS*
3. Add 1.5 ml of warm PBS and then 500 µl of MTT working solution to each well/Petri dish containing the cell monolayer
4. Incubate at 37ºC for two hours
5. In the meantime, mix together a working stock of solution A and solution B in a 50:1 ratio. *50 ml should be sufficient*
6. Remove from the incubator and examine under the microscope. *The solution is light sensitive so do not expose for too long*
7. If some cells have loosened, transfer the suspension into separate, marked 2 ml centrifuge tubes and spin down for 2 min at 1000 rpm. Decant the supernatant and then add 2 ml of the solution A/solution B mixture. Gently re-suspend and then add back to their respective wells/Petri dishes

8. If no cells have loosened then discard the supernatant and add 2 ml of the solution A/solution B mixture
9. Protect cells from light by covering with foil and shake vigorously for 5 min
10. After shaking, transfer to 2 ml centrifuge tubes and spin down for 2 min at 1400 rpm

Absorbance readings

9. Read the absorbance of the supernatant using a spectrophotometer (wavelength of 540 nm). *Use the solution A/solution B mixture as a blank*
10. If the absorbance values read above 1.0 then dilute further using appropriate volumes of solution A/solution B mixture

Protocol *3*

Protein extraction from cells

Solutions and reagents

Buffer A
20 mM Tris-HCl, pH 7.4,
137 mM NaCl
1 mM $CaCl_2$
1 mM $MgCl_2$
0.1 mM sodium orthovanadate

Buffer B (modified radioimmunoprecipitation (RIPA) buffer)
Tris–HCl 2.5mM, pH 7.4
EDTA 1 mM
NaF 50 mM
NaPPi 50 mM
Dithiothreitol 1 mM
Phenylmethylsulfonyl fluoride (PMSF) 0.1 mM
Benzamidine 1 mM
SBTI 4 mg/ml
Leupeptin 10 mg/ml
1% NP40
0.1% SDS
0.5% Na deoxycholate

- It is important to work on ice at all times in order to prevent cell proteins from denaturing.

Protein extraction

1. Discard the supernatants from cell culture dishes and place cells immediately on ice.
2. Rinse the cell monolayers three times in 5 ml of ice cold buffer A
3. Incubate for 10 min in 1 ml of buffer B
4. Scrape cells from culture dishes using a rubber policeman and transfer to 1.5 ml microcentrifuge tubes

Sonication

Sonication is performed in order to disrupt the cell membranes to release their contents.

1. Dilute cell sample extracts with 100 µl RIPA buffer
2. Sonicate cells in microcentrifuge tubes using gentle up and down movements x5
3. Allow contents to incubate on ice until the foam subsides
4. Decant the contents into new, marked microcentrifuge tubes

Centrifuging and storage

1. Centrifuge microcentrifuge tubes 4°C and 8000 rpm for 10 min
2. After centrifugation is completed, remove the microcentrifuge tubes and decant the supernatant into fresh microcentrifuge tubes that have been kept on ice in the meantime
3. Store lysates at -20°C and begin protein quantification or store for longer periods at -80°C

Protocol 4

Bradford Protein quantification

Bradford reagent (5X concentrated)

Dilute 500 mg of Coomassie Brilliant blue G in 250 ml 95% ethanol
Add 500 ml of phosphoric acid before mixing thoroughly
Make up to one litre with dH_2O
Filter and store at 4°C

Bradford working solution

Dilute stock in a 1:5 ratio with dH_2O
Filter using 2 filter papers (at the same time)
Solution should be a light brown colour

Bradford method

1. Thaw a 1mg/ml of BSA stock solution
2. Thaw protein samples if in -80°C freezer. *Keep on ice at all times*
3. Make up a working solution of 100 µl BSA:400 µl dH_2O. *Vortex the mixture*
4. Mark 7 microcentrifuge tubes for the standards as well as tubes for the samples to be tested
5. Now add BSA and water to marked microcentrifuge tubes as indicated in the table below:

Blank:	0 µl BSA	100 µl dH_20	
2 µg protein:	10 µl BSA	90 µl H_20	
4 µg protein:	20 µl BSA	80 µl H_20	
8 µg protein:	40 µl BSA	60 µl H_20	
12 µg protein:	60 µl BSA	40 µl H_20	
16 µg protein:	80 µl BSA	20 µl H_20	
20 µg protein:	100 µl BSA	0 µl H_20	
Each sample:	0 µl BSA	95 µl H_20	5 µl of sample protein

6. Vortex all the tubes briefly
7. Now add 900 µl of Bradford reagent to each microcentrifuge tube. *Vortex again*
8. Incubate at room temperature for ~5 min
9. Read absorbencies, twice each, at 595 nm

10. If sample values fall outside the range of the highest standard then dilute further using RIPA buffer.
11. Make use of excel to make a linear plot of absorbencies and then calculate the amount of each sample to be added to aliquots.

Protocol 5

Sample preparation

Laemmli sample buffer

Component	Volume
dH_2O	3.8 ml
0.5 M Tris-Hcl. pH 6.8	1.0 ml
Glycerol	0.8 ml
10% (w/v) SDS	1.6 ml
0.05% (w/v) bromophenol blue	0.4 ml

Procedure

1. Quantify proteins in cell extracts (protocol 4)
2. Set a beaker of water to boil or switch on the heating block
3. Make up a working solution of sample buffer containing 850 µl of Laemmli sample buffer and 150 µl 2 β-mercaptoethanol
4. Vortex the solution
5. Calculate the number of sample sets needed, each containing at least one representative of each protein sample
6. Add working sample buffer to each aliquot. *Do so under the fume hood*
7. Add a volume of sample buffer equal to 1/3 of the final volume
8. Add a volume of sample containing 50 µg of protein
9. Punch small, pin size, holes in each microcentrifuge tube then place in boiling water/on the heating block to stand for a period of 5 min.
10. Vortex each tube briefly
11. Spin tubes for a moment (~5 sec) using the tabletop centrifuge
12. Samples can now be stored at -80°C

Use of samples

For samples that have been stored in the -80℃ freezer:

1. Start by bringing a beaker of water to the boil or switch on the heating block
2. Remove samples from the freezer and allow them to thaw
3. Vortex each tube briefly
4. Make sure that small pin size holes have been punched in the top of each tube
5. Place in boiling water/on the heating block for a period of 5 min
6. Vortex briefly once again
7. Spin down momentarily (20 sec) on the tabletop centrifuge (*take care not to centrifuge for too long, especially if samples have been obtained from tissue*)
8. The samples can now be used for Western blotting analysis (protocol 5)

Protocol 6

SDS-PAGE and Western blotting

5X Electrode (Running) Buffer, pH 8.3

Component	Final percentage
Tris base	45 g
Glycine	216 g
SDS	15 ml

Make up to 3 litres with dH_20 and do not adjust pH

1. Clean pairs of inner and outer glass plates with methanol and a paper towel
2. Place the inner glass plate onto the larger outer plate and slide these into the green Mini Protean System, Bio-Rad assembly
3. Tighten the assembly by pushing the green clips outward
4. Place the assembly onto the rubber base, pushing down gently
5. Get two small beakers, two Pasteur pipettes and a small stirring bar
6. Fill one beaker with H_2O and get isobutanol ready
7. Separating gel recipe for 10% 0.75 mm gels:

	2 gels: µl	4 gels: µl
dH_2O	3850	7700
1.5M Tris-HCl pH 8.8	2500	5000
10% SDS (stock)	100	200
10% APS (0.1g/ml)	20	40
Acrylamide 40%	2500	5000
Temed	5	10

8. Add all constituents except for the APS and Temed and let the mixture stand for a few minutes so to allow it to degas
9. Add the APS first and stir briefly (~30seconds)
10. Add Temed and mix the solution momentarily

11. Quickly pour the mixture between the glass plates using a Pasteur pipette leaving enough space for the stacking gel
12. Add a layer of isobutanol using a fresh Pasteur pipette
13. Allow to set for 1 hr. Prepare running buffer and TBS-T in 1:10 dilutions
14. After 45 min has passed begin to prepare the stacking gel (4% recipe):

	2 gels: µl	4 gels: µl
dH_2O	3050	6100
0.5M Tris-HCl pH 6.8	1250	2500
10% SDS (stock)	50	100
10% APS (0.1g/ml)	50	100
Acrylamide 40%	500	1000
Temed	10	10

15. Once the gels are set (after 1 hr), wash off the isobutanol and make sure that the plates are dry
16. Add Temed to the stacking solution, mix quickly and add stack between the plates
17. Gently push combs (of the correct width) into the stacking gel
18. Leave to set for 30 min
19. At this stage, retrieve the standard marker (peqGOLD) from the freezer and allow it to warm to room temperature
20. Switch on the heating block (it must reach a temperature of 95°C)
21. Retrieve previously prepared samples from the -80°C freezer and allow them to thaw
22. Ready the electrophoresis apparatus for use
23. Once thawed, vortex each sample briefly before denaturing in the heating block for 5 min
24. In the mean time, carefully remove the combs and wash the gels gently with H_20 being careful not to damage the wells
25. Vortex each sample briefly before centrifuging by pulsing for a few seconds

26. Take the gel plates out of the assembly stand and place them into the U-shaped adaptor cassette. The small plates must be facing inwards
27. Place the U-shaped adaptor into the loading system and push the latches closed, away from your body
28. Carefully pour prepared running buffer into the middle compartment between the gel plates, allowing the buffer to flow over into the wells
29. Add 10µl of molecular weight marker into the first well on the left of each gel. Remember that the left of the far gel will be on your right hand side
30. Add your samples into each well using a micropipette and loading tips. Use a clean tip for every sample
31. Place the system into the outer running chamber, and add running buffer to approximately 1 cm below the wells
32. Place the green lid with electrical leads onto the cell system, making sure to attach the electrodes correctly (red to red and black to black).
33. Perform an initial ten minute run at 100 V (constant) and 400 mA.
34. Thereafter, perform a longer run (usually ~50 minutes) at 200 V (constant)
35. Turn off the power and disconnect the electrodes before removing the gel plates from the system. Proteins will slowly dissolve from the gel, so do not let the gels stand at this point. Move directly onto the transfer step
36. **Electrotransfer** can now be performed using the semi-dry apparatus (Bio-Rad)
37. Cut 8 Whatman 3 mm chromatography filter papers and one 0.2 micron PVDF membrane per gel
38. For every membrane soak three papers in anode buffer 1 (0.3 M Tris-base, pH 10.4, 20% methanol)
39. Soak one paper in anode buffer 2 (25 mM Tris-base, pH 10.4, 2% methanol)

40. Place these papers – first those from anode buffer one then from anode buffer two – onto the anode plate. Role them flat with a test tube to remove air bubbles
41. Soak one PVDF membrane in methanol for 15 seconds and then rinse with water before soaking it in anode buffer two. Place the membrane onto the anode buffer two papers already on the anode plate. Role again to remove any bubbles
42. Carefully remove gels from their respective plates – make sure that the gels do not tear in the process – and place them onto the membranes. Role with a wet tube to remove any bubbles that may have formed
43. Soak four papers in cathode buffer (25 mM Tris-base, 40 mM ε-aminohexanoic acid, pH 9.4, 20% methanol, and place these onto the gel
44. Close the system and run at limit 0.5 A and 15 V for one to two hours
45. Wash the membranes in copious amounts of prepared TBS-Tween (allow foam to develop). Wash three times for 5 minutes
46. Block the membranes in non-fat milk (5 g/100 ml TBS-T) for one to two hours on the belly dancer
47. Make up the primary antibody (5 µl in 5 ml TBS-T). Optimization is required for many antibodies. Different dilutions will need to be experimented with
48. Mix in the walk in freezer overnight.
49. Wash membranes in TBS-T with agitation. Three times five minutes each is sufficient
50. Place the membranes in the HRP-conjugated secondary antibody (1.25 µl in 5ml TBS-T). Incubate with agitation for one hour
51. To expose, use the ECL or ECL+ detection kit (Amersham biosciences) or LumiGLO Reserve™ CL substrate kit (KPL, Inc., USA)
52. Add 500 µl of each of the ECL cocktails provided (or 1:2 ratio for LumiGLO as per manufacturer's instructions) to a foil cover falcon tube and mix for a few seconds.

53. Cover the area of the membrane known to have the bands that you are looking for and leave to incubate for ~one minute
54. Expose membranes to x-ray film in a dark room

Protocol 7

Immunoprecipitation of PI3K

Reagents and solutions

Buffer A
20 mM Tris-HCl, pH 7.4,
137 mM NaCl
1 mM $CaCl_2$
1 mM $MgCl_2$
0.1 mM sodium orthovanadate

Buffer B (modified lysis) buffer
Tris–HCl 2.5mM, pH 7.4
EDTA 1 mM
NaF 50 mM
NaPPi 50 mM
Dithiothreitol 1 mM
Phenylmethylsulfonyl fluoride (PMSF) 0.1 mM
Benzamidine 1 mM
SBTI 4 mg/ml
Leupeptin 10 mg/ml
1% NP40
0.1% SDS
0.5% Na deoxycholate

Buffer C
20 mM Tris-HCl, pH 7.4
137 mM NaCl
1 mM $CaCl_2$
1 mM $MgCl_2$
1% NP-40
0.1 mM sodium orthovanadate

Buffer D
0.1 M Tris-HCl, pH 7.4
5 mM LiCl
0.1 mM sodium orthovanadate

Buffer E
10 mM Tris-HCl, pH 7.4,
150 mM NaCl,
5 mM EDTA
0.1 mM sodium orthovanadate

Procedure

1. Place buffers and microcentrifuge tubes on ice
2. Discard medium and immediately place the cells on ice
3. Rinse three times with ice-cold buffer A
4. Add 1 ml of ice-cold buffer B and allow to incubate for 20 min
5. Scrape adherent cells from the culture dishes and transfer to 1.5 ml microcentrifuge tubes
6. Sonicate using the lowest setting
7. Centrifuge at 4°C and 8000 rpm for 10 min
8. Transfer the supernatant to clean microcentrifuge tubes and perform a protein quantification
9. Add 10 µl of anti-PI3K p85/protein A-agarose slurry conjugate (Upstate Biotechnology, catalog #16-107) to cell lysates containing 500-1000 ug of protein
10. Gently rock the mixture at 4°C overnight
11. Collect the agarose beads by pulsing (5 seconds in a microcentrifuge at 14,000 x g) and drain off the supernatant
12. Wash the collected beads three times each in buffers C, D and E collecting the beads by pulsing between washes (5 seconds in a microcentrifuge at 14,000 x g)
13. Aspirate last wash completely

Protocol 8

Vital staining – Hoechst and PI

1. Remove the medium from your cells and wash two to three times with sterile 0.1 M PBS
2. Prepare fresh PI from the 5 µM stock (make up a 1:200 working solution) and spin down the PI working solution momentarily before use
3. Add enough PI to completely cover the cells (100 µl for a coverslip and ~1 ml for a 35 mm Petri dish)
4. Incubate at 4°C for 20 minutes
5. Aspirate and wash once with 0.1 M PBS
6. Add ice cold fixative (1:1 methanol/acetone) in order to permeabilize the cell membranes
7. Incubate for 10 minutes at 4°C
8. Using a micropipette, aspirate the fixative and leave the cells to air dry in the dark for approximately 20 minutes
9. Prepare a fresh Hoechst solution (Hoechst stock 5 µM: Make up a 1:200 solution in water (or 0.9% NaCl)). Store away from UV radiation at 4°C, and spin down the Hoechst working solution momentarily before use.
10. Rinse three times with sterile PBS
    - If cells have been grown on coverslips then they must be removed and placed, face up, onto labeled microscope slides at this point

11. Add enough Hoechst dye (1:200) to cover the cell monolayer completely (~100 µl for coverslips and 1 ml for 35 ml Petri dishes) and then incubate in the dark for a further 10 minutes
12. Wash the cell monolayer 5 times thoroughly
13. If staining has been done on coverslips then place a small drop of fluorescent mounting medium onto each slide and carefully place the washed coverslip face down onto the slide, spreading the mounting medium carefully underneath
14. Now place the slides face down onto tissue paper (already laid down) and cover with foil to protect from light. Leave like this overnight
15. Cells can now be stored at -20°C for ~2 weeks. *Wrap in foil to avoid any exposure to light*
16. Visualize using a fluorescence microscope

Protocol 9

Vital staining – Hoechst and Annexin V

1. Remove the medium from your cells and wash three times with sterile 0.1 M PBS
2. Add ice cold fixative (1:1 methanol/acetone) in order to permeabilise the cell membranes
3. Incubate at 4°C for 20 minutes
4. Using a micropipette, aspirate the fixative and leave the cells to air dry in the dark for approximately 20 minutes
5. Wash cell monolayers three times with 0.1 M PBS
6. Prepare 5% donkey serum in PBS (at least 100 µl per sample – make extra)
7. Incubate for 20 minutes at room temperature
8. Drain the serum, but do not rinse with PBS
9. Add 100 µl of anti-Annexin V primary antibody (dilution 1:50)
10. Incubate at room temperature for 90 minutes in a dark, humidified atmosphere
11. Rinse three times with sterile PBS
12. Add 100 µl of FITC or Texas red labelled secondary antibody (dilution 1:200)
13. Incubate for 30 minutes at room temperature in a dark, humidified atmosphere
14. Rinse three times with sterile PBS
15. Prepare a fresh Hoechst solution (Hoechst stock 5 µM: Make up a 1:200 solution in water (or 0.9% NaCl)). Store away from UV radiation at 4°C, and spin down the Hoechst working solution momentarily before use.
16. Add enough Hoechst dye (1:200) to cover the cell monolayer completely (~100 µl for coverslips and 1 ml for 35 ml Petri dishes)

17. Incubate in the dark for 10 minutes
18. Wash the cell monolayer 5 times thoroughly
19. If staining has been done on coverslips then place a small drop of fluorescent mounting medium onto each slide and carefully place the washed coverslip face down onto the slide, spreading the mounting medium carefully underneath
20. Now place the slides face down onto tissue paper (already laid down) and cover with foil to protect from light. Leave like this overnight
21. Cells can now be stored at -20°C for ~2 weeks. *Wrap in foil to avoid any exposure to light*
22. Visualize using a fluorescence microscope

Protocol 10 - DNA Fragmentation

Genomic DNA purification

Reagents

Lysis buffer	
2mM EDTA	2ml of 1M
100mM Tris-HCl (pH 8.0)	100ml of 1M
0.8% SDS (w/v)	8g
10mM NaCl	2ml of 5M

Mix for 1hr<
Make up to 1 liter with H_20
Store at room temperature

DNA loading buffer

0.25% Bromophenol blue
50% glycerol
Make up in H_2O

TAE buffer 50x	
2M Tris base	242g
1M acetate	57.1ml of glacial acetic acid (17.4M)
100mM EDTA	200ml of 0.5M EDTA (pH 8.0)

Lysis of cells from monolayer

1. Remove cells by trypsinization
2. Count on a hematocytometer
    - Place cells on ice in the meantime
3. Pellet by centrifugation for 10 min at 1200 rpm and 10ºC
4. Wash each pellet twice with sterile ice-cold PBS (centrifuging between washes)
5. Re-suspend pellets 3 ml of lysis buffer
6. Add RNase so as to have a final concentration of 20µg/ml
7. Incubate the mixture on a heating block at 37°C for 1hr
8. Add proteinase K so as to have a final concentration of 100µg/ml
9. Incubate on heating block at 45°C overnight

10. Inactivate the proteinase K the following day at 70°C for five minutes
11. Quench on ice for 5min
12. Centrifuge at 10 000 rpm for 15 min)
    - A tight white pellet of protein should be seen for proteinase K/SDS activity.
13. Decant supernatant into an equal volume of PCI (phenol/chloroform/isoamyl alcohol)
14. Mix slowly by inverting the microcentrifuge tube over end slowly for 3 min (phases should be well separated)
15. Centrifuge for 10 min at 10 000 rpm at room temperature
16. Remove the top (aqueous) phase containing the DNA and transfer to a new microcentrifuge tube.
17. Repeat steps 13 to 14
18. Add an equal volume of CI (cholorform/isoamyl alcohol, 24:1) and mix gently over end for 2 min
19. Centrifuge for 1 min at 10 000 rpm
20. Remove the top (aqueous) phase and transfer to a fresh microcentrifuge tube
21. Precipitate DNA by adding 40 µl NaCl and 1 ml of ice-cold 100% ethanol
22. Incubate at -20ºC for 1 hr
23. Centrifuge for 20 min at 14 000 rpm
24. Remove supernatant and wash the pellet once in 70% (v/v) ethanol
25. Spin down the genomic DNA for 5 min at 14 000 rpm
26. Drain the supernatant and air dry for a maximum time of 5 min
27. Re-suspend the pellet in 40 µl of Tris-EDTA, pH 7.5
28. Add 10 µl of each sample to 2 µl of loading dye

Gel preparation

1. Prepare 1X TAE from 50X TAE
2. Make up 1% agarose in 1X TAE buffer
3. Microwave the agarose solution for ~1 ½ minutes. Make sure that the solution does not bubble
4. Remove the flask containing the agarose solution from the microwave and allow it to cool to room temperature slowly (do not put on ice)
5. When the flask is cool enough to touch with a bear hand add ethidium bromide (1 µg/ml) to the solution
6. Add the comb to the electrophoresis tank and carefully pour the solution into the gel tank
7. Allow ½ hour for the gel to set before carefully removing the comb

Electrophoresis

1. Cover the gel in the same 1X TAE buffer used to make the agarose gel itself (cover the gel to only 1 mm above the wells)
2. Add the DNA ladder (typically 100 bp) to the left most well of the gel
3. Add DNA samples carefully using a micropipette
4. Resolve the gel by electrophoresis at 4 V/cm
5. After 40 min, examine the gel on a UV transilluminator